# WP3
# Monitoring network improvement for coastal flooding and extreme weather risk management

## Activity 3.2
## Radar monitoring network for coastal flooding and extreme weather

### D3.2.1 Radar data processing for network and the useful composite products for coastal monitoring

# PROJECT AND ACTIVITY DETAILS

| | |
|---|---|
| **Project Acronym** | AdriaMORE |
| **Project title** | Adriatic DSS exploitation for MOnitoring and Risk management of coastal Extreme weather and flooding |
| **Funding Line** | Priority Axis 2, Specific Objective 2.2 |
| **Project Partners** | LP Abruzzo Region (Italy)<br>P1 Dubrovnik and Neretva Region (Croatia)<br>P2 Meteorological and hydrological service (Croatia)<br>P3 National Research Council (Italy) |
| **Starting date** | January 1, 2018 |
| **Activity number** | 3.2 |
| **Activity Title** | Radar monitoring network for coastal flooding and extreme weather |
| **Work Package** | WP3: Monitoring network improvement for coastal flooding and extreme weather risk management |
| **Activity Summary** | Activity 3.2, within Work Package 3, is devoted to improve the effectiveness of radars measurements by mean the creation of radar composite by utilizing data provided by Italian and Croatian radar network |
| **Deliverable number** | 3.2.1 |
| **Deliverable Summary** | This deliverable is aimed at describing the radar's mosaic algorithm chain developed and the related composite products generated |
| **Main Author** | Errico Picciotti, errico.picciotti@aquila.infn.it |
| **Main Author's organization** | CETEMPS |
| **Other Author's** | Stefano Barbieri, Saverio Di Fabio and Zvonko Komericki |
| **Data of issue** | November 30, 2018 |
| **Total Number of pages** | 109 |
| **Distribution list** | Italy-Croatia CBC Programme, AdriaMORE partners |

*This document has been produced with the contribution of the EU co-financing and the Interreg Italy-Croatia CBC Programme. The content reflects the author's views; the Programme authorities are not liable for any use that may be made of the information contained therein.*

# Table of contents

# 1. INTRODUCTION

**Hydro-meteorological** and other marine hazards triggered by meteorological events, affecting the Adriatic areas represent a dramatic threat which needs to be faced by enhancing monitoring and forecasting systems. In this respect, **AdriaMORE project** proposes increasing of the management capacity of the response to marine and coastal hazards in the Adriatic basin.

AdriaMORE goal is to improve an existing integrated hydro-meteorological risk management platform focusing on the Adriatic coastal areas of Italy and Croatia capitalizing the major achievements of ADRIARadNet and CapRadNet projects. The latter, successfully completed under the IPA Adriatic CBC Programme, were devoted to create a cross-border infrastructure of observing and forecasting systems for building real-time risk scenarios for civil protection purpose.

To this end, one of AdriaMORE's specific objective is the improving the **effectiveness of radar measurements** in Adriatic coastal area by means of the creation of a rain composite utilizing data provided by Italian and Croatian radar network. This objective has been performed in the action 3.2 of the WP3 of AdriaMORE project whose the main result is constituted by the **Output entitled "One radar network mosaic data SW to enhance the monitoring coastal flood"**.

Two deliverables have contributed to the achievement of the above project Output:

- one aimed at describing the radar's mosaic algorithm chain developed and the related composite products (**deliverable 3.2.1**)
- one aimed at describing the useful radar products to be used against extreme weather events, it can be applied at radars having different technical characteristics (**deliverable 3.2.2**).

The latter is described in another document while the **deliverable 3.2.1**, subject of this paper, has been organized as follows.

In the **chapter 2** some principles of radar meteorology are introduced: history, main utilizations, radar types and useful products as well as the sources data uncertainty.

In the **chapter 3** the main outcomes of ADRIARadNet and CapRadNet projects are recalled focusing on the aspects concerning the activity 3.2 of AdriaMORE project. Moreover, advantages and disadvantages of X-band systems are introduced as well as some examples of their use within EU-funded or National projects.

In the **chapter 4** a review of the main radar network in the world and Europe is conducted focusing on those operative in Italy and Croatia. Furthermore, the heterogeneous radar network in the complex orography of Abruzzo Region is detailed described.

In the **chapter 5** the weather radar network software developed (called CRAMS) is analysed in detail in every single module with examples of application by utilizing Italian and Croatia radars data. This chapter can be considered as the core of this deliverable.

In the **chapter 6** the performances of the different merging strategies operating in the CRAMS have been carried out by means of three cases study utilizing ground truth data as a reference.

Summary and outlooks are given in the **chapter 7** while the references here used are listed in the **chapter 8**.

Lastly, **annex 1** shows the functions that characterize the CRAMS scheme in the form of pseudocode.

# 2. WEATHER RADAR OVERVIEW

## 2.1 History

The measurement of rainfall rate and amount is critical to a wide range of applications including space and atmospheric sciences, environmental and agricultural research, hydrology, and water resources management. The point observations based on traditional rain gauges have many limitations because of the spatial and temporal variability of precipitation. In the past four decades, the use of **weather radar** has greatly changed quantitative rainfall estimation by providing spatially continuous estimates of rainfall at small temporal sampling intervals. This now serves as the primary rainfall observing system in many places around the world, with the usage of rainfall gauge measurements for bias corrections, and for merging with the radar estimates.

The term **RADAR** as the abbreviation of **RA**dio **D**etection **A**nd **R**anging was first used by the U.S. Navy in 1940 and adopted universally in 1943. It was originally called Radio Direction Finding (R.D.F.) in England.

Primarily, the radar consists of a **transmitter** to generate microwave signal, an **antenna** to send the signal out to space and to receive energy scattered (echoes) by targets around, a **receiver** to detect and process the received signals by means of processors and a **display** to graphically present the signal in usable form (**figure 2.1, left panel**).

The transmitter generates a microwave pulse which is routed through the circulator and waveguide and radiated by the antenna. The latter emits the transmitter pulse in a symmetrical pencil beam. The atmosphere around the radar is scanned by moving the antenna in azimuth and elevation following meteorological scanning strategies. After the transmit pulse is terminated, the receiver is connected via the circulator to the antenna. The receive phase starts and the receiver is acquiring the signals scattered by the targets. This phase lasts until the next pulse is transmitted.

It is worth mentioning which radar's antenna are often subject to severe weather. So, some enclosure is needed for antennas to survive and to perform under adverse weather conditions. These enclosures are called as **radome**. A radome (radar dome) is a weatherproof enclosure used to protect an antenna. It is used mainly to prevent ice (especially freezing rain) from accumulating directly onto the metal surface of the antenna (**figure 2.1, right panel**).

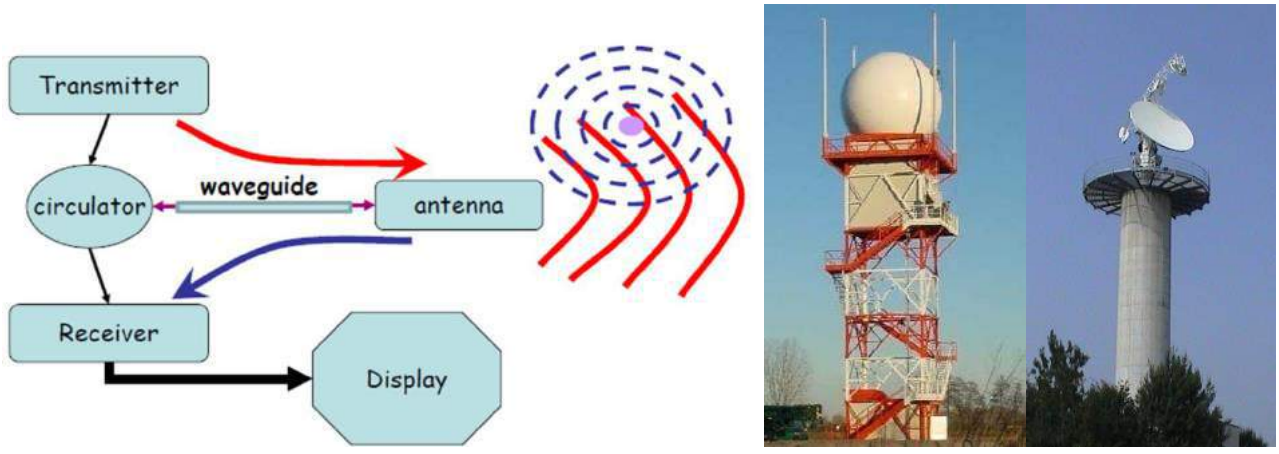


***Figure 2.1*** *General radar block diagram (left) and radar antenna with and without radome (right)*

Operation principle of a radar is very simple in theory. Radar emits a radio signal in a certain frequency into its surroundings and receives the reflected signal from any object (**figure 2.2, left panel**). In general, weather radars detect precipitation echoes using multi-elevation volume scans, it is worth mentioning that a volume radar is a well-defined standard structure formed by a set of PPI (or sweep) scan at different elevation angles (**figure 2.2, right panel**).
The volume radar is generated and recorded to be processed in real time (i.e. product generation) or later (case study analysis etc.).

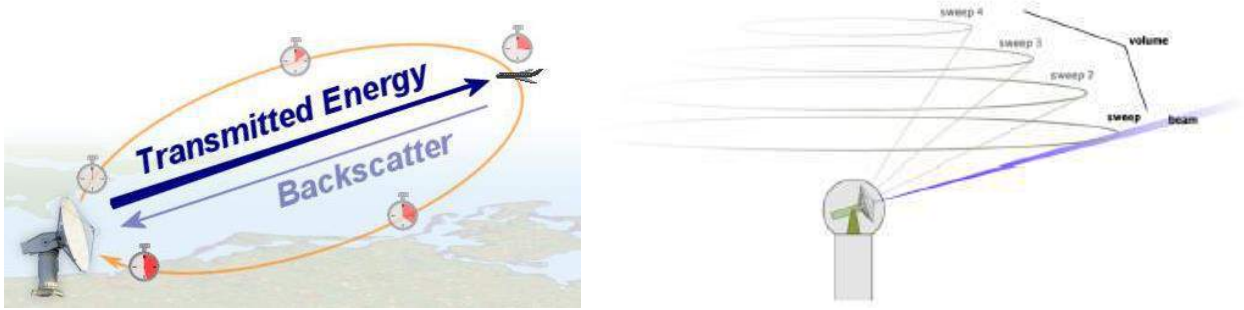


***Figure 2.2*** *Radar principle (left panel) and a typical volume scan (right panel)*

After the processing of this signal, the distance, type, shape, size and motion of the object can be estimated based on the strength and frequency shift of the returned signal. The returned signal (echo) from any target measured by the radar is generally called as "reflectivity". The latter, expresses in decibel (dBZ), depends mainly to droplet size but also to its concentration as well as on the type of precipitation (**figure 2.3**).

| dBZ | Rain Rate | Comments |
|---|---|---|
| 10 | ~0.2 | Significant but mostly non-precipitating clouds |
| 20 | ~1 | Drizzle, very light rain |
| 30 | ~3 | Light rain |
| 40 | ~10 | Moderate rain, showers |
| 50 | ~50 | Heavy rain, thundershowers, some hail possible |
| 60 | ~200 | Extremely heavy rain, severe thunderstorm, hail likely |

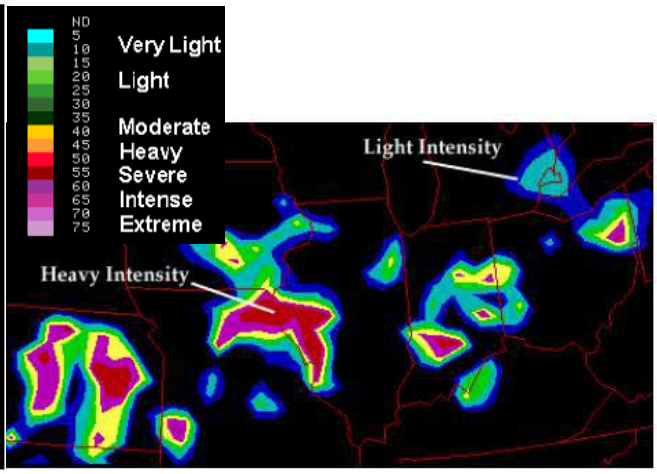


***Figure 2.3*** *Correspondence between radar reflectivity and rain rate (left panel) and a typical radar map (right panel)*

Although the starting of the research and development studies for radars are dated to the first half of 1800s, the radars have been used for tracking the weather systems since early 1950s, after the 2nd World War. Radars with the capability of the reflectivity measurements only were put into operation for the detection and tracking of weather phenomena such as thunderstorms and cyclones with limited moving target indication capability.

After 1970s, by the development of the Doppler technology, it would be possible to get the velocity and direction information of the meteorological targets more accurately as well as the intensity and location of them.
In addition to the Doppler technology, the researches on the polarimetric radars since late 1990s have brought out new approaches and opportunities for radar operations, particularly for hail detection and hydrometeor classification, and dual polarization technology has been put into operational use after 2000s with new features and benefits for users. These new benefits provided by dual polarization radars urge the radar users either to upgrade the existing systems for dual polarization features or to have new systems with this capability. Furthermore, advanced signal processing and data processing methods have also increased the capability of the weather radars significantly.

### 2.2 Main utilizations of weather radars

Although the hydrometeors in the atmosphere as the main targets for weather radars vary from the very small particles of non-precipitation clouds to big hail drops, radars are capable of detecting and classifying them. On the other hand, non-meteorological targets such as obstacles, birds, insect and dust clouds can also be detected by weather radars.
It will not be wrong to assert that weather radars as active remote sensing systems, at least for today, are the only and essential instruments as active remote sensing systems which can provide real time (less than 15 minutes depending on the scanning strategy and processing features), accurate and high resolution (up to 150 m) weather information in large scale area (up to 500 km depending on the frequency used) particularly for nowcasting purposes.
Although the short list above demonstrates that weather radars are used mainly for preparing the warnings against severe weather conditions, they can provide many information and products for several purposes with the capabilities summarized below:

a. Determination of time, quantity and location of the precipitation occurred,
b. Estimation of time, quantity and location of expected precipitation,
c. Tracking the weather systems by estimating the intensity, direction and velocity,
d. Providing real time data for numerical weather prediction models as well as hydrological forecasting models,
e. Identification of precipitation type (hydrometeor classification),
f. Supporting the disaster management and hazard mitigation activities by means of early warnings against hazardous heavy rain, flash flood, hail, hurricane, etc.,
g. Improving the aviation safety by means of en-route surveillance,
h. Supporting marine meteorology and road meteorology services,
i. Determination of wind shear, microburst, macroburst, downburst and strong winds with spatial, temporal and vectoral information at the airports and flight regions,
j. Real time monitoring of the location, surface and travelling of cold and warm fronts,
k. Not conventional applications such as study of bird migration, monitoring of sand storms and detection and quantitative retrieval of volcanic ash.

## 2.3 Weather radar types

The weather radars may be classified in several ways due to the criteria of the classification, e.g. receiving and transmitting type, operating frequency band, polarization type, type of transmitter, Doppler, non-Doppler, etc. The most common classification and types are described briefly in this part.

### 2.3.1 Frequency Bands of Weather Radars

Generally, weather radars are classified by the frequency band used. The mostly used weather radars are C-Band, S-Band and X-Band radars respectively whose characteristic are described below and resumed in **table 2.1**.

**a) S-band radars**

Those radars operate on a wavelength of 8-15 cm and a frequency of 2-4 GHz. Because of the wavelength and frequency, S-band radars are not easily attenuated. This makes them useful for near and far range weather observation. It requires a large antenna dish and a large motor to power it. S-band radars are generally used to detect and track severe weather phenomena in long ranges such as tornado, hurricane, etc.

**b) C-band radars**

Those radars operate on a wavelength of 4-8 cm and a frequency of 4-8 GHz. The signal is more easily attenuated, so this type of radar is best used for short range weather observation. Also, due to the small size of the radar, it can therefore be portable. The frequency allows C-band radars to create a smaller beam width using a smaller dish. C-band radars also do not require as much power as an S-band radar. C-band radars are very suitable for precipitation measurements.

**c) X-band radars**

Those radars operate on a wavelength of 2.5-4 cm and a frequency of 8-12 GHz. Because of the smaller wavelength, the X-band radar is more sensitive and can detect smaller particles. These radars are used for studies on cloud development because they can detect the tiny water particles and also used to detect light precipitation. X-band radars also attenuate very easily, so they are used for only very short-range weather observation. Furthermore, X-band is very suitable for mobile radar applications.

| | S-Band Radars | C-Band Radars | X-Band Radars |
|---|---|---|---|
| FREQUENCY | 2-4 GHz | 4-8 GHz | 8-12 GHz |
| WAVE LENGTH | 15-7.5 cm | 7.5-3.8 cm | 3.8-2.5 cm |
| TYPICAL RANGE | 300-500 km | 120-240 km | 50-100 km |
| PEAK POWER | 500 kW- 1MW | 250-500 kW | 10-100 kW |
| MEASURING SENSITIVITY | Rain, snow, hail | Rain, snow, hail, drizzle | Rain, snow, hail, light drizzle |
| ATMOSPHERIC ATTENUATION | Less attenuation as compared to C-Band and X-Band | Less attenuation as compared to X-Band while much attenuation as compared to S-Band | Much attenuation as compared to C-Band and S-Band |
| TYPICAL ANTENNA SIZE | 7.5 m | 4.2 m | 2.5 m |

***Table 2.1** A roughly comparison of 3 types weather radars mostly used*

### 2.3.2 Non-Doppler and Doppler Weather Radars

**a) Non-Doppler Weather Radars**

These types of weather radar are called as “conventional weather radars”. Non-Doppler radars can make the reflectivity measurements to estimate the distance and intensity of the targets with limited capability for moving target indication by using some clutter suppression algorithms.

**b) Doppler weather radars**

Doppler weather radars are capable of obtaining information about the velocity, direction and strength of the targets by using Doppler effect and advanced processing algorithms as well. If a target is moving relative to radar, this will cause a change in the frequency of received signal proportional to the amount of the movement. This is called as Doppler Effect or Doppler Shift and velocity of the target can be calculated by using this information.

### 2.3.3 Single Polarization Radars and Polarimetric Radars

**a) Single Polarization Weather Radars**

Electromagnetic or radio waves consist of electric (E) and magnetic (H) force fields, which are perpendicular to each other and to the direction of propagation of the wave front, propagate through space at the speed of light. Electric and magnetic fields are always perpendicular to each other. So, it is possible to specify the orientation of the electromagnetic radiation by specifying the orientation of one of those fields. Most of the weather radars use the linear horizontal polarization by considering that it performs very well to detect the main weather targets based on the suitability of their shapes and distribution.

**b) Polarimetric Radars**

Most weather radars transmit and receive radio waves with a single horizontal polarization. That is, the direction of the electric field wave crest is aligned along the horizontal axis. Polarimetric radars, on the other hand, transmit and receive both horizontal and vertical polarizations. Since polarimetric radars transmit and receive two polarizations of radio waves, they are sometimes referred to as dual-polarization radars. Polarimetric Doppler Weather Radars are getting more popular because they improve the accuracy of quantitative precipitation measurement and hydrometeor classification significantly with additional transmitting and processing functionality allowing further information on the directionality of the reflected electromagnetic energy received.

## 2.4 Basic products of weather radars

The radar observables for dual-polarization systems include copolar reflectivity factor in both horizontal ($Z_{hh}$) and vertical polarization ($Z_{vv}$), differential reflectivity ($Z_{dr}$), linear depolarization ration ($L_{dr}$) and differential specific phase shift ($K_{dp}$). It is worth mentioning that single-polarization system includes only horizontal ($Z_{hh}$) reflectivity measurement. Both systems can include also radial velocity (V) and spectral width (W) if have doppler capability.

Main useful radar products are shown in **table 2.2**, they are generally created from the volume acquired during the scan. Radar products are usually automatically generated at each acquisition time and can be displayed on radar monitoring screen.

| Product Name | Features |
|---|---|
| PPI<br>Plan Position Indicator | It is a slant-range display of radar echo data acquired from one antenna rotation with the antenna at a given elevation angle. |
| RHI<br>Range Height Indicator | Display on which radar signals are shown with height as the vertical axis and range as the horizontal axis, forming a vertical cross section of a cloud or precipitation system. |
| VMI<br>Vertical Maximum Indicator | Gives a maximum value of reflectivity above each vertical column of data. This radar product is useful for a quick surveillance of regions of convective precipitation to locate both mature and newly developing thunderstorm |
| HVMI<br>Horizontal Vertical Maximum Indicator | As the VMI but with maximum value given also along two horizontal direction |
| Echo TOP<br>Top Height of reflectivity echo | It shows the elevations that the precipitation echoes, or reflectivities, extend up to in the atmosphere. Echo Top is similar to cloud top, but usually the top of the cloud will be somewhat higher than the top of the precipitation echoes. It is generally measured in [km] |
| LBM<br>Lowest Bin Map | It is a reflectivity map create with lowest level data in each column and can be used for precipitation estimates |
| VIL<br>Vertically Integrated Liquid | The VIL value at a certain location is the sum of all observed radar reflectivities (converted to liquid water content) in a vertical column above this location. The unit of VIL is [kg/m$^2$] and it can be regarded as a measure for the potential rainfall |
| CAPPI<br>Constant Altitude Plan Position Indicator | It is a horizontal cross-section at a specified altitude produced from data volume through interpolation |
| SRI<br>Surface Rainfall Intensity | Instantaneous rain rate in [mm/h], can be derived from reflectivity data using various relationship |
| SRT<br>Surface Rainfall Total | It is the accumulated rain in [mm] and can be calculate from SRI, generally is available for 1, 3,6,12 and 24 hours |
| CLASSIFICATION | The product is aimed at partitioning the radar volume in terms of microphysical hydrometeor types (rain, hail, snow, etc). It is applied only at dual polarization radar. A technique for hail detection is applied to single polarization radar |
| COMPOSITE | The composite products can be generated by combining the data from different radars in the network. These products can be used efficiently by the forecasters to make an overall interpretation and comparison of data from different radars for a more accurate forecasting. |

***Table 2.2** List of main useful radar products*

## 2.5 Sources of radar data uncertainty

There are numerous sources of errors that affect radar measurements of reflectivity volumes or surface precipitation, which have been comprehensively discussed by many authors **[e.g. Collier, 1996; Meischner, 2004; Šálek, 2004; Michelson, 2005]**. Hardware sources of errors are related to electronics stability, antenna accuracy, and signal processing accuracy **[Gekat, 2004].** Other non-meteorological errors are results of electromagnetic interference with the sun and other microwave emitters, attenuation due to a wet or snow (ice) covered radome, ground clutter **[Germann, 2004]**, anomalous propagation of radar beam due to specific atmosphere temperature or moisture gradient **[Bebbington, 2007]**, and biological echoes from birds, insects, etc. Next group of errors is associated with scan strategy, radar beam geometry and interpolation between sampling points, as well as the broadening of the beam width with increasing distance from the radar site.

Moreover, the beam may be blocked due to topography **[Bech, 2003]** and by nearby objects like trees and buildings, or not fully filled when the size of precipitation echo is relatively small or the precipitation is at low altitude in relation to the antenna elevation (so called overshooting).

Apart from the above-mentioned non-precipitation errors, meteorologically related factors influence precipitation estimation from weather radar measurements. Attenuation by hydrometeors, which depends on precipitation phase (rain, snow, melting snow, graupel or hail), intensity, and radar wavelength, particularly C and X band, may cause the strong underestimation in precipitation, especially in case of hail **[Doviak, 1993]**.

Another source of error is Z–R relation which expresses the dependence of precipitation intensity R on radar reflectivity Z. This empirical formula is influenced by drop size distribution, which varies for different precipitation phases, intensities, and types of precipitation: convective or non-convective **[Šálek, 2004]**. The melting layer located at the altitude where ice melts to rain additionally introduces uncertainty into precipitation estimation. Since water is much more conductive than ice, a thin layer of water covering melting snowflakes causes strong overestimation in radar reflectivity. This effect is known as the bright band **[Battan, 1973; Goltz, 2006]**.

Moreover, the non-uniform vertical profile of precipitation leads to problems with the estimation of surface precipitation from radar measurement **[e.g. Franco, 2002; Einfalt, 2008]**, and these vertical profiles may strongly vary in space and time **[Zawadzki, 2006].**

A sketch of the main source of uncertainty id given in **figure 2.4**.

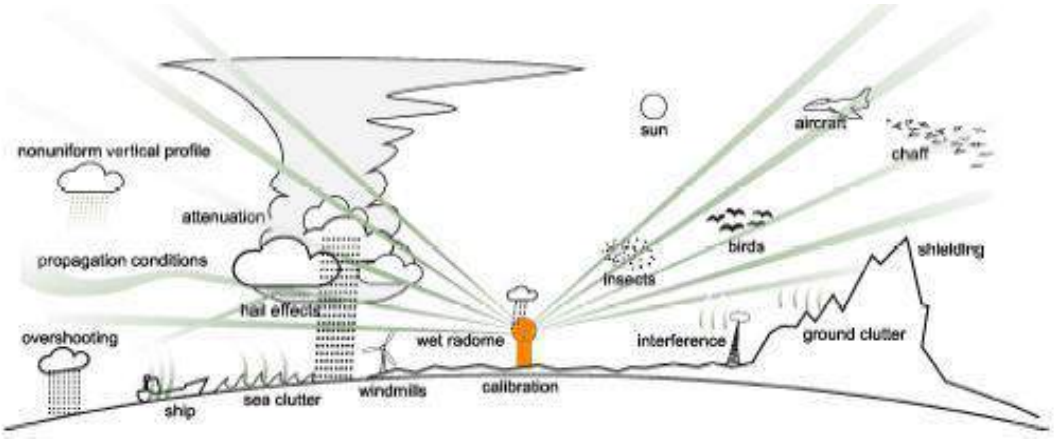


***Figure 2.4*** *Phenomena affecting radar measurements of reflectivity*

# 3. KNOWLEDGE EXPLOITED

Some achievements of activity 3.2 was built on knowledge of previous EU projects: namely ADRIARadNet and CapRadNet.

The **ADRIARadNet project** (http://cetemps.aquila.infn.it/adriaradnet/) has successfully designed an innovative Decision Support System (DSS) to enhance the response capacity to extreme weather events affecting the safety of people in the Adriatic area.

The DSS main components are: (i) an observational network, composed by four X-band mini-radars and satellite sensors; (ii) an early-warning system coupling hydrometeorological numerical forecast and observational data assimilation; (iii) an integrated ICT web-based platform for data sharing and consultation to support decisions on hydro-meteorological hazards.

The **CapRadNet project** (http://cetemps.aquila.infn.it/capradnet/) has been accomplishment five feasibility studies and realized new tools and infrastructures covering some issues in maritime, coastal, airport and metropolitan environments whose common denominator is the hydro-meteorological hazard.

In the next two sections ADRIARadNet and CapRadNet projects are recalled focusing on the aspects concerning the activity 3.2 only.

Moreover, in the third section advantages and disadvantages of X-band systems are introduced and some examples of their use within EU-funded or National projects are also given.

## 3.1 The ADRIARADNET project

One of the primary goals of ADRIARadNet project (financed within the second call of IPA Adriatic CBC Programme 2007-2013) was to install and testing **four low cost, X-band mini-radar.** Two dual-polarization systems have been installed in Italy (Cingoli and Tortoreto sites) while two single-polarization systems have been installed in Croatian and Albanian territories (Dubrovnik and Durres sites). In **figure 3.1** are shown the location of these systems while in **figure 3.2** the pictures of each installation.

These installations have enhanced the observational network in the territories involved; as matter of fact, only three weather radars existed in Croatia before the ADRIARadNet project, installed inland, leaving the Dalmatian coastline basically uncovered. There were no radar installations available in Albania and Marche Region, as well. The Abruzzo Region, although well instrumented, had a gap in its northern and central coastline area.

After the deployment and set-up activities, the four radars were left in continuous operational mode and fully tested during the experimental campaign planned within the project.

The installed mini-radar system has proved useful for:

1) facilitating the establishment of low-cost weather radar monitoring networks that would be particularly attractive to developing countries lacking the funds to implement and operate nationwide networks on the basis of high-power radar units;

2) developing small networks to provide in situ weather surveillance of small cities and flood prone areas not well covered by existing operational national radar networks, thus filling up the geographical gaps in the radar network coverage;

3) local deployment on small size platforms requiring low power consumption and easily remotely controlled to facilitate specialized field observations in remote areas.

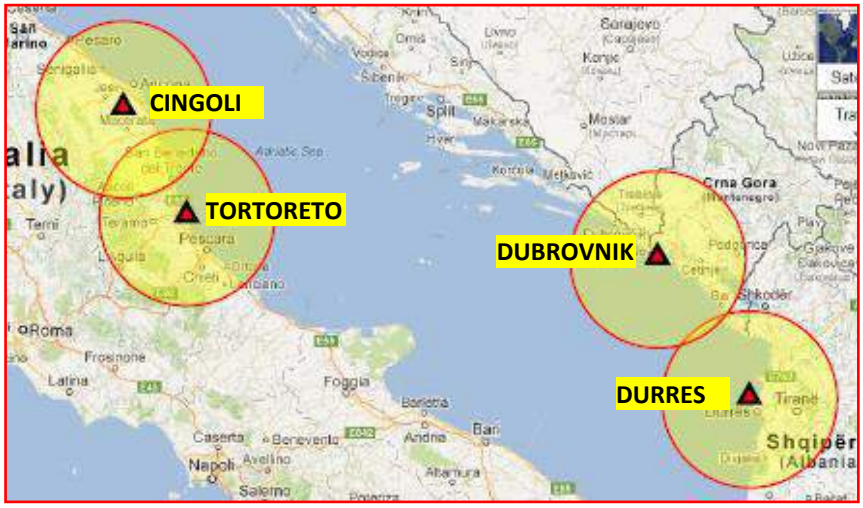


***Figure 3.1*** *Location of the four X-band mini-radars installed within the ADRIARadNet project*

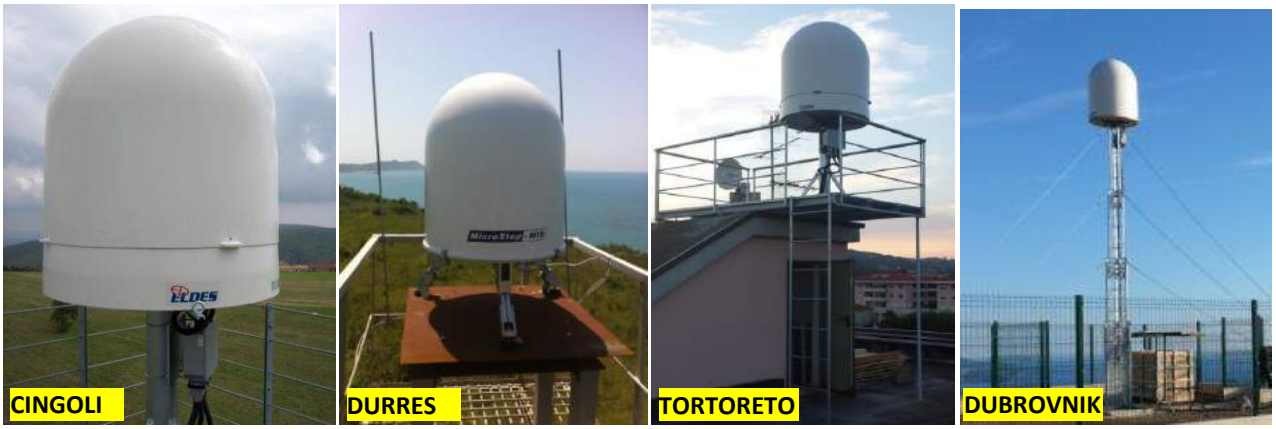


***Figure 3.2*** *Pictures of the four X-band mini-radars installed within the ADRIARadNet project*

Therefore X-band radars provide a possible tool in hydrologic forecasting for urban areas and small-scale basins. However, the use of sophisticated hardware systems, even though of essential importance, is not enough. The drawback is that X-band signals may be heavily attenuated in intense rainfall and hail, such as that found in convective systems. So, radar algorithms able to process raw radar data, enhance their quality, extract from them accurate products useful for example for initializing hydrological as well as meteorological models, are active parts of the radar system. Thus, the capability to invert the X-band radar measurements into useful hydro-meteorological products is then crucial to understand the full potential of X-band radar system.

For this purpose, algorithms for X-band radar which have been developed and optimized within the ADRIARadNet project for single and dual polarization systems. These algorithms, called RadarALG tool (see **figure 3.3**) have been used for the four mini-radar data analysis during and after the experimental campaign carry out in the project. Various operational aspects were examined to extract quantitative information from radar data and to provide reliable products.

In particular, hydrometeor classification (see **figure 3.4**), path-attenuation correction, rain-rate estimation and nowcasting deserved a special attention being the core of any hydro-meteorological application.
Some of these algorithms have been reused and adapted for AdriaMORE purposes.

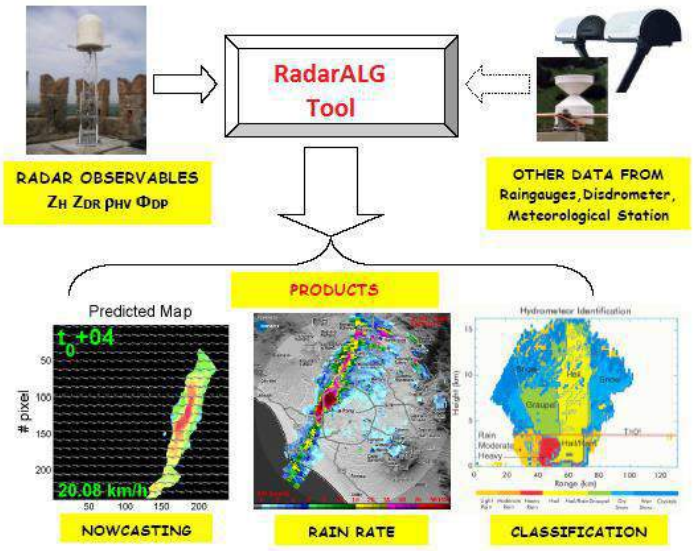


***Figure 3.3*** *RadarALG tool convert radar observable into hydro-meteorological products, some reference data, if available, can be used to assess the goodness of the algorithms*

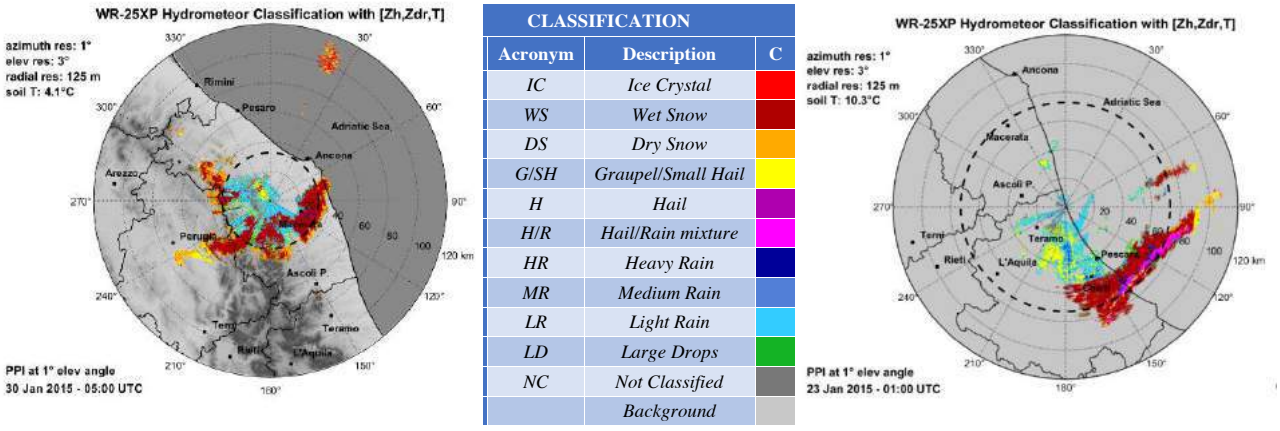


| CLASSIFICATION | | |
|---|---|---|
| Acronym | Description | C |
| *IC* | *Ice Crystal* | |
| *WS* | *Wet Snow* | |
| *DS* | *Dry Snow* | |
| *G/SH* | *Graupel/Small Hail* | |
| *H* | *Hail* | |
| *H/R* | *Hail/Rain mixture* | |
| *HR* | *Heavy Rain* | |
| *MR* | *Medium Rain* | |
| *LR* | *Light Rain* | |
| *LD* | *Large Drops* | |
| *NC* | *Not Classified* | |
| | *Background* | |

***Figure 3.4*** *Two examples of hydrometeor classification for Cingoli (left panel) and Tortoreto (right panel) radars*

### 3.2 The CAPRADNET project

One specific objective of CapRadNet project (financed within the *targeted call on EUSAIR* call of IPA Adriatic CBC Programme 2007-2013) was the realization of a feasibility study aimed at improving the management of severe weather events on the airport flight operations by utilizing meteorological model and weather radar data. Moreover, a single-polarization X-band mini-radar has been installed 5 km far from Pescara Airport in the municipality of Cepagatti. In **figure 3.5** is shown the pictures of the installation and a VMI reflectivity map taken during a rainy event.

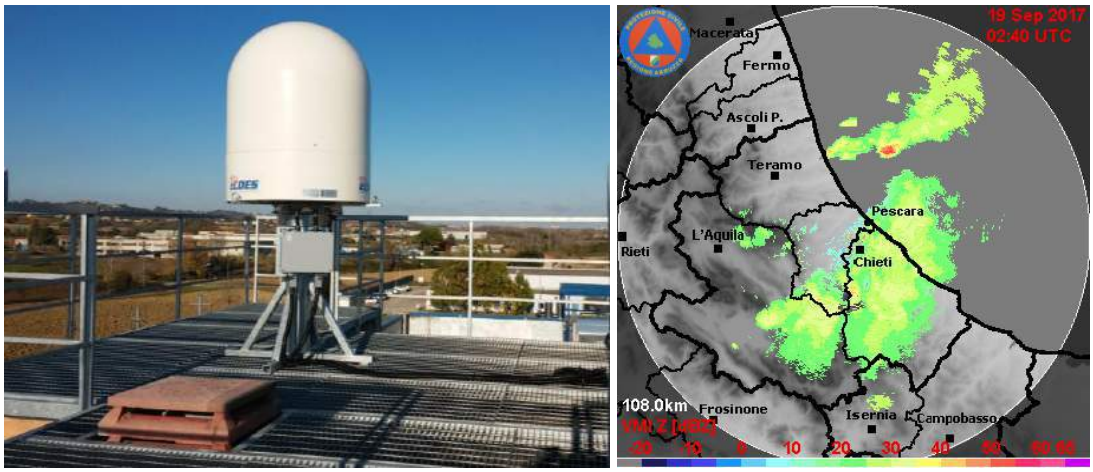


***Figure 3.5*** *Pictures of the X-band mini-radar installed in Cepagatti (left panel) and a VMI reflectivity map taken during a rainy event*

Application of weather radar data in Air Traffic Management (ATM) systems is caused by sufficiently high reliability of detection of areas with dangerous for aviation weather, especially of convective origin **(figure 3.6)**.

It is worth mentioning that convective system such as thunderstorms and related phenomena can close airports, degrade airport capacities for acceptance and departure, and hinder or stop ground operations. Convective hazards en-route lead to rerouting and diversions that result in excess operating costs and lost passenger time. Heavy precipitation, lightning and hail damage can remove aircraft from operations and result in both lost revenues and excess maintenance costs.


***Figure 3.6*** *Pictures of meteorological hazards for flight operations*

Ground based weather radar information has been recognized as necessary for the safety and regularity of international air navigation and is thus a defined standard in the service provision for operators and flight crew members. In the past weather radar products were first and foremost used in the strategic pre-flight planning by operators and flight crew members. In recent years this usage is gradually moving to an increasing use of ground-based weather radar data for in-flight re-planning, tactical use in Air Traffic Control (ATC) and even usage for aircrafts in flight.
**X-band weather radar** can be installed also in proximity of the **airport surveillance radar,** the latter, is a radar system used at airports to detect and display the position of aircraft in the airspace around airports and operates in the range of 2,7 to 2,9 GHz.

**Weather radars** use high-power, narrow "pencil beams," which scan relatively slowly in azimuth and elevation to provide accurate measurements of precipitation. By contrast, **aircraft surveillance radars** typically use much broader, fan-shaped radar beams that scan rapidly to provide the frequent target echoes necessary for reliable tracking. Different beam patterns are required for aircraft and weather surveillance. To define the three-dimensional structure of storms, weather radars employ narrow pencil beams that are scanned in azimuth and elevation. Aircraft surveillance radars use broad beams that are fan shaped in elevation. The beam is scanned in azimuth only at a high rate to provide the rapid sequence of target echoes needed to track fast-moving aircraft. **Figure 3.7** illustrates these contrasting surveillance strategies, showing a Weather Radar and an Airport Surveillance Radar both located in the immediate vicinity of an airport outside an urban area.

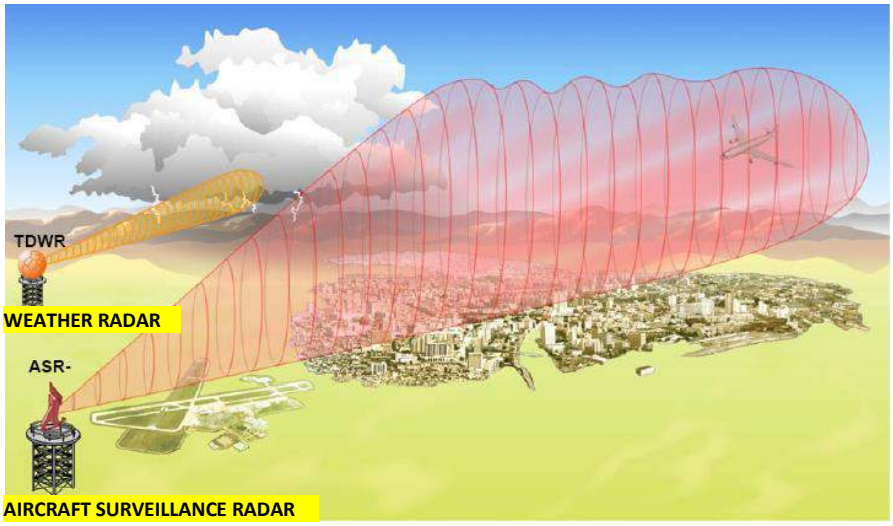


***Figure 3.7** Contrasting surveillance strategies between a Weather Radar and an Airport Surveillance Radar*

Within the feasibility study a suitable radar process chain has been designed. This chain, called **RASP-FLIGHT** (Radar Advanced Single-polarization Processing chain for FLIGHT operation) utilize as input the reflectivity giving as output some useful products against meteorological hazards for flight operations.
Some of these algorithms have been reused and adapted for AdriaMORE purposes.

### 3.3 Focus on the X-band weather radars

From the hydrologic perspective, where the domain of interest is often limited in size to a county, or a research validation site, higher frequency radars (X band) can provide rainfall products with higher spatial and temporal resolution but at a significantly lower cost. This lower cost is due to the fact that higher frequency radars can provide high spatial and temporal resolution products with much smaller antenna. The smaller size and lighter structure often allow the radars to be installed on mobile platforms (trucks, trailers), which yields flexibility in network configuration, remote deployment and a lower maintenance cost (**figure 3.8**).


***Figure 3.8*** *X-band radar installed on fixed (left) and mobile platform (right panel)*

Thus nowadays, X-band radars represent a cost-effective solution because these radars are much cheaper (in direct cost, infrastructure and maintenance costs) than traditional C-band or S-band radars. This fact has revived in the recent years the interest of the scientific and the operational communities about X-band radar; these systems are now considered a convenient solution for applications such as rainfall monitoring over a small watershed, to fill gaps in operational radar network and for improving lower atmosphere coverage, and capability to trace and track storm cells in the presence of small scale and high impact cases.

As mentioned in chapter 1, their main disadvantage is represented by the attenuation due to propagation through precipitation that determines important errors in radar rainfall estimation obtained from parameters derived from power measurements. During strong rain events we can have even a total signal loss **(figure 3.9)**.

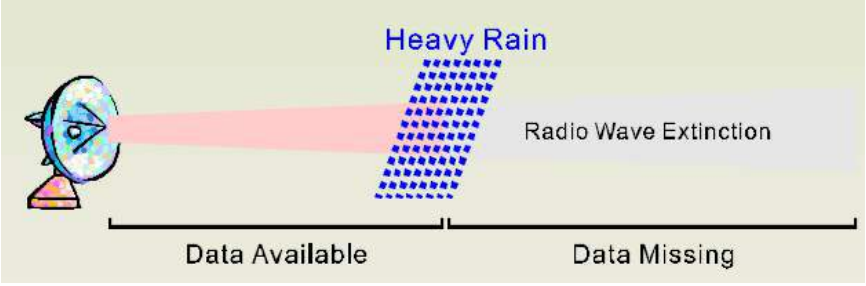


***Figure 3.9*** *The presence of heavy precipitation can lead to a complete extinction of the radar signal especially at X-band*

As an example of that issue in **figure 3.10**, we present data from the 2002 IHOP experiment that took place in Oklahoma [**Domaszczynski, 2012**]. During the experiment, collocated S-band and X-band radars operated simultaneously, which allowed for the direct comparison of radar returns and associated attenuation. Figure 3.8 illustrates that the X-band radar suffered total signal attenuation after passing over a region of extreme rainfall.
Another example of comparison is shown in **figure 3.11**, also here the attenuation undergone at X-band is well evident.
In an event of a total signal loss, successful correction for attenuation is not possible with a single-radar approach due to the lack of a valuable reference signal. This problem can only be addressed by providing additional radar information from a separate source that has not experienced total signal loss. This is where the concept of radar networks becomes useful especially in X-band.

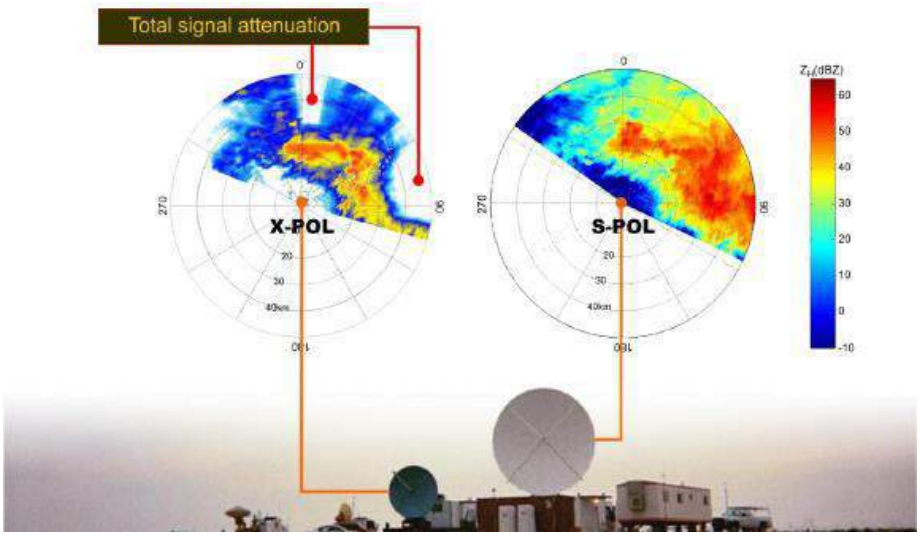


***Figure 3.10*** *Example of total signal attenuation experienced by X-band radar (left panel) as compared to a S-band radar (right panel), both images refer at the same event of heavy precipitation*

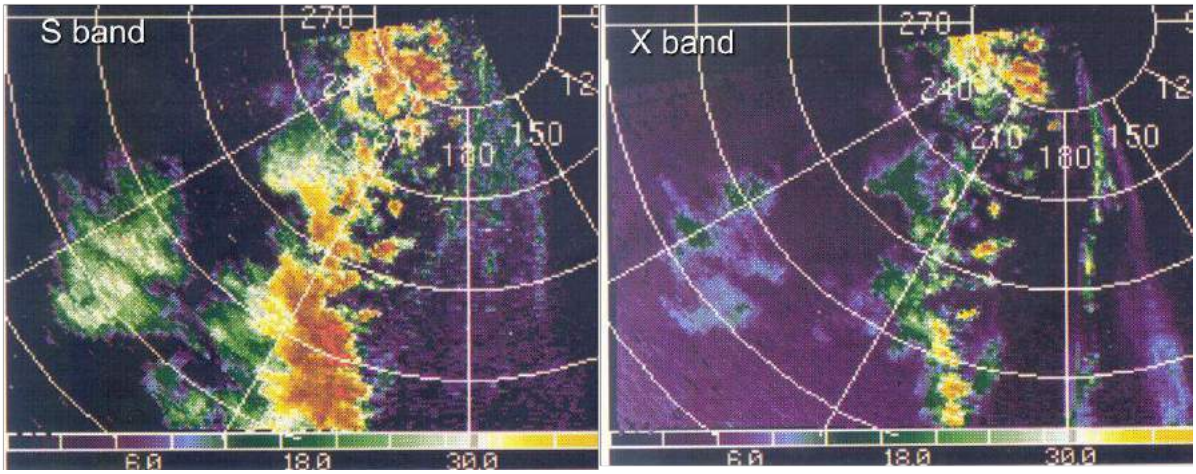


***Figure 3.11*** *Example of severe signal attenuation experienced by X-band radar (right panel) as compared to a S-band radar (left pane), both images refer at the same event of heavy precipitation*

Another example of X band signal extinction comes from the measurement campaign carried out within the AdriaRadNet project **[Picciotti, 2014]** and shown in **figure 3.12**. Comparing the measurements of the Cingoli radar with the Tortoreto ones the extinction of the signal suffered by the first radar is evident. On the contrary, in **figure 3.13** an example of extinction of the signal suffered by the Tortoreto radar is shown, due to heavy precipitation occurring in the Marche Region coast.

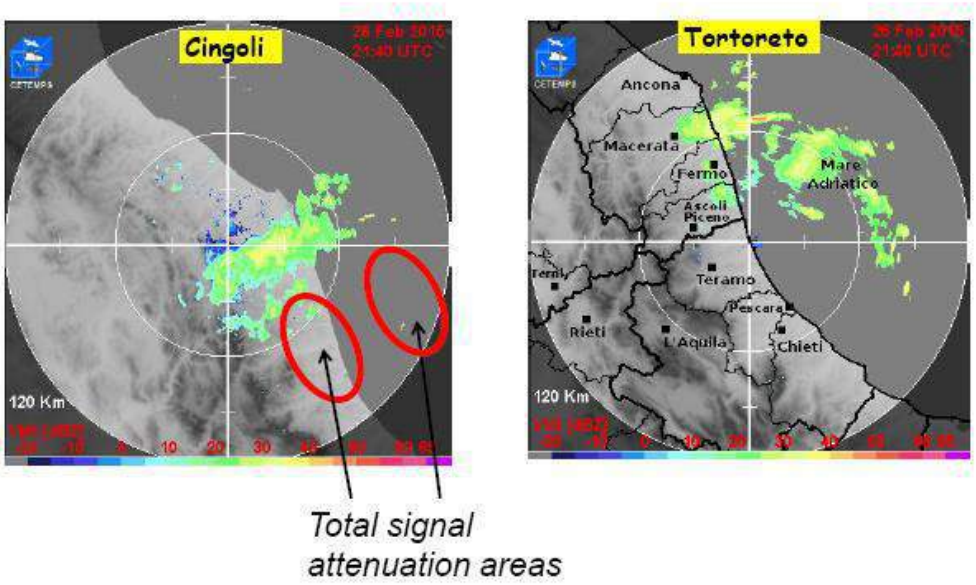


***Figure 3.12*** *Example of signal attenuation experienced by Cingoli radar (left panel) as compared to Tortoreto radar (right panel)*

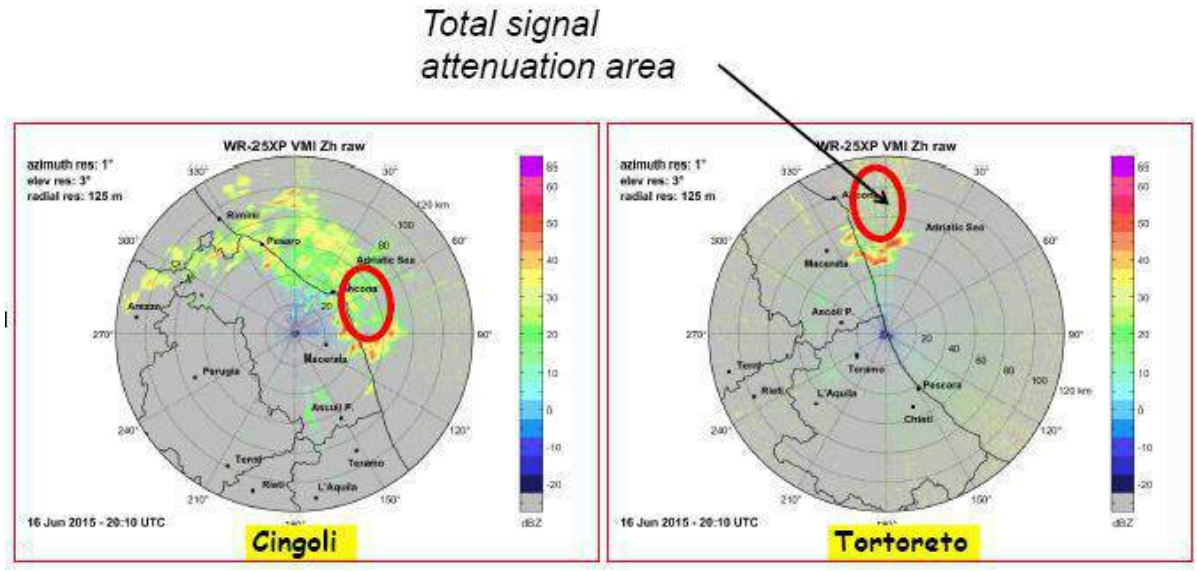


***Figure 3.13*** *Example of signal attenuation experienced by Tortoreto radar (right panel) as compared to Cingoli radar (left panel)*

As mentioned before, the importance and widespread demand for high quality rainfall information at local and global scales drives many research activities focusing on different aspects of precipitation observation and motivates a continuous search for better and more reliable precipitation estimation techniques by using network of radar. Integration of different types of radars is relevant in urban drainage in order to achieve the best combination of high resolution and long range. The potential gain could be the theoretical improvement of spatial resolution close to the X-band radar for high quality rainfall information and a better range with the S- and C-band radar. On the other hand, it is clear that the differences antenna geometry scanning strategy and wavelength poses some challenges when trying to combine different types of radar. In practice, operating a network of several radars (nodes) as a single instrument means that information from individual radars is shared in data post-processing. In this case, the quality of the final rainfall products varies depending on how many nodes are used, how radar data are merged, and what quality control steps are implemented.

In the following we give a brief description of different radar network, especially with respect to the systems operating at X-band frequencies, which have been tested during several EU-funded or National projects focused on operational systems.

In the project **ForeAlps** (Meteo-hydrological Forecast and Observations for improved water Resource management in the ALPS) [**Bertoldo, 2012**], Alcotra programme 2003 – 2007, were tested low-cost X-band microrad network in Italy.

In the project called **RHYTMME** (Risques Hydro-météorologiques en Territoires de Montagnes et Méditerranéens) [**Westrelin, 2012**] a network of 4 polarimetric X-band radars has been deployed in the south of France (**figure 3.14).**

In the project called **HYDRORAD** (Integrated advanced distributed system for hydro-meteorological monitoring and forecasting using low-cost high-performance X-band mini-radar and cellular network infrastructures) [**Picciotti, 2013**] a network of 3 polarimetric X-band radars has been deployed in the Moldova for a measurement campaign. The composite products have been successfully tested and compared against a state-of-the-art radar (X-POL) and against in situ weather stations measurements (**figure 3.15**). The project has been successfully completed and was funded by Seventh Framework Programme, FP7.

In the framework of two projects, **ResMar** (Réseau pour l'Environnement dans l'Espace Maritime) and **PROTERINA-2** (La seconde étape pour la protection contre les risques naturels: les investissements sur le territoire) under the Cross-Border Cooperation Programme Italy-France "Maritime" [**Antonini, 2017**], a radar network over the Tyrrhenian Sea has been tested (**figure 3.16**). This network includes three new X-band radar systems, installed in Tuscany region (**figure 3.17**), that cover almost all the regional coasts and two radars at C- and S- band installed in Sardinia (Monte Rasu) and Corsica (Aleria).

In the USA, the project **CASA** (Center for Collaborative Adaptive Sensing of the Atmosphere; **[Junyent, 2010]** aims to deploy an experimental network of small X-band polarimetric radars in Oklahoma as a proof of concept of a new paradigm for precipitation sensing based on low cost X-band polarimetric radar with overlapping coverage (**figure 3.18**).

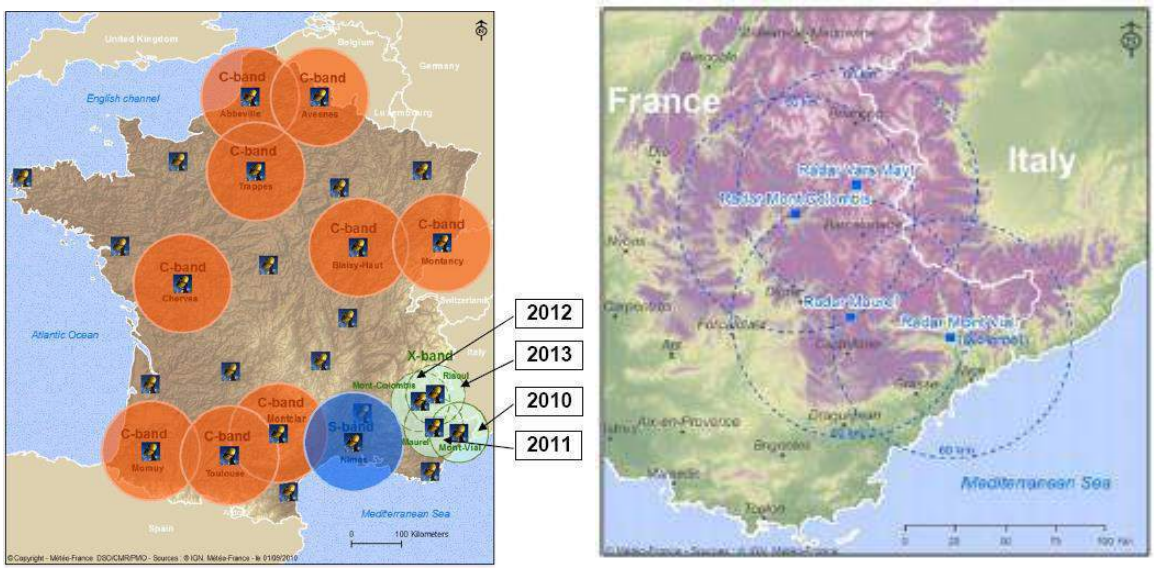


***Figure 3.14*** *The location of the four X-band radars installed within RHYTMME project (left panel) and their network coverage (right panel)*

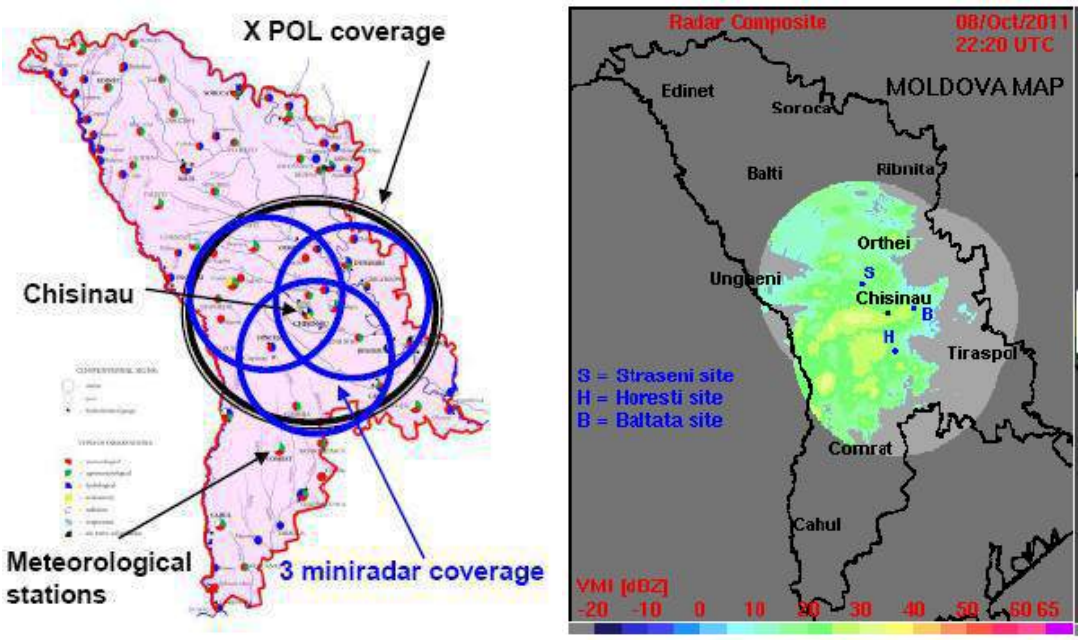


***Figure 3.15*** *Location and coverage of X-band radars network in Moldova tested in the framework of Hydrorad project (left panel) and their reflectivity composite (right panel)*

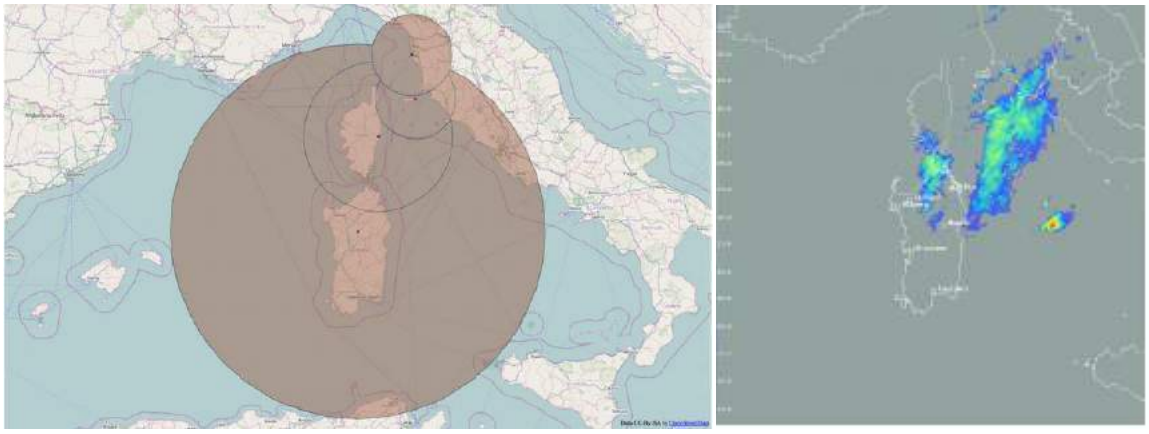

***Figure 3.16*** *The nominal overlapping area between radar systems of Tyrrhenian Sea network (left panel) and an example of composite realized in the framework of ResMar e PROTERINA-2 projects (right panel)*

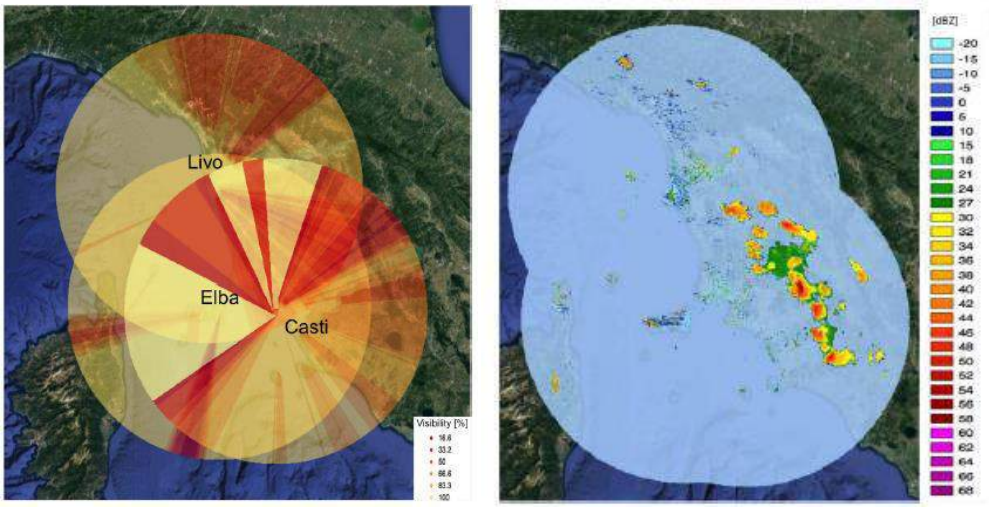


***Figure 3.17*** *Simulated visibility map of the Tuscan X-band weather radar network considering a scan elevation angle of 1.5 degree (left panel) and an example of reflectivity composite (right panel)*

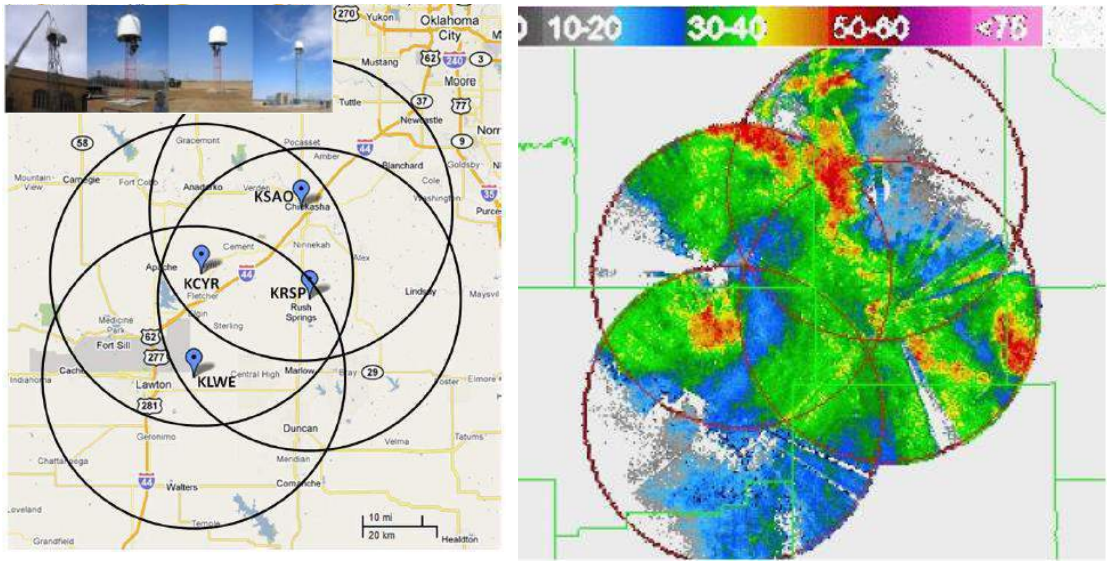


***Figure 3.18*** *Photographs, location and coverage of four CASA X-band radars installed in southwestern Oklahoma (left panel) and a reflectivity composite map (right panel)*

In Japan, the **NIED** (National Research Institute for Earth Science and Disaster Prevention) deployed an experimental network of three X-band radars (X-NET) in the Tokyo metropolitan area to improve the coverage of the regular C-band radar network of the Japan Meteorological Agency **[Maesaka, 2011]**. The NIED's results boosted Ministry of Land, Infrastructure, Transport and Tourism (MLIT) to start deploying the X-band MP radars in Japan. MLIT deployed 26 radars in four great urban areas (Tokyo, Nagoya, Kinki and Fukuoka) and local major cities (see **figure 3.19**).

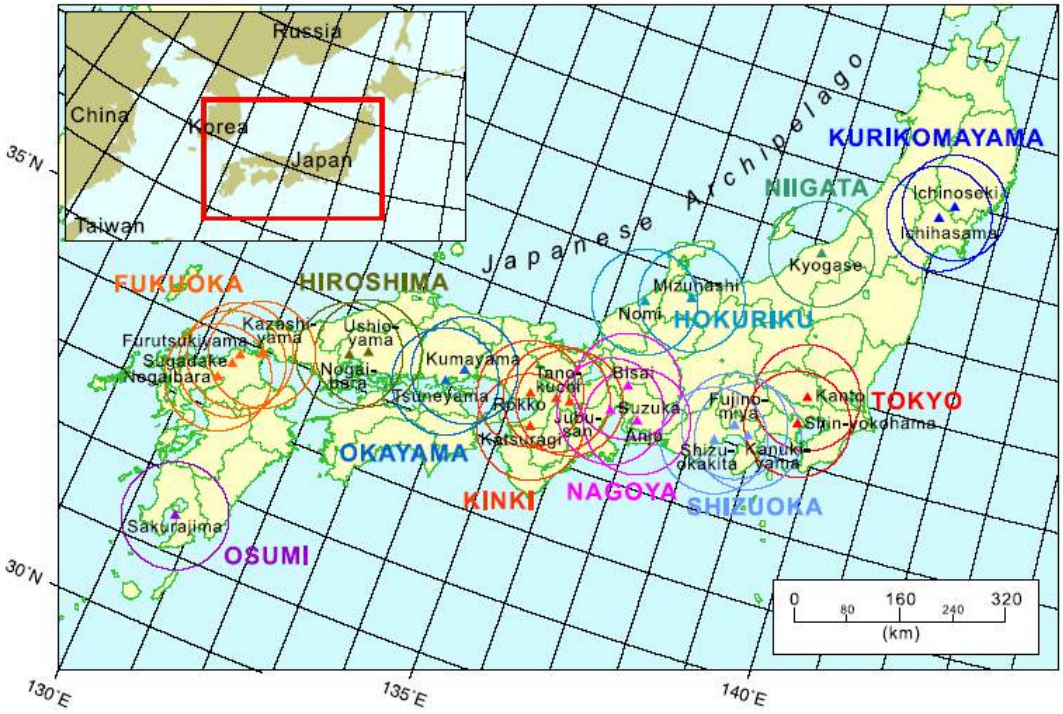


***Figure 3.19*** *Radar distributions and their coverages of MLIT X-band MP radar network. Triangles indicate the radar locations. Circles indicate the observation ranges (r = 80 km). Capital and bold letters indicate the area names. Each radar belongs to a particular area; the radar (triangle and circle) with the same color as the capital and bold letters belongs to the area*

It is worth mentioning that X-band weather radar sometimes misses precipitation echoes behind heavy rainfall by the rain attenuation. We cannot know if there is a rainfall or not in this radio wave extinction area. When the distribution of rainfall intensity is graphically drawn, this area should be shown not as "no rain" area but as unknown area where it may be rain (grey shades in the following two figures).

**Figure 3.20** shows the example Plan Position Indicators (PPIs) of the rainfall intensities estimated by this MLIT system. At the time, a heavy rain accompanied by Typhoon went through Nagoya area. Because the maximum intensity of this rain was about 100 mm/h, many radio wave extinction areas were detected (grey shades in figure 3.20).

**Figure 3.21** shows the areal composite of the estimated rainfall intensity in Nagoya area. The estimated intensities of the five radars shown in figure 3.20 were used to create this composite. It is important to highlight that the radio wave extinction area was compensated by other radars in the overlapped observation area.

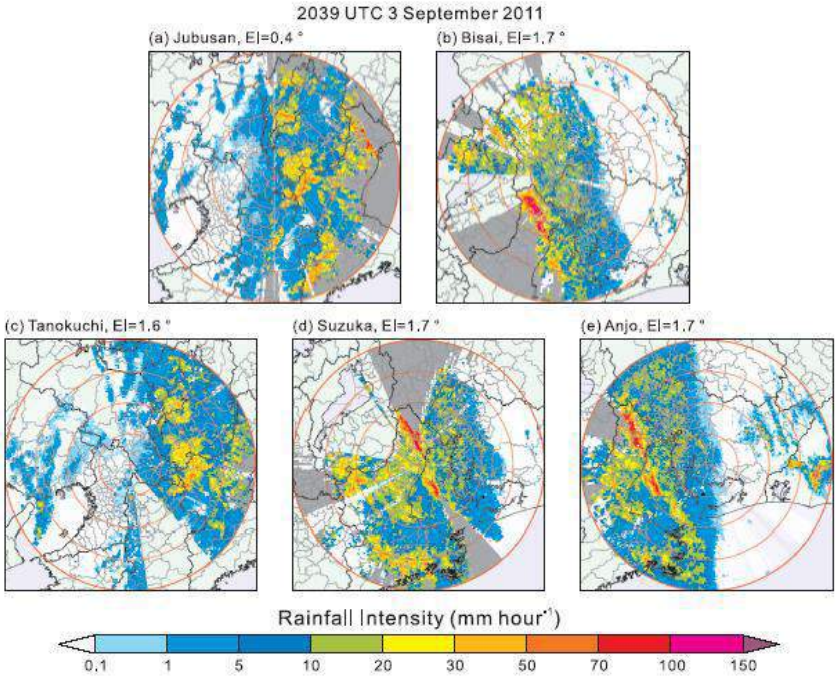


***Figure 3.20*** *PPIs of the estimated rainfall intensity in Nagoya area at 2039 UTC 3 September 2011. a) Jubusan radar, b) Bisai radar, c) Tanokuchi radar, d) Suzuka radar and e) Anjo radar. Gray shade indicates the radio wave extinction area*

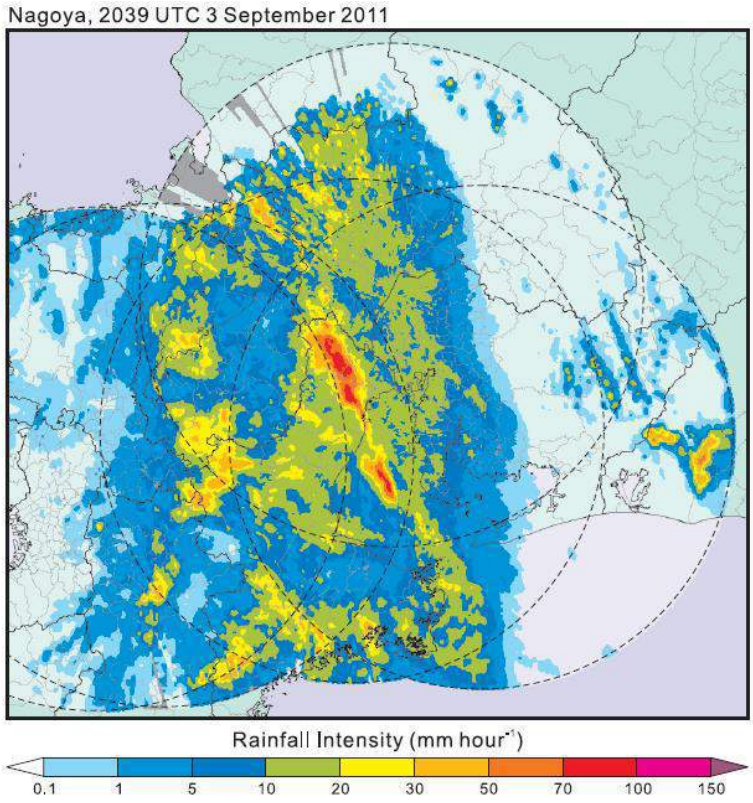


***Figure 3.21*** *Areal composite of the estimated rainfall intensity in Nagoya area at 2039 UTC 3 September 2011. Broken circles are the observation ranges of the radars used to create this composite. Gray shade indicates the radio wave extinction area.*

# 4. NETWORK OF WEATHER RADAR

## 4.1 Advantages of simultaneous observation of precipitation

As shown in the previous chapter, the simultaneous observation of precipitation by multiple radars creates new prospects to overcome signal attenuation as well as signal extinction. Besides dense radar networks allow getting better Quantitative Precipitation Estimates (QPE) than those obtained with individual radars. Not only taking the advantage of a larger coverage but improving quality of rainfall estimates in overlapping areas as well. Well-known sources of error (see section 2.5) as those associated with range can be mitigated through radar mosaics.

One of the challenges in compositing is the number of different available data products from the different radars. Requirements for compositing are: (i) radar data quality control of the single radars, using various filtering and correction algorithms and (ii) the mapping of the corrected radar data onto a uniform rectangular grid with a homogeneous data presentation with availability in near real time (**figure 4.1**).

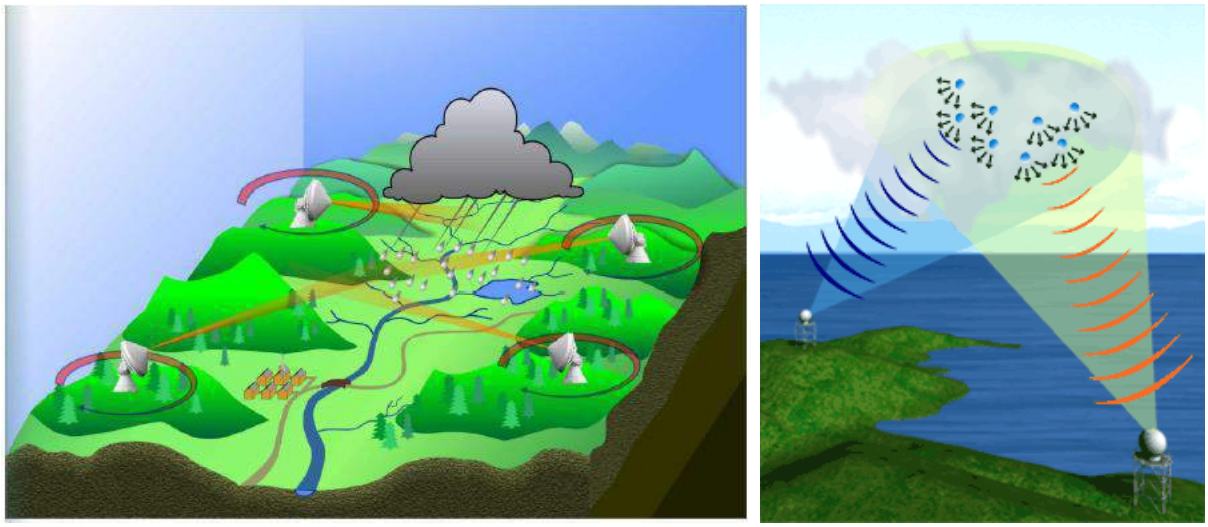

***Figure 4.1*** *Conceptual images illustrating a network of radars operated as a single instrument*

Thus, the creation of composite products from multiple radar scans offers a number of advantages compared to the contemplation of single scan data, the main advantages are:

- **Cover a larger area**
  - overcome the limited coverage of single radar sites
  - more accurate measure at farther range
- **Overlapping coverage for a given geographic area**
  - improve rain estimation due to simultaneous observation
  - inter-calibration of the network's radars
  - reduction of attenuation, ground clutter and blocking effects
- **Observation redundancy**
  - giving guarantees in case of failure of one observing system
- **Overcome total signal attenuation especially at X band**
  - have a useful measure in areas with signal extinction

The composite can be generated directly from volume data acquired during the scan from each radar or from some specific products generated by each single radar. In the first case reflectivity 3D observations from individual radars can be combines onto a unified 3D cartesian grid (**figure 4.2**) while in the latter case reflectivity 2D products from individual radars can be combines onto a unified 2D cartesian grid (**figure 4.3**).
The main differences between 3D and 2D mosaics are well described in **[Lakshmanan, 2014]**.

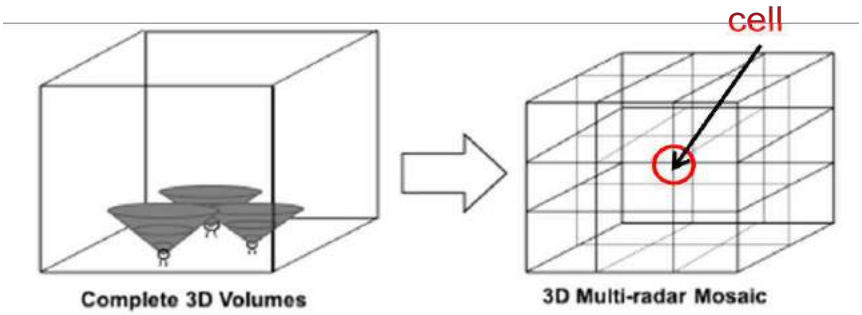


***Figure 4.2*** *Composite from volumetric measurements: each single radar 3D polar data has to combined onto a unified 3D cartesian grid*

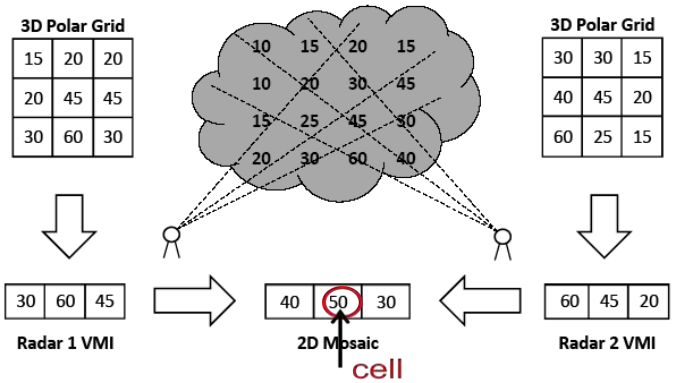


***Figure 4.3*** *Composite from specific products: each single radar 2D products data has to combined onto a unified 2D cartesian grid. In the above example is shown a composition by mean VMI product*

There are several ways to combine data from multiple radars, the most common are listed below:

1. to attribute to the common cell the mean or the maximum value of reflectivity
2. to assign to the common cell the reflectivity value of the nearest radar
3. to combine the data through a weighted average, where the weight is inversely proportional to the distance from the radar
4. to attribute to the common cell the value corresponding to the minimum PIA (Path Integrated Attenuation)
5. to attribute to the common cell the value corresponding to the minimum distance from the earth surface
6. to attribute to the common cell the value corresponding to the higher quality index

These techniques can be applied to both 3D and / or 2D mosaics, those adopted within CRAMS chain are described in the section 5.5.

### 4.2 Radar network across the world

The inherent spatial and temporal variability of precipitation makes rainfall one of the most difficult geophysical variables to measure anywhere, and yet it is one of the most important for advancing hydro-meteorological predictions. Arguably, weather radar's capability to monitor precipitation at high spatial and temporal scales has stimulated great interest and support within the hydro-meteorological community **[Hossain, 2004].**

Dense radar networks allow getting better quantitative rainfall information than those obtained with individual radars. Not only taking the advantage of a larger coverage but improving quality of rainfall estimates in overlapping areas as well. Well-known sources of error as attenuation by intense rainfall or errors associated with range can be mitigated through radar mosaics.

Several meteorological services across the world are using networks of weather surveillance radars (**figure 4.4**) which can advance precipitation monitoring with direct implications on the improvement of real-time forecasting of river floods and flash floods in ungauged basins.

The figure 4.4 shows that almost complete coverage is achieved for North and Central America, as well as Western and Central Europe. Good coverage is also available for the Middle East, South, Southeast and East Asia, and Australia. Large parts of Africa and South America remain uncovered, yet, as well as vast parts of Russia.

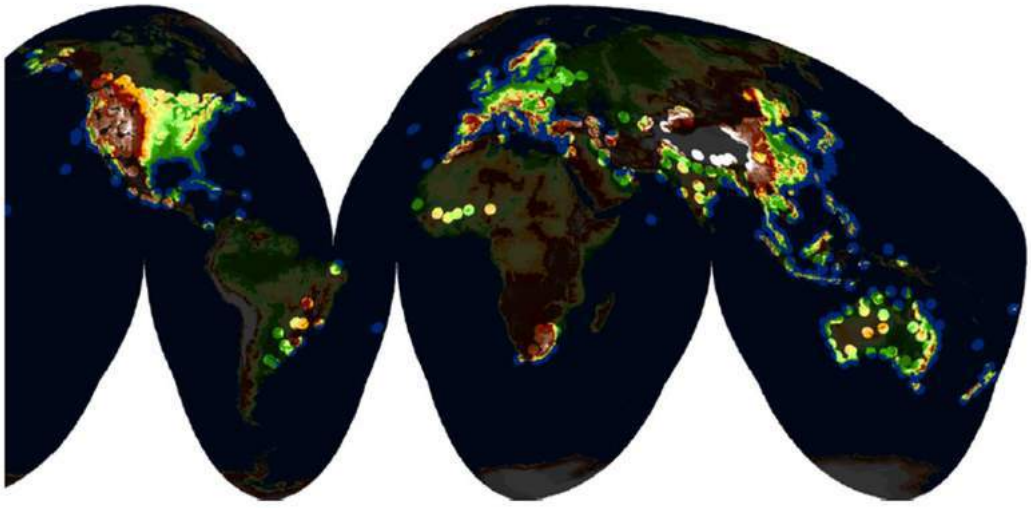

***Figure 4.4*** *Current weather radar coverage provided by national weather services, for computing the area illuminated by weather radars, we assumed a maximum range of 200 km per radar device*

The typical operating frequency of weather radars can span over many bands. For example, NEXRAD, the national weather radar network in the United States, uses S-band radars that operate at 3GHz, see in **figure 4.5** an example of composite. The Canadian national weather network utilizes radars operating at C-band (5.5 GHz), see in **figure 4.6** their installation site while the about 150 radars of China network work at C- and S-band equally distributed, S-band radar are mainly distributed in east and coastal areas in southern China while C band radar are mainly located in the northern and western parts of China. You can see in **figure 4.7** the location and an example of composite. Operating at such frequencies allows radars to provide valuable information for ranges over 200 km **[Sauvageot, 1992].**

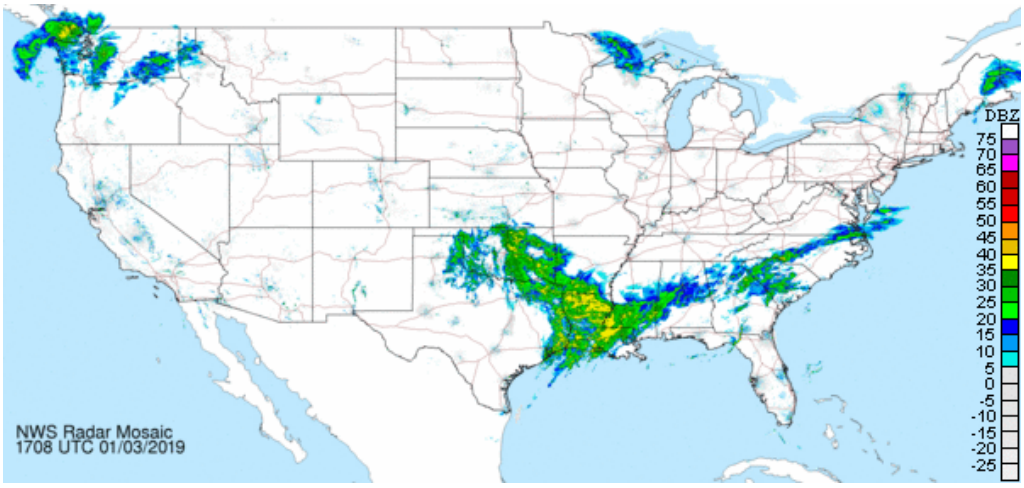


***Figure 4.5*** *Reflectivity composite images taken from the network of the 159 S-band Doppler weather radars operated by the National Weather Service (NWS) in the United States*

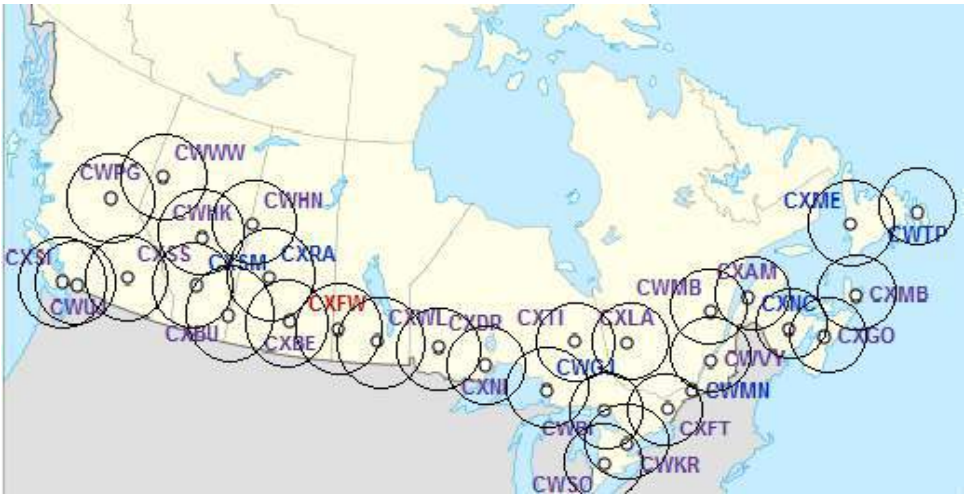


***Figure 4.6*** *The Canadian weather radar network consists of 31 weather radars spanning Canada's most populated regions. Their primary purpose is the early detection of precipitation, its motion and the threat it poses to life and property*

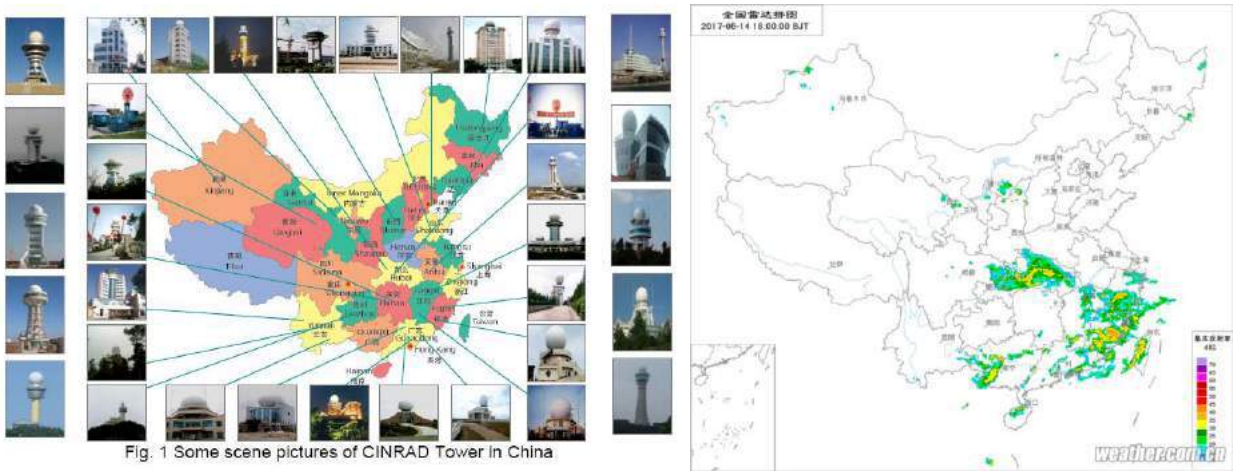


***Figure 4.7*** *Location of C- and S-band China radar network (left panel) and an example of reflectivity composite (right panel)*

In **Europe**, almost all nations have their own radar network, most of them work in C-band while a small part work in the S-band, nonetheless, many challenges remain, particularly from a hydrological perspective.

From a scientific point of view, these challenges particularly arise from the multitude of potential error sources which are typically inhomogeneous in space and time. These error sources can introduce severe bias in quantitative hydrological studies, e.g. hydrological modelling and forecasting. Hence, it requires the combination of state-of-the-art correction algorithms to make the data useful for hydrological applications. Although many algorithms have been published in peer-reviewed journals, the level of documentation often is not sufficient for a straightforward reimplementation.

From a technical point of view, other barriers exist that prevent hydrologists (and other users) from working with weather radar data; the first being a multitude of different file formats for data storage and exchange. Although the OPERA project (http://www.eumetnet.eu/opera) has taken steps towards harmonizing the data exchange in Europe, different dialects still exist in addition to a large variety of legacy formats. Many radar data come in complex, and sometimes proprietary binary formats which require a lot of expertise in handling, or even the use of commercial software products. Other technical barriers are a lack of experience in working with polar coordinates and in georeferencing three-dimensional scan data, as well as the lack of out-of-the-box spatial visualisation tools outside GIS working environments.

It is worth mentioning that OPERA Project aims to harmonize European radar data and products, through the provision of a European platform wherein expertise on operationally-oriented weather radar issues is exchanged. OPERA manages, develops, collects radar volume, from each European available radar system, and produces quality-controlled radar products composite **(figure 4.8).**

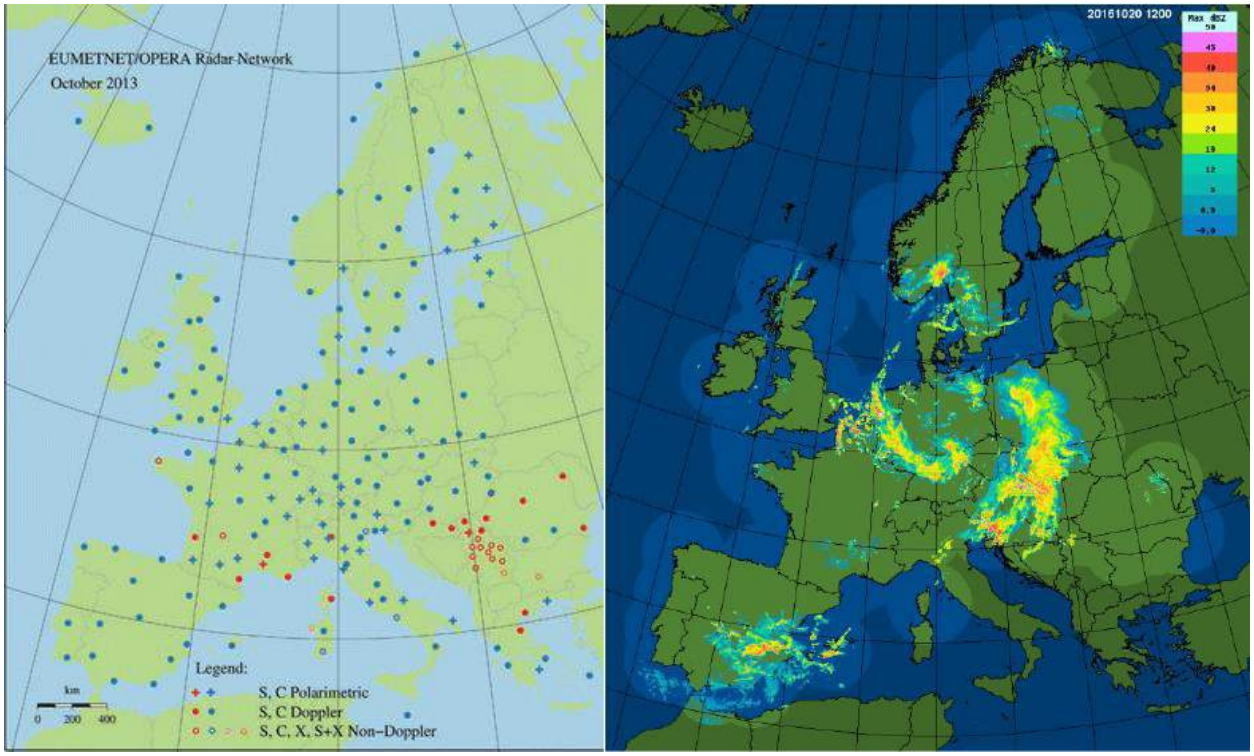


***Figure 4.8*** *Radar network of OPERA (left panel) and an example of reflectivity composite (right panel)*

### 4.3 Italian and Croatian network

The **Croatian operational radar network** is currently constituted by three S-band systems, installed inland (**figure 4.9, left panel**), leaving the Adriatic coastline basically uncovered. In the next year thanks to the METMONIC project, started on November 2017, the existing three S-band weather radars are going to be replaced with new weather radars and three new radars are going to be placed along the Adriatic coast. All six radar will be at C-band with doppler and dual polarization capability (**figure 4.9, right panel**).

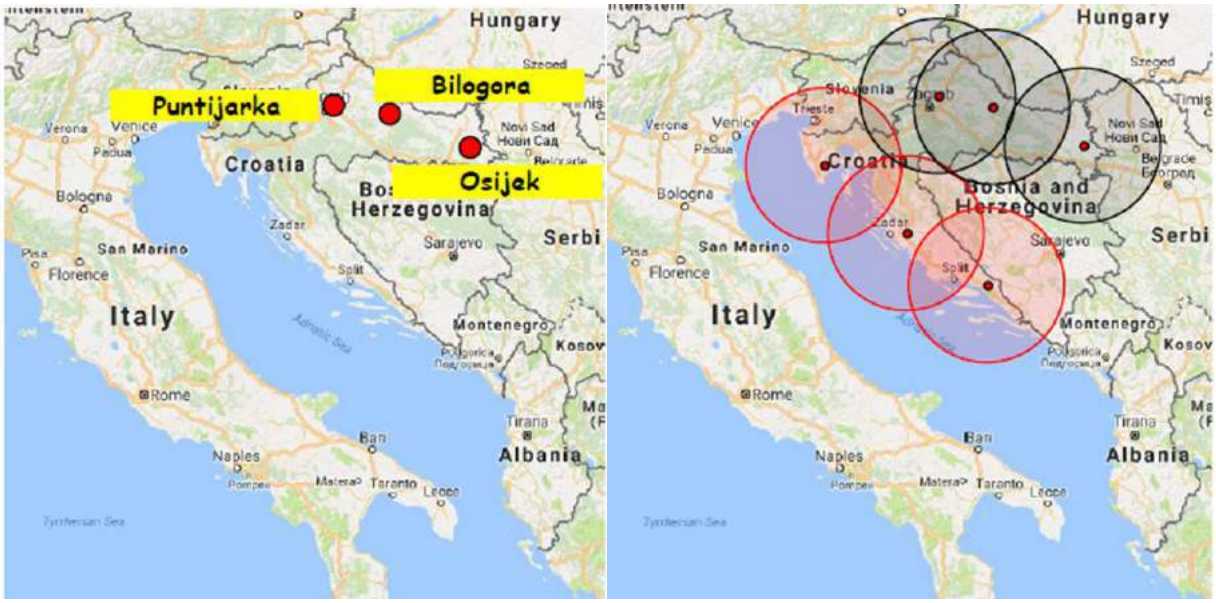


***Figure 4.9*** *Currently Croatian radar network sites (left panel) and those planned in the framework of METMONIC project (right panel). Black circles indicate the coverage of the radar to be replace while red circles the coverage of the new installations along the Adriatic coastline near Pula, Zadar and Vis*

It is worth mentioning that the purpose of the strategic project METMONIC (Modernization of Croatian Meteorological Measurements Network) is the establishment of a modern and high-quality system of automatic surface meteorological stations, meteorological-oceanographic buoys and remote measurement systems, including meteorological radars. In total, 450 modern automatic meteorological systems will provide traceable, reliable, high quality and timely information on the state of the atmosphere and the sea throughout the territory of the Republic of Croatia.

The project, co-financed by the European Regional Development Fund (ERDF), is managed by the the Meteorological and Hydrological Service of Croatia (DHMZ) which is PP2 of AdriaMORE project.

Ultimately METMONIC project will significantly contribute to:

- improvement of early-warnings to severe weather and natural disasters;
- development of human, technical and scientific capacities;
- international exchange of information
- developing of meteorological products tailored to the needs of users
- modernization of all components of the DHMZ observation system, easier access to its archives and databases and accompanying infrastructure.

Find in the following more details about the currently Croatian radar network.
As mentioned before, it consists of three long range S-band radars, shown in **figure 4.10**, installed in the continental part of Croatia. First one is near Zagreb, (Puntijarka radar), the second one is near Virovitica, (Bilogora radar) and third one is near Osijek (Osijek radar). All three are manufactured by EEC and were modernized to the SIGMET Radar Signal Processor with IRIS software.
The technical specifications are practically the same for all three radars, they are working in the same volume scan task schedule. It is starting every 15 minutes with elevation 0.5° and last elevation is 26.4°. Approximate time for volume scan is 5 minutes. Then the data are processed with IRIS software. These radars are managed by the DHMZ partner of AdriaMORE project.


***Figure 4.10*** *Pictures of the three S-band radars operative in Croatian territory*

The Croatian network is completed by Dubrovnik radar (see section 3.1) currently under maintenance due to hardware problems, it is managed by the Dubrovnik Neretva Region, partner of the AdriaMORE project. In the **table 4.1** the technical specifications of these radars are resumed.

| Features | Unit | Puntijarka | Bilogora | Osijek | Dubrovnik |
|---|---|---|---|---|---|
| Model | --- | DWSR 74 S | DWSR 88 S | DWSR 74 S | WR-10X |
| Data of installation | [year] | 1982 | 1993 | 1982 | 2014 |
| Latitude | [deg] | 45.907 | 45.883 | 45.502 | 42,635 |
| Longitude | [deg] | 15.968 | 17.200 | 18.561 | 18,139 |
| Height (over sea level) | [m] | 1024 | 258 | 105 | 302 |
| Polarization capability | --- | NO | NO | NO | NO |
| Band (frequency) | [GHz] | S (2,8) | S (2,8) | S (2,8) | X (9,41) |
| Peak Power | [kW] | 550 | 550 | 550 | 10 |
| Antenna Gain | [dB] | 37 | 37 | 37 | 35 |
| Maximum Range | [km] | 240 | 240 | 240 | 108 |
| Gate resolution | [m] | 1000 | 1000 | 1000 | 450 |
| Temporal resolution | [min] | 15 | 15 | 15 | 10 |
| Beamwidth | [deg] | 2,1 | 2,1 | 2,1 | 3,0 |

***Table 4.1*** *Technical specifications of the installed radars in Croatia*

The **Italian operational radar network [Vulpiani, 2008]** is currently composed by 22 systems, **(figure 4.11)** mostly at C-band and with dual-polarization capability, managed by a federation of national and regional bodies including the Department of Civil Protection (DPC), the Air Force, the regional weather services, and the National Aviation Authority (ENAV).
The DPC collects and processes the radar volume provided by every network partner to generate and distribute national-level products. The rainfall products are mainly used for monitoring purposes within the national early-warning system. Consequently, specific activities are carried out to assess the related quality.
The applied processing chain attempts to deal with the main error sources by associating them a quality indicator, i.e. contamination by non-weather returns, attenuation, vertical variability of precipitation, beam broadening and drop size distribution variability affecting the inversion technique.
The main national-level composite products generated in real time by DPC and disseminated at national and regional level are:
- the vertical maximum intensity (VMI, dBZ)
- the constant altitude plan position indicator (CAPPI, dBZ)
- the surface rain intensity (SRI, mm/h)
- the accumulated surface rain total (SRT, mm) at various hours.

All products are obtained over a grid of 1400×1400 km$^2$ with spatial resolution of 1 km and temporal resolution of 10 minutes.
In the next year additional radar installations are planned in the centre and south of Italy in areas not yet well covered.


***Figure 4.11*** *Location of the radar belonging to the Italian Network*

Two examples of composite for Croatian (left panel) and Italian radar network (right panel) are shown in **figures 4.12 and 4.13**, both images are taken on December 14, 2018 at 03:00 and 13:00 UTC respectively.

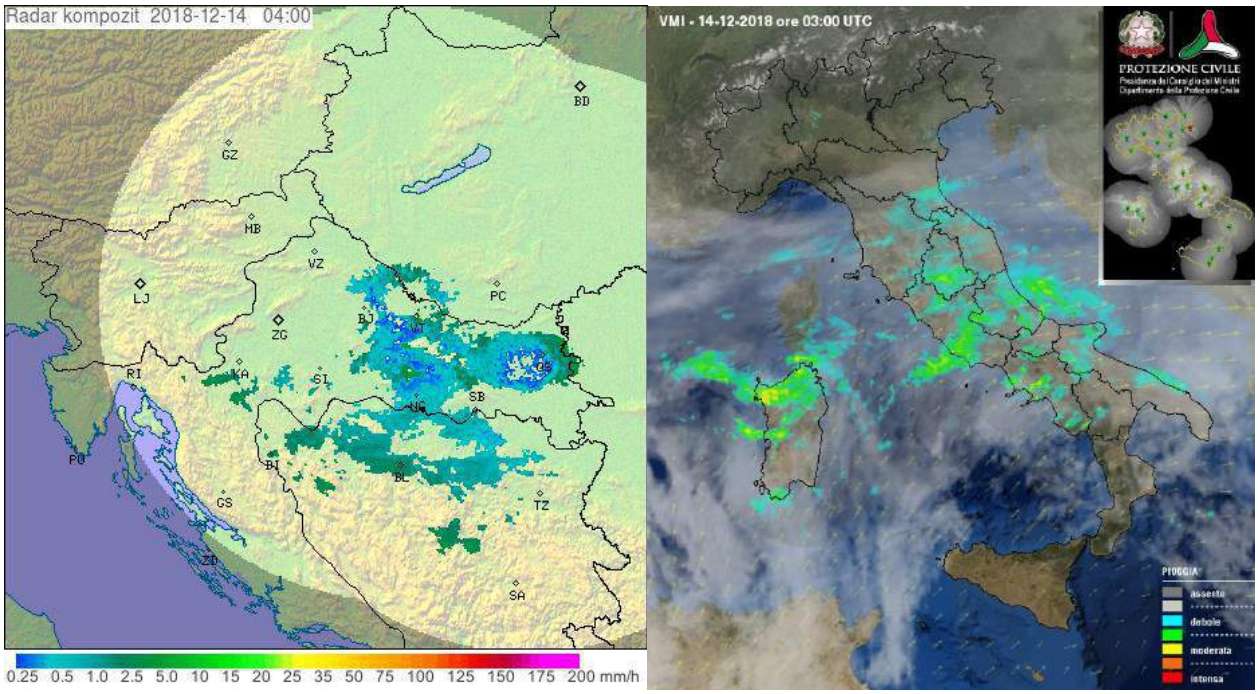


***Figure 4.12*** *Examples of composite for Croatian (rain, left panel) and Italian radar network (reflectivity, right panel) taken on December 14, 2018 at 03:00 UTC*

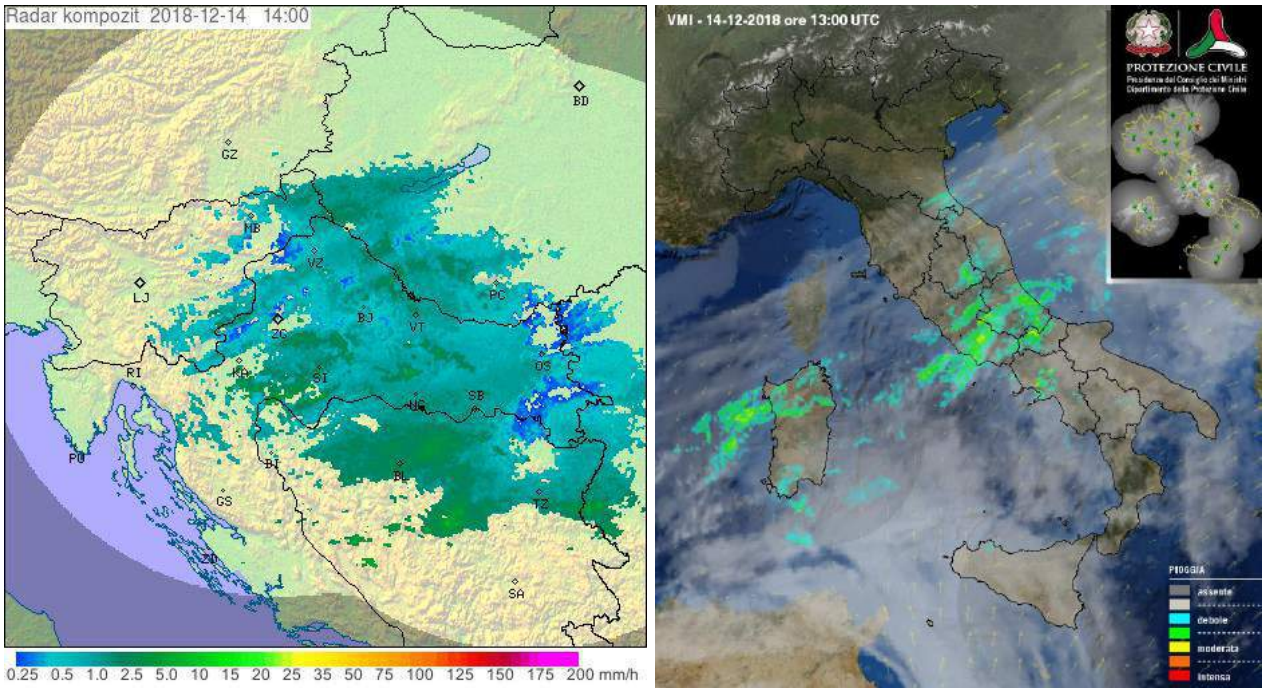


***Figure 4.13*** *Examples of composite for Croatian (rain, left panel) and Italian radar network (reflectivity, right panel) taken on December 14, 2018 at 13:00 UTC*

### 4.4 Heterogeneous radar network in the Abruzzo Region

In this section the Abruzzo radar network is described in detail since its data will be widely used in the next chapter to test the CRAMPS chain developed.

In the Central Italy area floods, even in the form of flash floods, represent a recurrent problem, especially during the fall season. The damages associated to these events are very significant both in terms of human and social costs and losses of unique monuments and cultural heritage.

The hydrological risks of Abruzzo Region, in the centre of Italy, are further enhanced by its complex orography, which is characterized by high mountainous, relatively small catchments, river basins and Adriatic Sea (**figure 4.14 left panel**). Its climatology is such that there is a predominance of low-to-moderate rainfall, having stratiform nature with high temporal persistence. Embedded convective rain may be also present mainly due to orographic effects.

In such conditions, rainfall monitoring must be performed by exploiting all sources of data: rain gauge network, satellite radiometers and ground-based weather radars. Each source is needed to have a detailed picture of the rain field at ground with a fairly accurate spatial texture and resolution.

Functional Centre of Abruzzo Region (CFA) is part of Civil Protection Regional System with functions of forecast, monitoring and warning regarding meteorological, hydrological, hydraulic and wildfire risk. It is the regional meteorological service for Abruzzo and includes the institutional duties of the daily operational meteorological surveillance, for example the emission of weather-hydrological alert bulletins (**figure 4.14 right panel**). For its activities, CFA uses data in real time from the hydro-meteorological stations and radar network located in the Abruzzo territory. The Centre of Excellence (CETEMPS) of the University of L'Aquila is a joint effort of the Dept. of Physics and the Dept. of Electrical Engineering, funded by the Ministry of Education and University of Italy starting from 2001. The research activity concerns mainly remote sensing, atmospheric physics, meteorology and hydrology. It supports the CFA in the daily operational meteorological forecast and surveillance.

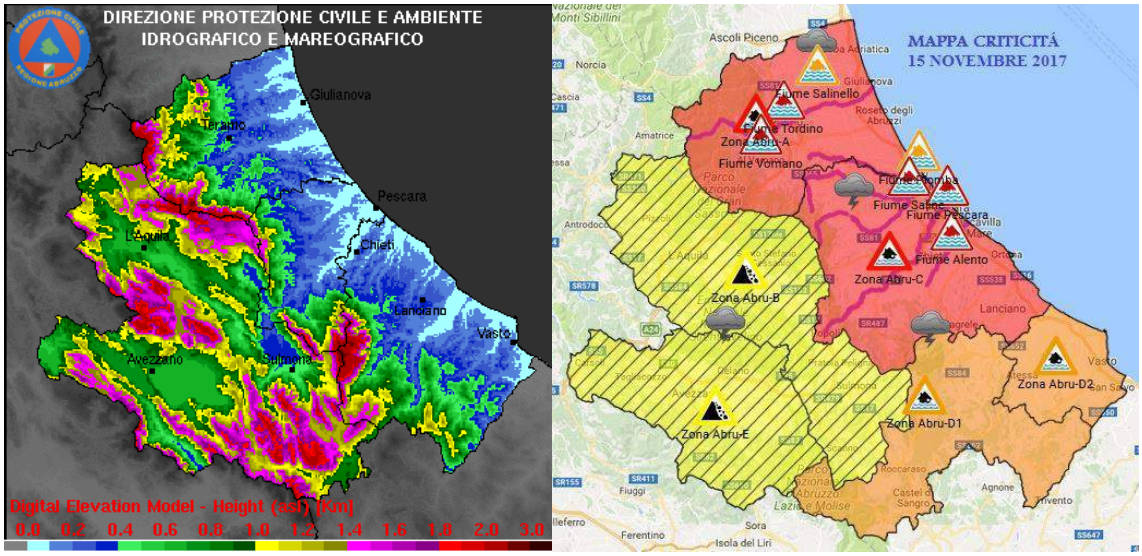


***Figure 4.14*** *The complex orography of Abruzzo region (left panel) and the warning map issued on November 15, 2017 by CFA with maximum alert for the areas falling within the Pescara river basin (right panel)*

The Abruzzo radar network design was driven by the needs of the CFA for the detection and warning of severe weather and related hydrological risks, which requires high redundancy, availability and accuracy of radar data.

Operating a meteorological radar is generally a challenging task when in presence of a significant beam blockage as in complex orography **[Marzano, 2004].** Apart from enhanced ground clutter, mountainous obstructions of the radar beam can significantly reduce the radar visibility and, thus, its monitoring capabilities.

As known, any fruitful usage of network radar data either for quantitative precipitation estimation or just for operational monitoring, must deal with a careful check of data quality. This aspect is particularly critical for networks with heterogeneity radar having different system features, moreover complex orographic environment introduces additional difficulties in the matching of observations of the same phenomenon from different radars during the mosaicking. In this respect, a dedicated algorithmic chain, able to process raw data, enhance their quality, extract from them accurate and useful hydro-meteorological products have been developed and customized for the different installations.

The Abruzzo radar network is constituted by four radars located at the sites of Monte Midia, Cepagatti, Tortoreto and L'Aquila respectively. The main criteria taken into account to support the choice of the sites were: 1) identification of priority coverage areas for population centres based on the expected paths of storms; 2) environmental impacts, terrain features and local obstructions; 3) electromagnetic interference; 4) financial resources and costs; 5) communications to the site, namely, accessible roads, electrical lines, phone lines enabled for data connections, water supply, etc.

During 2006 a new project for installing a C-band weather radar in Central Italy, at Monte Midia site, has been successfully accomplished. The site is at the border between the Abruzzo and Lazio regions in Central Italy. Monte Midia top height is at 1710 meter and covering most Central Italy, including the Abruzzo inland and the urban area of Rome. The project, sponsored by the Italian Department of Civil Protection (DPC), has been a synergic work, coordinated by the CETEMPS and including both regional authorities (CFA) and Italian company (Telespazio) **[Marzano, 2012]**. Monte Midia radar is part of the Italian operational weather radar network described in section 4.3.

As described in the chapter 3, in the framework of AdriaRadNet and CapRadNet projects and spin-off activities of HYDRORAD project three new X-band radar systems have been installed in Abruzzo Region. One X-band radar has been installed in 2012 at L'Aquila, another in 2014 at Tortoreto and the third one at Cepagatti five km far from Pescara airport in 2016. These systems cover almost all the regional coasts and partially overlap and complement the existing national radar network, their choice derived from a balance between the available economic and financial resources of the related projects and the need for qualitatively valuable observations, related to the CFA activities for civil protection purposes.

All these four systems are jointly operated by the CFA and CETEMPS.

Moreover, in the south part of Abruzzo region, a dual-polarization C-band radar, located in Tufillo, has been installed and managed by the DPC. The Tufillo radar is operative since 2008 and is part of the Italian operational weather radar network described in section 4.3.

Some general technical specifications of all radar systems installed in Abruzzo Region are shown in **table 4.2** while their location and pictures are given in **figure 4.15.**

| Features | Unit | M. Midia (MM) | Tortoreto (TO) | Cepagatti (CE) | L'Aquila (AQ) | Tufillo (TU) |
|---|---|---|---|---|---|---|
| Model | --- | DWSR-93C | WR-25XP | WR-10X | WR-25XP | METEOR 660C |
| Data of installation | [year] | 2006 | 2014 | 2016 | 2012 | 2008 |
| Latitude | [deg] | 42,06 | 42,78 | 42,40 | 42,37 | 41,94 |
| Longitude | [deg] | 13,18 | 13,94 | 14,14 | 13,35 | 14,25 |
| Height (over sea level) | [m] | 1710 | 10 | 50 | 665 | 692 |
| Polarization capability | --- | NO | YES | NO | YES | YES |
| Band (frequency) | [GHz] | C (5,57) | X (9,41) | X (9,41) | X (9,41) | C (5,60) |
| Peak Power | [kW] | 250 | 25 | 10 | 25 | 500 |
| Antenna Gain | [dB] | 40,5 | 35 | 35 | 35 | 45 |
| Maximum Range | [km] | 120 | 120 | 108 | 60 | 175 |
| Gate resolution | [m] | 125 | 125 | 450 | 125 | 150 |
| Temporal resolution | [min] | 10 | 10 | 10 | 10 | 10 |
| Beamwidth | [deg] | 1,6 | 3,0 | 3,0 | 3,0 | 1,0 |

***Table 4.2*** *Technical specifications of the installed radars in Abruzzo Region*

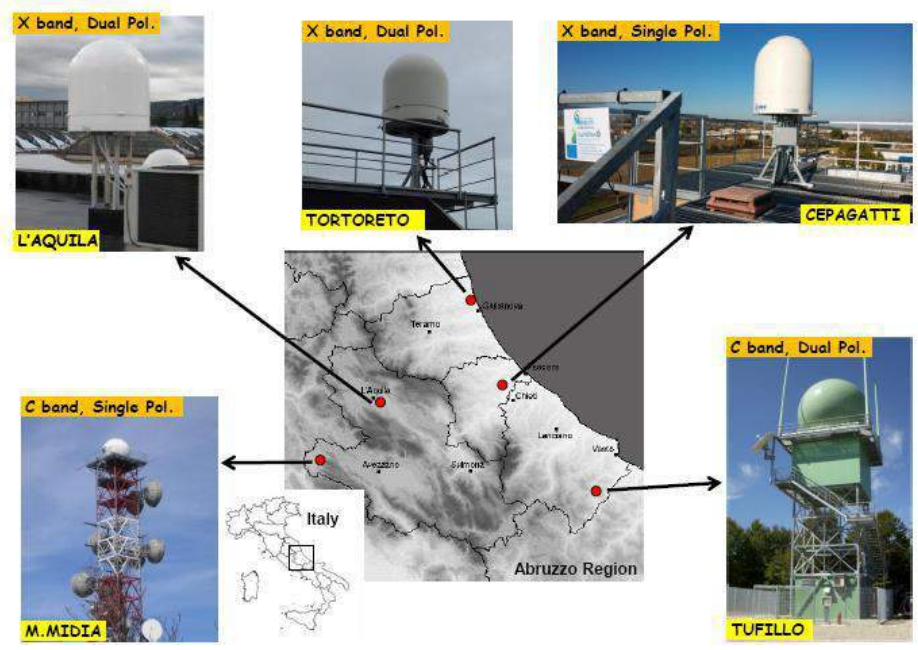


***Figure 4.15*** *Location and pictures of the radars installed in Abruzzo Region in the center of Italy*

Summing up, the radar coverage of the Abruzzo Region is currently ensured by:
- a single polarization band C radar, located in Monte Midia near Tagliacozzo (AQ);
- a double polarization band C radar, located at Il Monte near Tufillo (CH);
- a double polarization band X radar, located in Tortoreto (TE);
- a double polarization X-band radar, located in L'Aquila (AQ);
- a single polarization X-band radar, located at Cepagatti (PE).

# 5. DESCRIPTION OF THE CRAMS CHAIN

The potential of weather radar observations for hydrological and meteorological research and applications is undisputed, particularly with increasing world-wide radar coverage. However, some barriers prevent the use of weather radar data. These barriers are of both scientific and technical nature. The former refers to inherent measurement errors and artefacts, the latter to aspects such as reading specific data formats, geo-referencing, mosaicking and visualisation.

This chapter describes the block diagram of the data processing algorithm for radar network, called **CRAMS** (Cetemps Radar Advanced Mosaic Software), developed in the framework of the AdriaMORE project and adopted for the creation of composite products. The general scheme of the CRAMS is shown in **figure 5.1**, it is designed to provide the tools required for building complete radar processing chains.

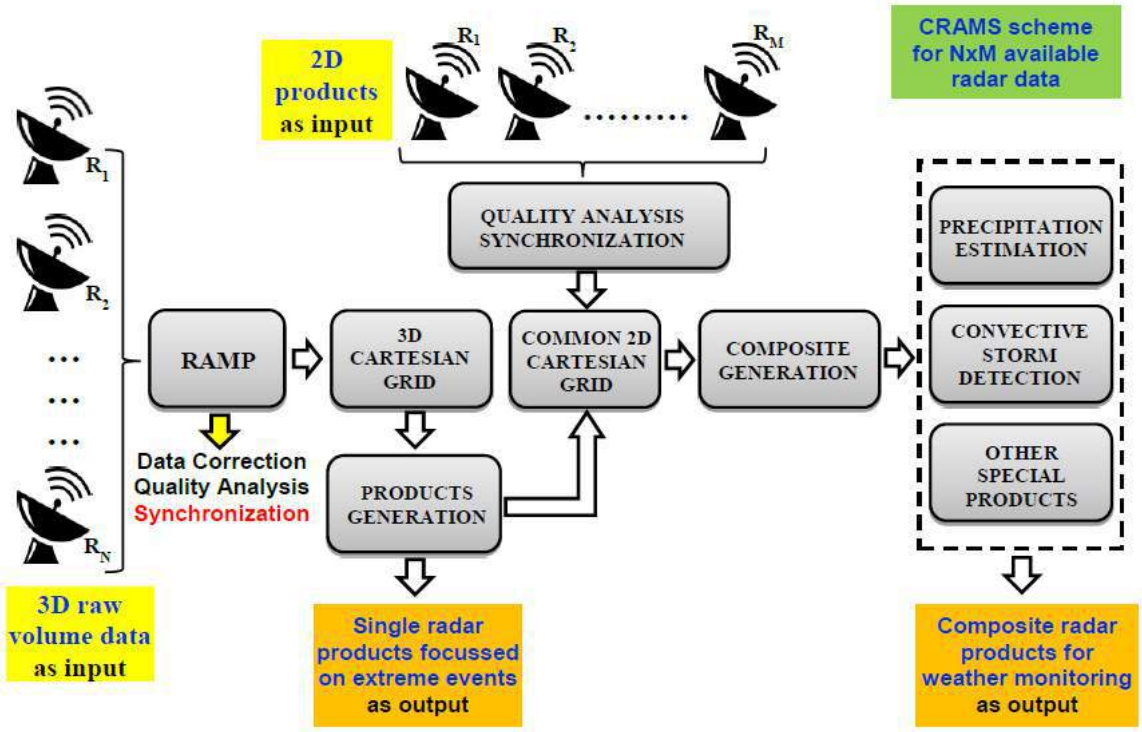


***Figure 5.1*** *Block diagram of the radar data processing and mosaicking algorithm (CRAMS)*

As seen in the section 4.1, starting from the measurements of several radars, the composite can be generated with:

a) **3D Mosaic**, that is directly from the volumes data acquired during the scanning of each radar (usually with 3D polar format);
b) **2D Mosaic**, that is starting from some specific products generated by each single radar (usually with two-dimensional format) such as VMI, SRI, SRT and other useful products.

Due to incorporate 2D products as input (for radar for which volumetric data is not available), it was decided to utilize the 2D mosaic scheme, adapting all available radar products in a common two-dimensional Cartesian grid. This is the scheme referred in figure 5.1.

It is worth mentioning that 2D mosaic is the simplest compromise, to reduce the computational complexity and the data rate although 2D products lack the height information which is critical for severe weather forecasting. This is the approach suggested by **[Charba, 2005]** and carried by the U.S. National Weather Service to create mosaics operationally at 2 km resolution.

The general scheme shown in figure 5.1 can be applied to any radar network configuration.
Given the availability of data and for project purpose, in the following it is applied to the Abruzzo Region Network as well as Croatian radar network.
See in **figures 5.2a and 5.2b** how the general scheme of figure 5.1 has been adapted to the Abruzzo and Croatian radar network.
As regards **Abruzzo network**, in an operational configuration the implemented mosaicking software can takes as input a complete volume scan from L'Aquila (AQ), Monte Midia (MM), Cepagatti (CE) and Tortoreto (TO) radars and some 2D product from Tufillo (TU) radar (all routinely collected every 10 minutes with synchronised start time).

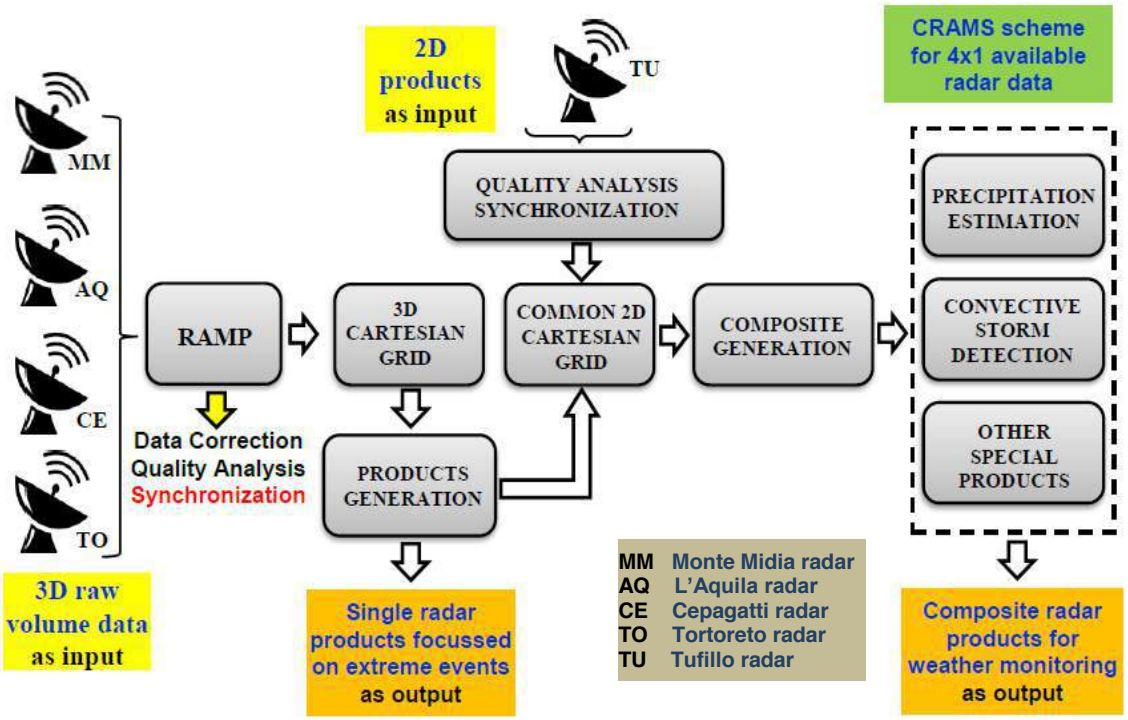


***Figure 5.2a*** *Block diagram of the radar data processing and mosaicking algorithm (CRAMS) as applied to the Abruzzo Region radar network*

For Abruzzo network preliminary results of CRAMS application were shown at the ERAD (European Conference on Radar in Meteorology and Hydrology) conference, held in Ede, Holland in July 2018. Every two years, ERAD promote the exchange of knowledge among students, researchers, engineers, radar operators and end users of meteorological radar, as well as providing a platform for transferring knowledge from research to operational use (and vice versa) of weather radar **[Picciotti, 2018]**.

As regard **Croatian network**, in an operational configuration the implemented mosaicking software can takes as input a complete volume scan from Bilogora (BI), Osijek (OS) and Puntijarka (PU) radars (routinely collected every 15 minutes with synchronised start time).

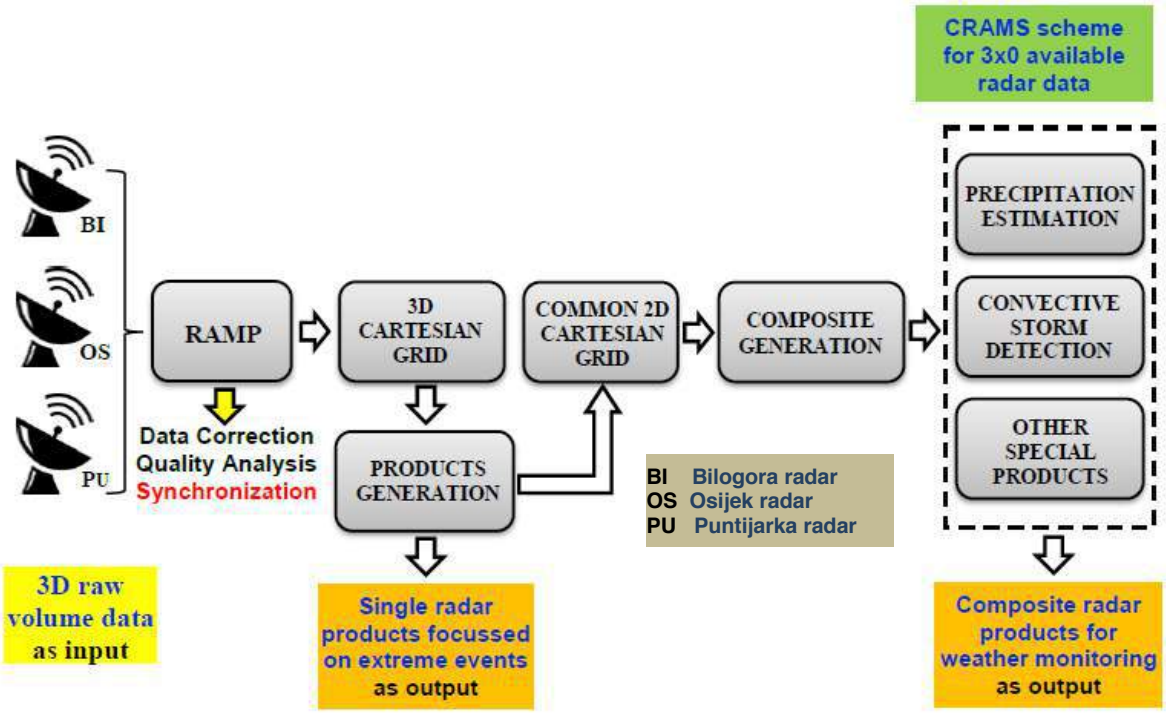


***Figure 5.2b*** *Block diagram of the radar data processing and mosaicking algorithm (CRAMS) as applied to the Croatian radar network*

In the next sections the CRAMS structure is analysed in detail in every single module, referring, for simplicity of treatment and to show examples of application, to the general scheme "adapted" for the Abruzzo region and Croatian radar network.

**Annex 1** shows the functions that characterize the CRAMS scheme in the form of pseudocode. This is a high-level informal description of the operating principles of algorithms that uses the structural conventions of a normal programming language, but is intended for human reading rather than automatic reading. The pseudocode generally omits the essential details for understanding the algorithm machine, such as variable declarations, system-specific code and some subroutines, and is enriched with details of natural language description, where convenient, or with a compact mathematical notation.

CRAMS chain has been developed in Python language (http://python.org), this is an open source, high level interpreted language with an extensive built-in standard library. It has a clear syntax, is well documented and easy to learn. Using Python also allows embedding lower-level programming languages such as C/C++ or FORTRAN. This option can be used to include external code, but also to optimise the performance of selected functions.

Finally, we emphasize that measurements made by weather radars contain a tremendous amount of information, yet considerable effort must be made to extract out scientifically and operationally meaningful products.

### 5.1 Correction, characterization of data quality and synchronization

The RAMP module is fully described in the **deliverable 3.2.2**, anyway for reader convenience a summary of its functionality is given in this section.

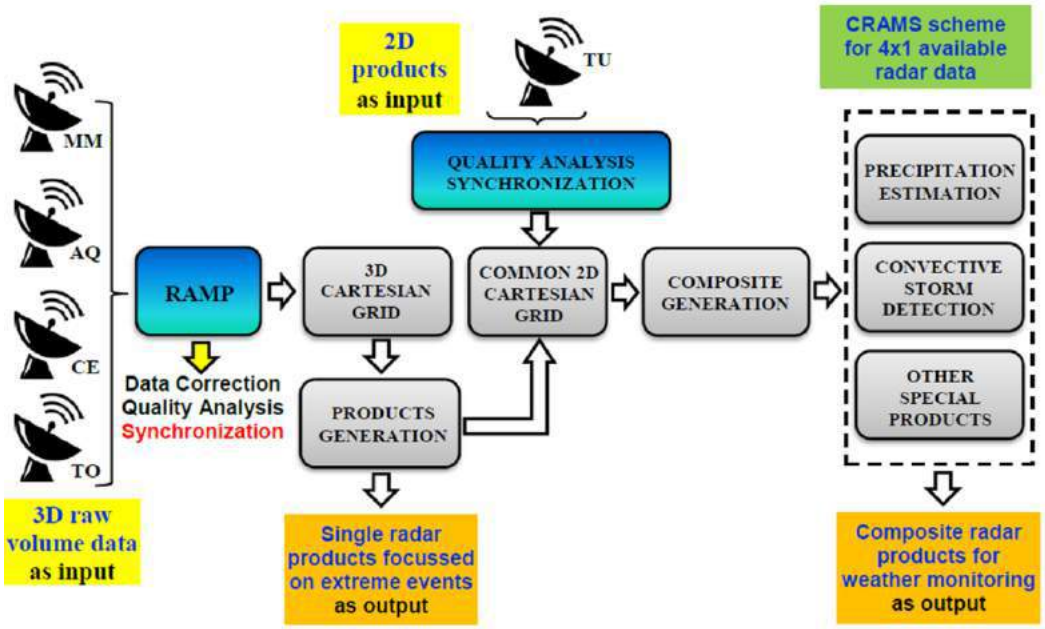


***Figure 5.3a*** *Block diagram of the radar data processing and mosaicking algorithm (CRAMS) as applied to the Abruzzo Region radar network, the modules described in this section are highlighted*

It is worth mentioning it is necessary to have a uniform time reference for all the radar data observations before the mosaicking. The individual radars are not temporally synchronized (volume scans follow different patterns and even if they start at the same time all the scans do not ends at the same time) thus a synchronization is needed both for volumetric 3D and 2D products data we have as input. This is accomplished in the blocks highlighted in **figures 5.3a and 5.3b.**

As regards Abruzzo network, we recall that the Tufillo radar is managed by the Department of Civil Protection (DPC), and the data are received through the various 2D products of the national radar composite (VMI, SRI, SRT, CAPPI) which DPC distributes at a regional level and national, every 10 minutes, in real time. The use of the Tufillo radar products derives from the need to cover the southern part of the Abruzzo Region in an optimal manner.
Thus, from Tufillo (TU) radar is currently available only two-dimensional products that has already been treated for the correction of the main sources of error. In this case, only a temporal synchronization of the data is performed, in order to ensure the complete overlapping of the observations with those of the other radars. The quality associated to the Tufillo products is also estimated as explained later.

For the radar of L'Aquila (AQ), Cepagatti (CE), Tortoreto (TO) and Monte Midia (MM) the volumetric data are available. In this case the temporal synchronization of the observations which have time resolution of 10 minutes is performed before RAMP application.

As regards Croatian network for Bilogora (BI), Osijek (OS) and Puntijarka (PU) radars the volumetric data are available. In this case the temporal synchronization of the observations which have time resolution of 15 minutes is performed before RAMP application.

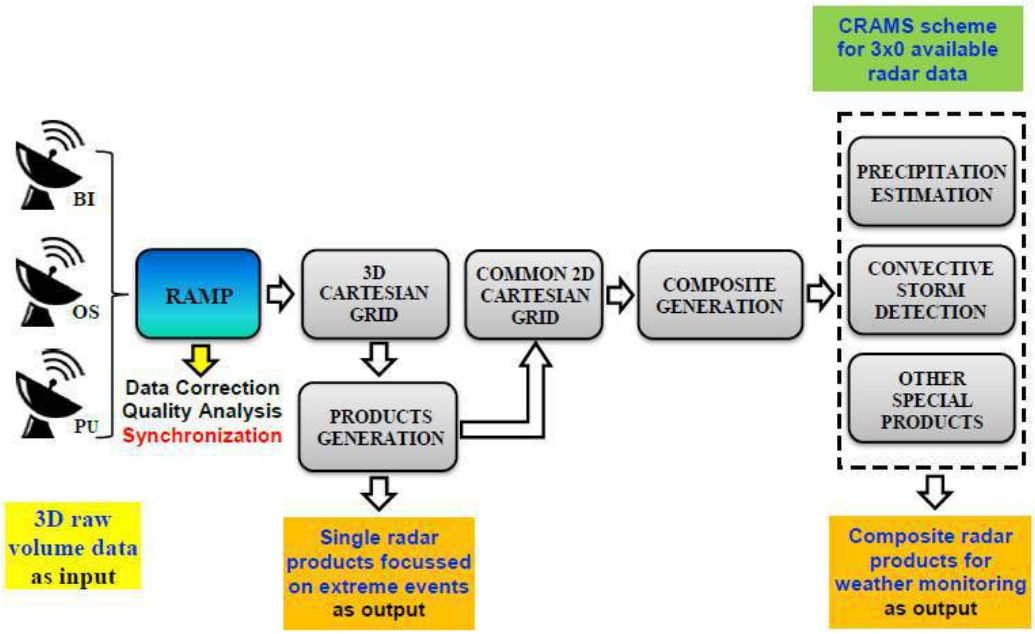


***Figure 5.3b*** *Block diagram of the radar data processing and mosaicking algorithm (CRAMS) as applied to the Croatian radar network, the modules described in this section are highlighted*

As mentioned in section 2.5, there are numerous sources of errors that may affect radar measurements. Among these, the most important are the following: radar calibration, ground clutter, beam blockage, wet-radome attenuation, rain attenuation, beam-broadening, non-uniform beam filling, vertical variability of precipitation and WLAN interferences. At X-band, attenuation may generate detrimental effects in quantitative precipitation applications, especially in convective events. Dual-polarization radars have the potential to provide additional information to overcome many of the uncertainties in contrast to situation when only the conventional reflectivity Z and Doppler information are available.

Due to the complexity of radar measurement and processing it is practically impossible to eliminate these errors completely or at least to evaluate each error separately. On the other hand, precise information about the data reliability is important for the end user.

To address this, in the framework of AdriaMORE project a specific processing chain called **RAMP (Radar Advanced Multiband Processing)** has been developed starting from some results of AdriaRadNet and CapRadNet projects (see chapter 3).

After a radar scan, raw data are generated as so-called volumes, i.e. 3-D polar data and once a raw volume scan is fully received, the data are processed through the RAMP in order to compensating or at least to identifying the most common error sources for each radar device. That to ensure

harmonized technical and software platforms on which each radar data, with different features, can be processed before the products generation at single radar level as well as before the composite.
The scheme of RAMP chain is presented in **figure 5.4**. The employed algorithms are functionally divided into two paths: one for data corrections and the second for data quality characterization. Particular quality algorithms can be switched on or off in the scheme. In general, algorithms for the 3D data quality control and characterization can be divided into categories based on analysis of: scan geometry, reflectivity data structure and technical characteristics.
The scheme should be an objective procedure, i.e. independent of platform (quality of data from different radar could be easy to compare) for the application at different radar data.

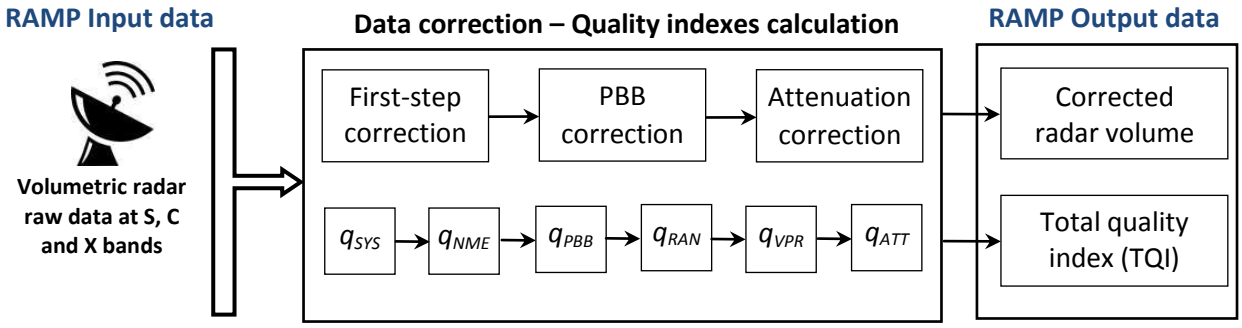


***Figure 5.4** Weather radar data processing chain (RAMP)*

The main steps for data correction and quality characterization within the proposed RAMP chain can be summarized as follows, anyhow you can find the details of the algorithms as well as examples of application in the deliverable 3.2.2.

### 5.1.1 First-step correction

For each radar, a specific first-step correction of volumetric data is applied. Ground-clutter, specks, WLAN interference, biological and others non-meteorological echoes have been removed from the reflectivity (Z) field by exploiting the textural spatial correlation of meteorological targets with respect to artefacts **[Barbieri, 2017].** Uncertain data are flagged but not removed. For dual-polarization systems a median smoothing filter and bias correction has been applied to the differential reflectivity ($Z_{dr}$), a compensation is applied to the correlation coefficient ($\rho_{hv}$) and the differential phase ($\Phi_{dp}$) has been processed by a multistage smoothing filter for $K_{dp}$ estimation **[Barbieri, 2014].**
An example of application of reflectivity correction is shown in **figure 5.5** for Monte Midia radar.

### 5.1.2 Partial beam blockage correction

Radars operating in complex orographic areas usually suffer from partial or total beam blockage by surrounding targets at their lowest elevation scans. The need for radar quantitative precipitation estimates in such environments led to the development of PBB (Partial Beam Blockage) corrections. When a radar beam intercepts a mountain, two situations are possible: 1) only part of the beam cross section illuminates the intercepted topography (partial blockage), or 2) the radar beam is completely blocked (total blockage).

A geometrical approach is applied to calculate the degree of the beam blockage. This approach is based on calculation of which part of radar beam cross-section is blocked, for any elevation angle, by any topographical object. For this purpose, the degree of PBB is computed from a high-resolution (250 m) digital terrain map (DTM), the radar technical characteristics and its sampling strategy. For each radar pixel (or bin) of the entire volume scan PBB is computed and usually is expressed in percentage. The Partial Beam Blockage correction can be applied to radar bins partially shielded according to vary schemes [**Tabary, 2007; Fulton, 1998; Fornasiero, 2005**].
In the scheme here adopted an occlusion of the beam of the order of less than 10% is considered negligible and is not corrected while an occlusion that exceeds 70% is rejected. If radar bins are partially shielded between 10% and 70% the radar reflectivity measurement is modified by adding 1-4 dB depending on the degree of occultation. As an example, in **figure 5.6** are shown the visibility maps at the first operational elevation for the radar of Bilogora and Osijek.

### 5.1.3 Path attenuation correction

The attenuation that the radar signal undergoes in the presence of heavy precipitation determines an underestimation of the measured reflectivity and differential reflectivity that increases with the increase in the distance from the radar and the intensity of the precipitation in progress. This problem is particularly important in the X-band and can also lead to the complete extinction of the signal **[Maki, 2012]**. We must therefore try to compensate both the reflectivity (Z) and the differential reflectivity ($Z_{dr}$), the latter present in the double polarization systems only.
For single-polarization radar the attenuation is computed with an iterative procedure that involves the estimation of the two-way path integrated attenuation (PIA) along the entire beam path **[Osrodka, 2012].** For dual polarization systems the PIA can be found by using the reconstructed differential phase shift too **[Bringi, 2001]**.
Find in **figure 5.7** an example of correction for the attenuation for Cepagatti radar.

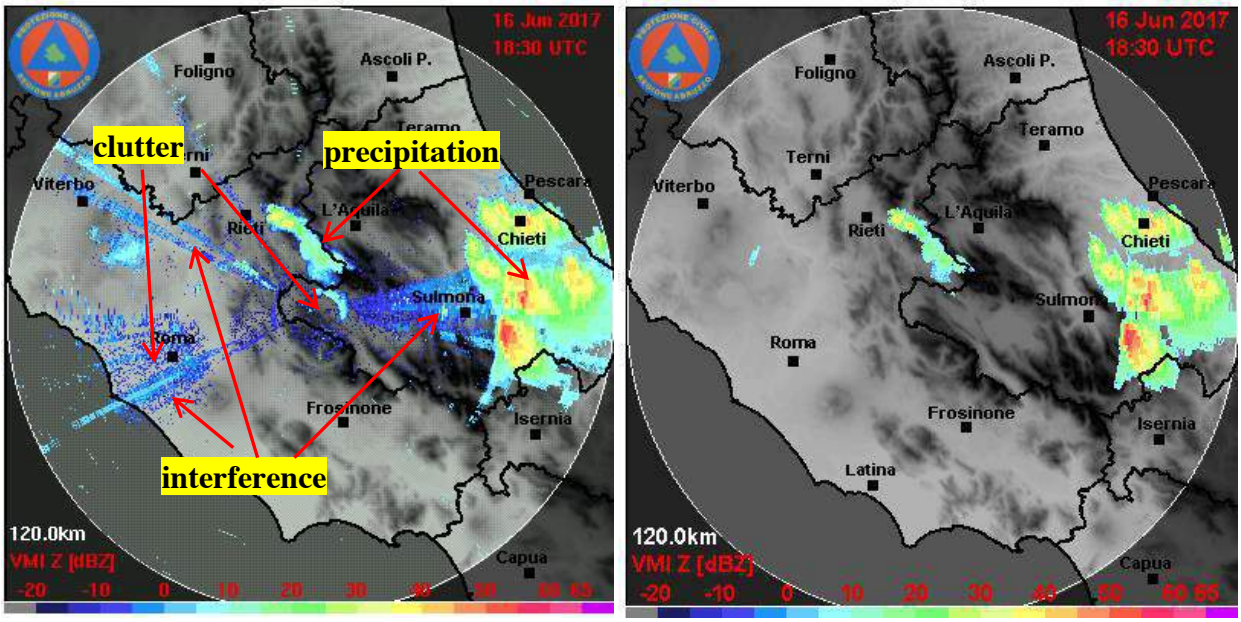


***Figure 5.5*** *Uncorrected reflectivity image (left panel) as input at RAMP chain and the related output (right panel) after that "First step correction" has been applied at Monte Midia radar for the precipitation event occurred on June 16, 2017*

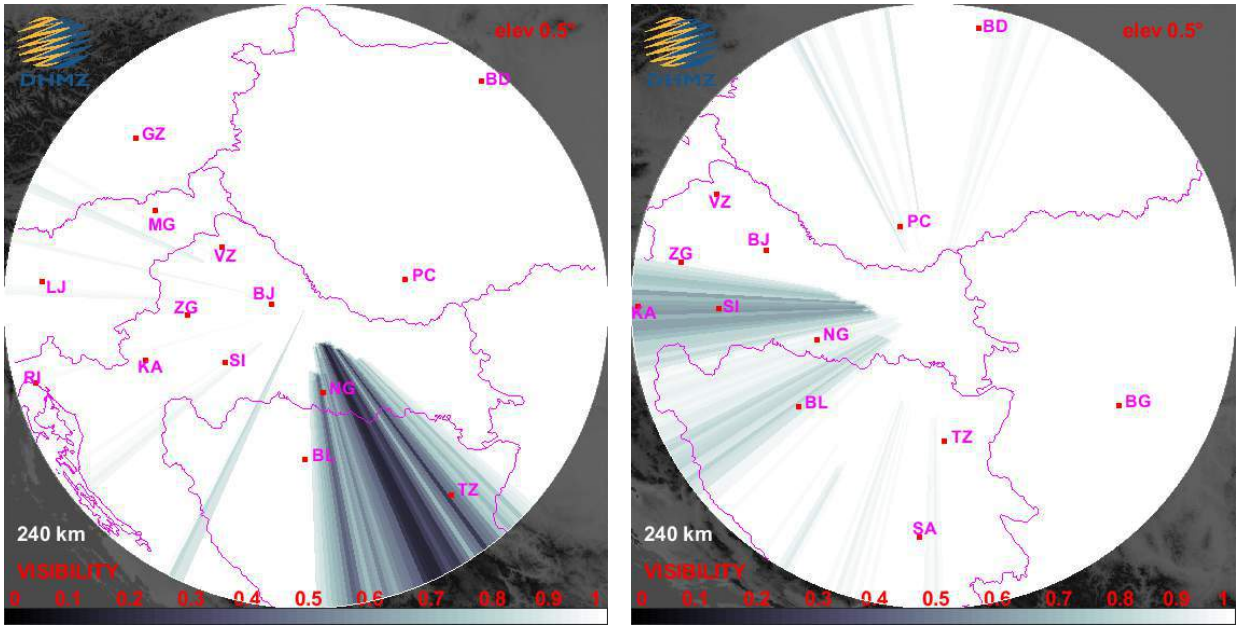


***Figure 5.6*** *Beam occlusions for Bilogora (left panel) and Osijek (right panel) radars at 0.5 degree of elevation angle the colors range from white, that is complete visibility, to black, that is no visibility*

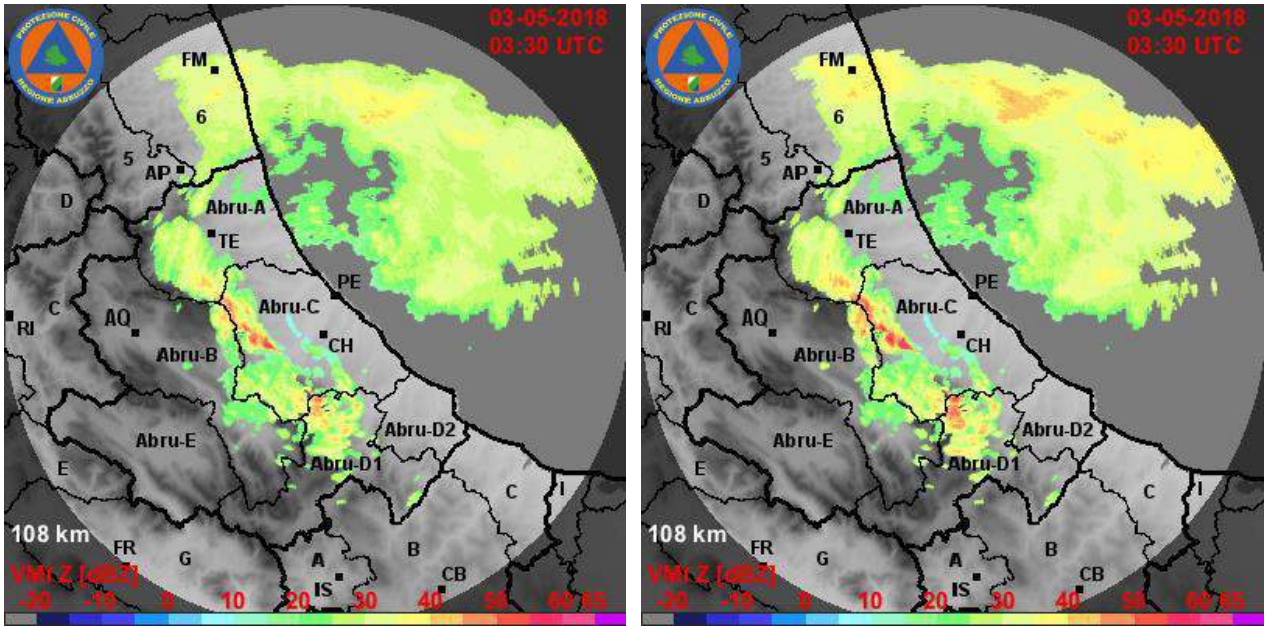


***Figure 5.7*** *VMI map of uncorrected reflectivity (left) and corrected for the attenuation (right) using the iterative method for an X-band weather radar (Cepagatti)*

### 5.1.4 Total quality information

The quantitative estimation of error magnitude is necessary not only in order to gain general knowledge about data uncertainty but also to apply quality information in further data processing, e.g. in the generation of standard or user-related specific products.

One of the most common approaches in the characterisation of the quality of weather radar data is to employ ($q_i$), which is defined as a unitless quantity that provides information on the data reliability in a digital scale.

The idea of the quality index scheme is based on selection of quality factors, determination of their quality indices and computation of one total quality index.
Assuming that any radar systems are well maintained, the quality analysis, for AdriaMORE purpose, has been focused on the following error sources resumed in the **table 5.1**.
For each error an individual quality index ($q_i$) is calculated in each radar pixel volume through appropriate tests, giving as output an unitless quantity expressed by numbers from 0 (bad quality) to 1 (excellent quality).

| Quality Index | Source of error | Note |
|---|---|---|
| $q_{SYS}$ | Radar system technical parameters | It is static within the whole radar range as well as in time and taken into account several factors as in [Osrodka, 2012] |
| $q_{NME}$ | Non-meteorological echo | Pixel affected by non-meteorological echoes are removed, for the uncertain pixel a value of 0.5 is applied, the others data are set to 1. |
| $q_{PBB}$ | Partial beam blocking | It is computed from the corrected data taking into account the PBB value as in [Barbieri, 2017] |
| $q_{RAN}$ | Long range measurement | This quality factor decreases with increasing distance from the radar, it is computed as in [Rinollo, 2013] |
| $q_{ATT}$ | Rain path attenuation | It is computed from the corrected data taking into account the PIA value as in [Barbieri, 2017] |
| $q_{VPR}$ | Inhomogeneous vertical profile of reflectivity | The compensation of this effect is not performed in RAMP, the quality index associated is estimated as in [Friedrich,2006] |

***Table 5.1*** *Group of quality index and related source of errors to which they refer*

In the case of 2D products as input it is not possible to determine some of the individual quality indexes (attenuation, height of measurement and non-meteorological echoes), in which case the value of their quality is conventionally set equal to 1. Some examples of the individual quality index are given in **figure 5.8a.**

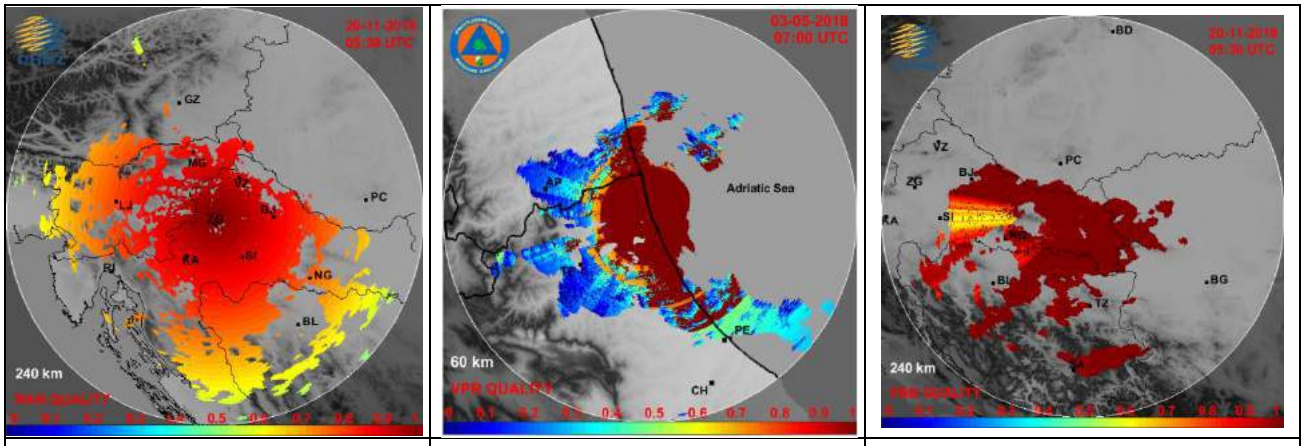


| $q_{RAN}$ of Puntijarka's radar | $q_{VPR}$ of Tortoreto's radar | $q_{PBB}$ of Osijek's radar |
|---|---|---|

***Figure 5.8a*** *Examples of individual quality indices for the Monte Midia, Cepagatti and Tortoreto radars*

The Total Quality Index (TQI) in each radar pixel can be retrieved by combining all the individual quality indicators. A multiplicative combination rule is here used:

$$TQI = q_{SYS} \cdot q_{NME} \cdot q_{PBB} \cdot q_{RAN} \cdot q_{ATT} \cdot q_{VPR}$$

**Figure 5.8b** shows the effect of the RAMP chain for the reflectivity data of the Monte Midia, Tortoreto and Osijek radars relating to precipitation events. It can be noted the elimination of some non-meteorological echoes and the attenuation correction. The corresponding maps of TQI are also shown once the individual quality indices defined by **table 5.1** have been calculated.

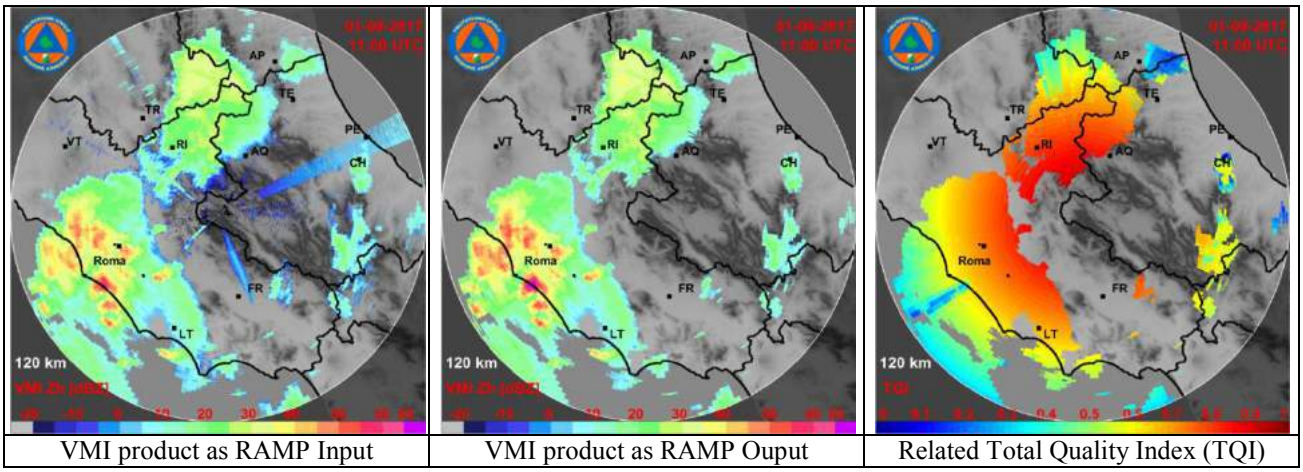


| VMI product as RAMP Input | VMI product as RAMP Ouput | Related Total Quality Index (TQI) |
|---|---|---|

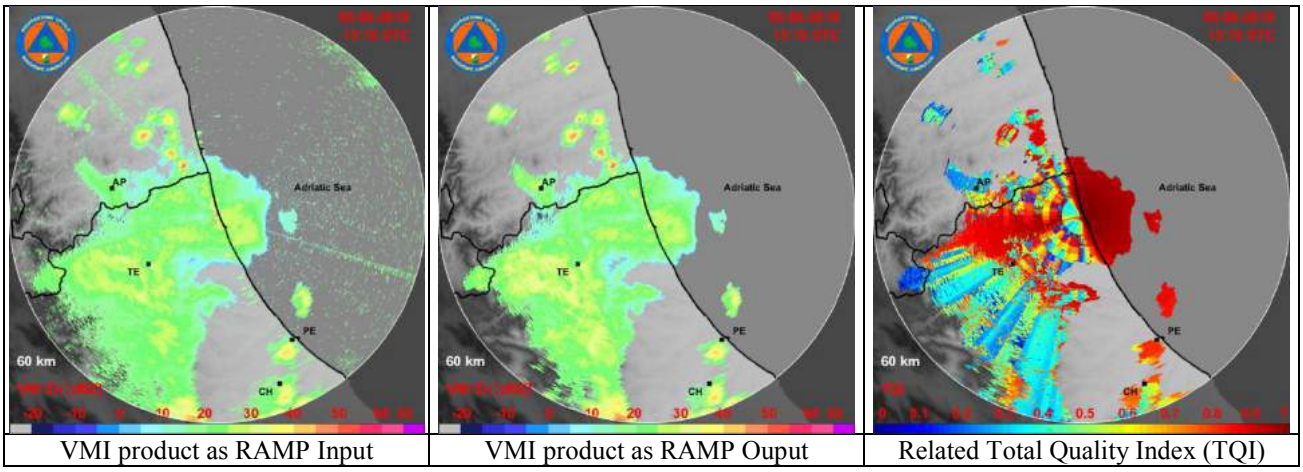


| VMI product as RAMP Input | VMI product as RAMP Ouput | Related Total Quality Index (TQI) |
|---|---|---|

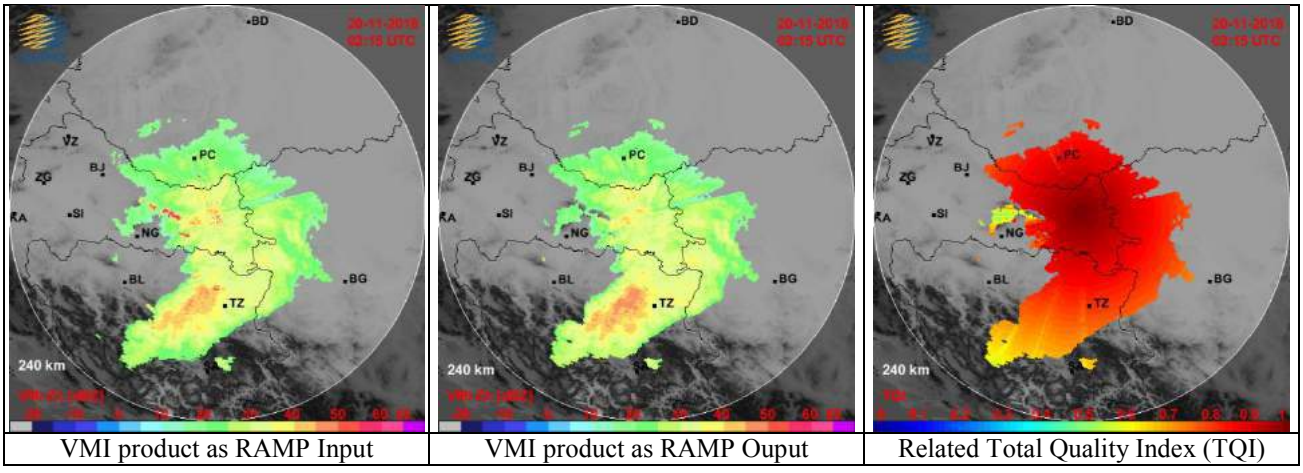


| VMI product as RAMP Input | VMI product as RAMP Ouput | Related Total Quality Index (TQI) |
|---|---|---|

***Figure 5.8b*** *VMI products as input (left column) and output (central column) at RAMP chain for some events with precipitation for the Monte Midia (first row) Tortoreto (second row) and Osijek (third row) radars. The right column shows the overall quality matrices for the same events.*

### 5.2 Resampling onto a 3D Cartesian grid

In this part of the CRAMS algorithm (highlighted in **figure 5.9**) the data volumes of each radar, consisting of 3D corrected reflectivity observations in polar format (polar coordinates), are recombined on a specific and well-defined three-dimensional Cartesian grid as sketched in **figure 5.10** preserving height information and the desired spatial resolution and grid extension.

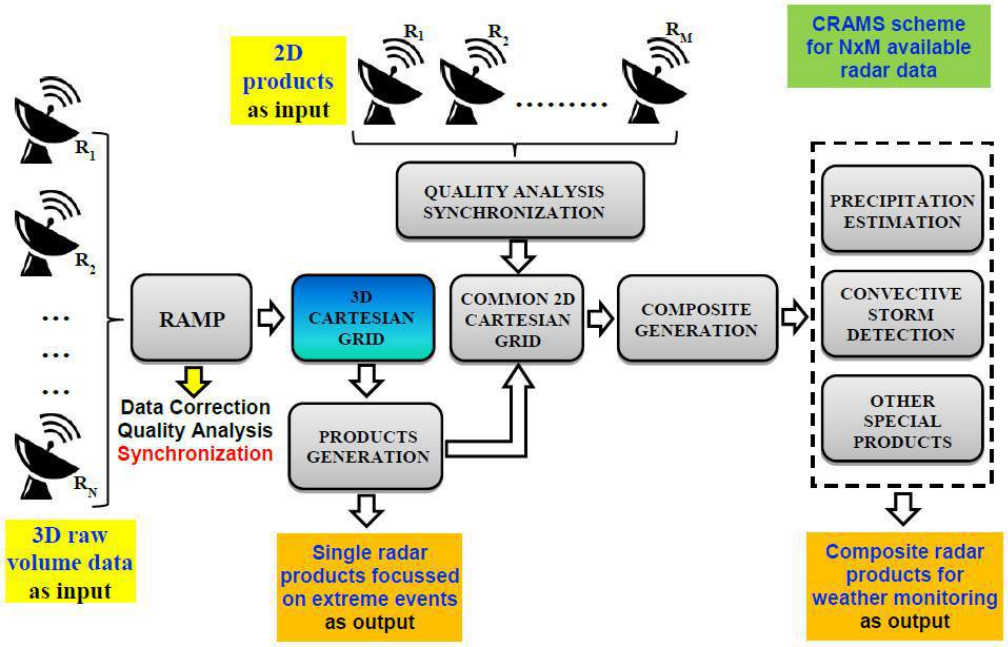


***Figure 5.9*** *Block diagram of the radar data processing and mosaicking algorithm (CRAMS), the module described in this section is highlighted*

The volume of each single radar is first converted into cylindrical and then into cartesian coordinates. The size of the cartesian grid is determined by the maximum range of each single radar and the elevations used in the scans. Its resolution in width and length is chosen so as to maintain the same radial resolution of the various radars, while in height it is fixed at 0.5 km for each radar of both the Abruzzo and Croatian network. For example, the cartesian grid of Cepagatti radar has a width and length equal to 216 km (twice the maximum range) with a resolution of 450 m and height equal to the maximum altitude reached by its highest elevation (5 deg) to the maximum range (10 km) with a resolution of 0.5 km, i.e. a grid of dimensions 480x480x20.

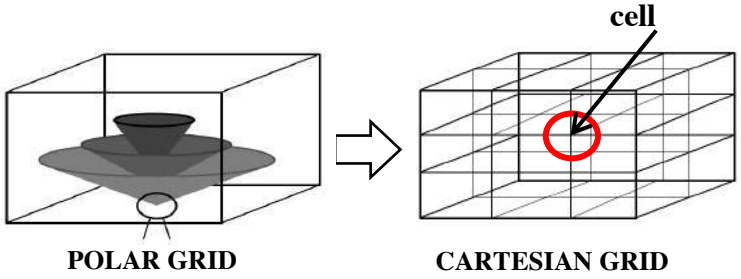


***Figure 5.10*** *Every single polar 3D volume radar data is converted in Cartesian coordinates combined onto a 3D Cartesian grid consisting of a certain number of elementary cells*

**Figure 5.11** shows examples of the correct reflectivity volume of some individual radar in the respective 3D Cartesian grids.

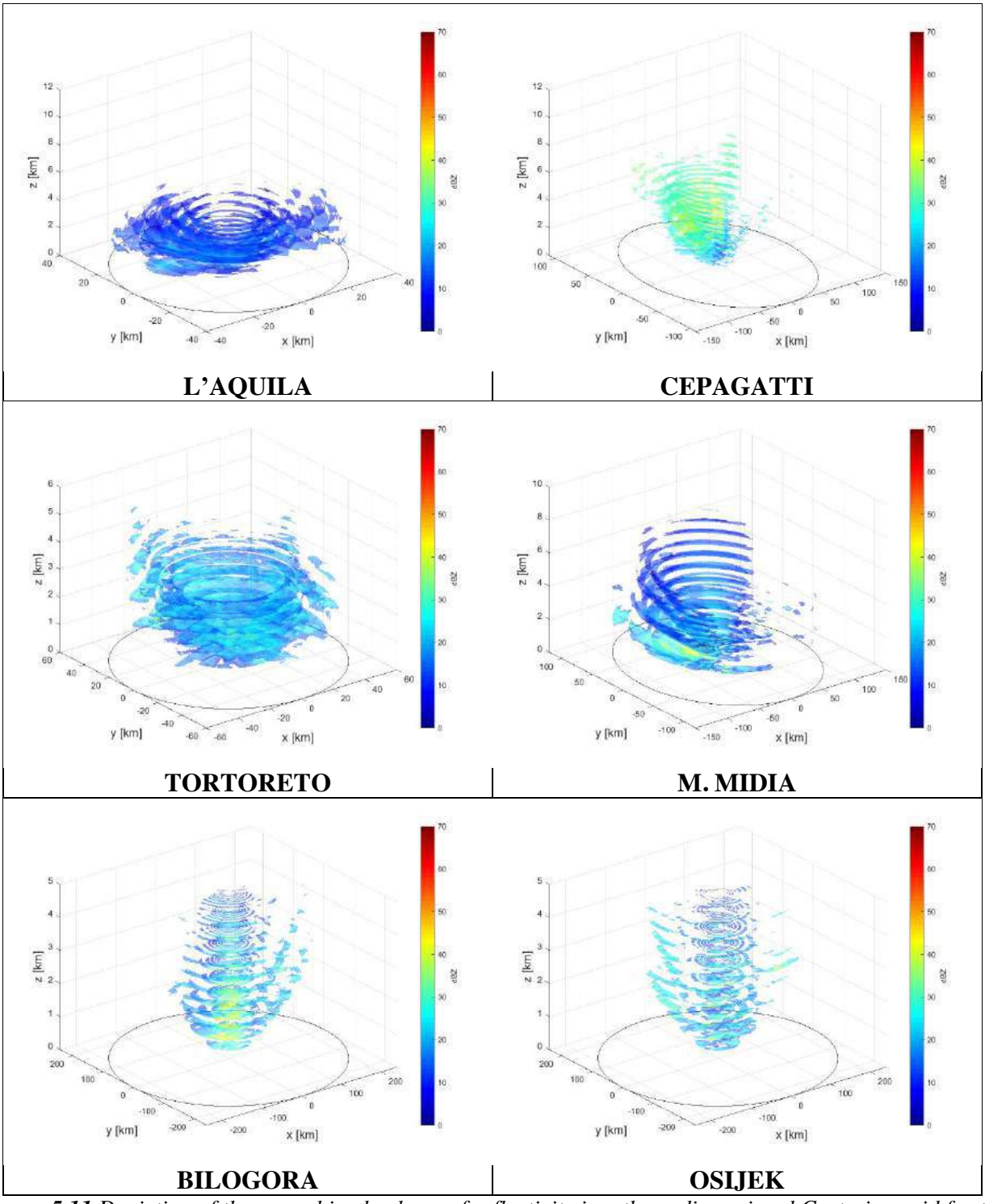


***Figure 5.11*** *Depiction of the recombined volume of reflectivity in a three-dimensional Cartesian grid for the L'Aquila, Cepagatti, Tortoreto, Monte Midia, Bilogora and Osijek radars*

### 5.3 Products generation at single-radar level

This module is fully described in the deliverable 3.2.2, anyway for reader convenience a brief description is given in this section. In the **figure 5.12** is highlighted the part of the CRAMS chain assigned to the generation of sophisticated radar products at single-radar level. Practically, the corrected volumes consist of sets of measurement gates organized in polar scans related to the rotation of an antenna at selected elevation angles. Based on the transfer from polar to Cartesian representations through a certain interpolation method the corrected volumes are processed to obtain various 2-D Cartesian products from single radar measurements dedicated to specific user requirements. These are generally two-dimensional representations with dimensions and resolution depending on the characteristics of the radar to which it refers.

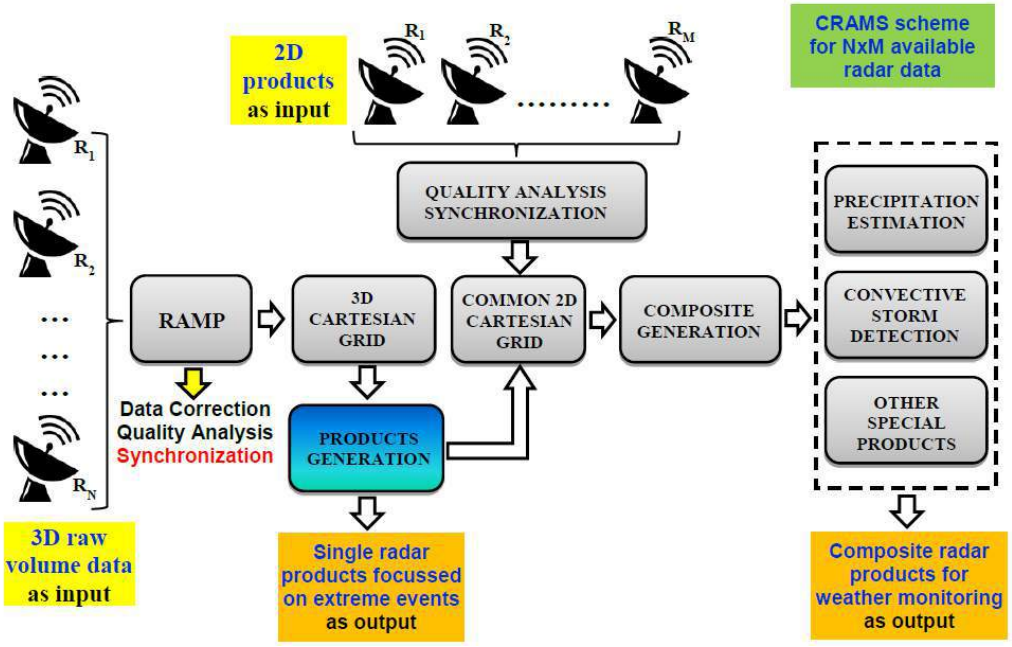


***Figure 5.12*** *Block diagram of the radar data processing and mosaicking algorithm (CRAMS), the module described in this section is highlighted*

For AdriaMORE's goals, products focused on extreme events (listed in **table 5.2**) have been taken into account, that for: (1) to examine in detail severe weather events of particular interest, (2) to have useful products in case of the relative composite products were not available and (3) to generate the products to be mosaicked with the other radars' available products.

As mentioned before, all the modules devoted to the generation of the products at single-radar level (**figure 5.13**) will be described in detail in the deliverable 3.2.2 with the standard algorithms for their generation and examples of application.

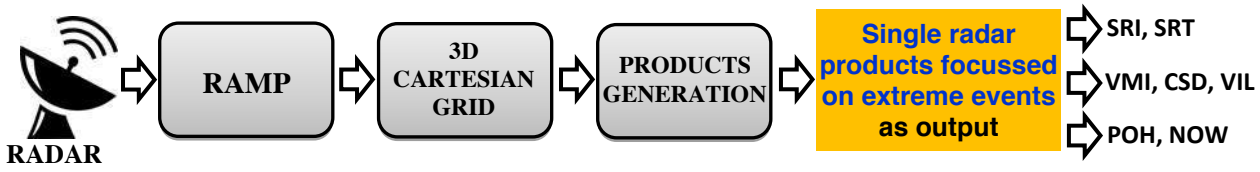


***Figure 5.13*** *Part of the CRAMS chain devoted to the products generation at single-radar level*

| PRODUCT NUMBER | PRODUCT NAME | PRODUCT SYMBOL | SHORT DESCRIPTION |
|---|---|---|---|
| 1 | Vertical maximum of reflectivity | VMI | This product is useful for a quick surveillance of region covered by the radar |
| 2 | Convective storm detection | CSD | The product is aimed at distinguish stratiform and convective precipitation |
| 3 | Short time prediction | NOW | The product is aimed at short-term forecast (nowcasting) of convective cells motion. |
| 4 | Precipitation estimation | SRI SRT | These products estimate the ground instantaneous (SRI) and accumulated (SRT) rain over radar coverage area. |
| 5 | Vertically Integrated Liquid | VIL | This product can be used as a measure for the potential strong rainfall |
| 6 | Hail detection | POH | The product is aimed at hail detection which is one of the most danger phenomena. |

***Table 5.2*** *List of the products at single-radar level implemented within CRAMS chain*

In the **figures 5.14 and 5.15** some examples of the products listed in table 5.2 are shown.

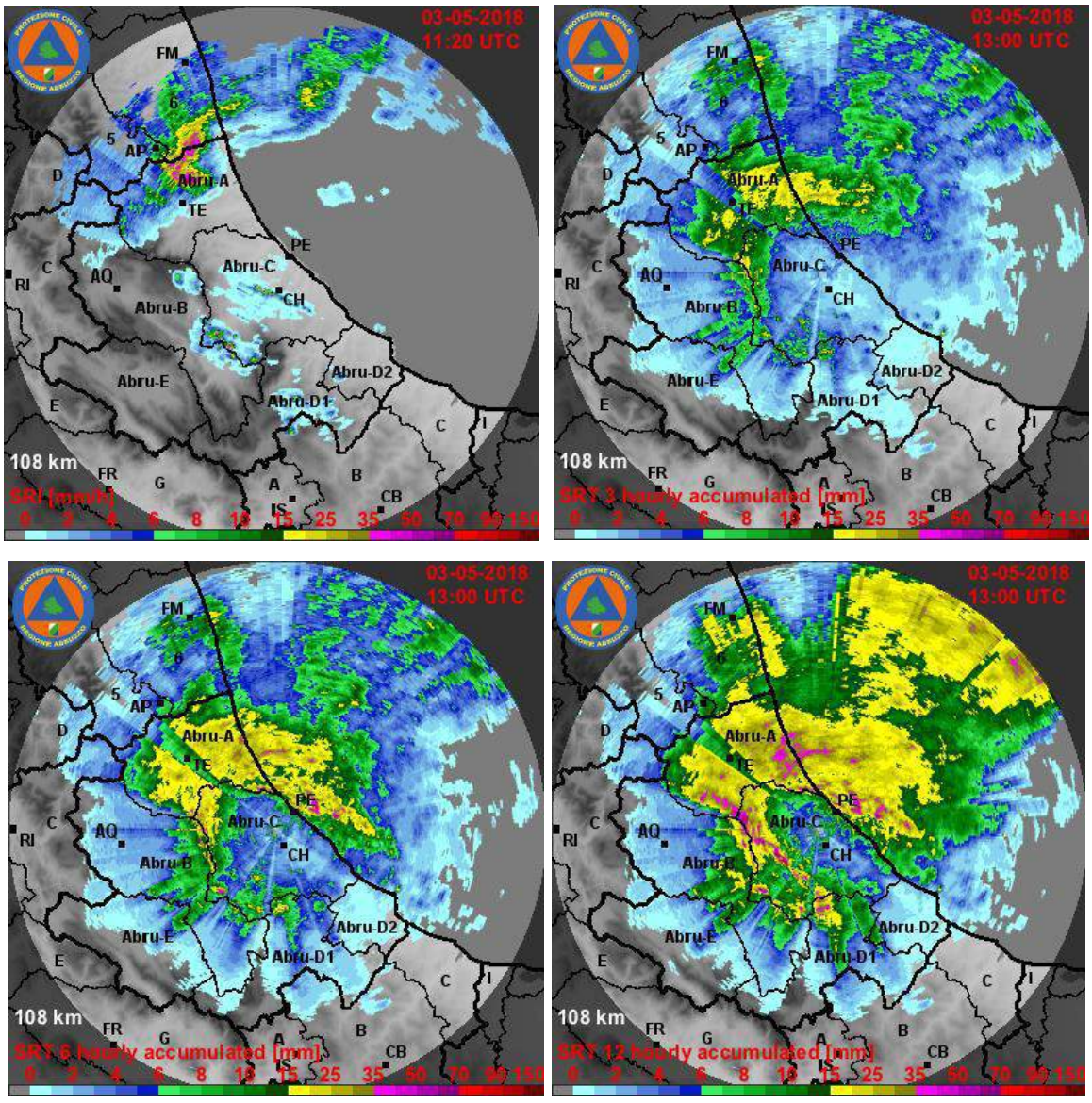


***Figure 5.14*** *Examples of rain rate estimation (SRI) and cumulated precipitation (SRT) for Cepagatti radar*

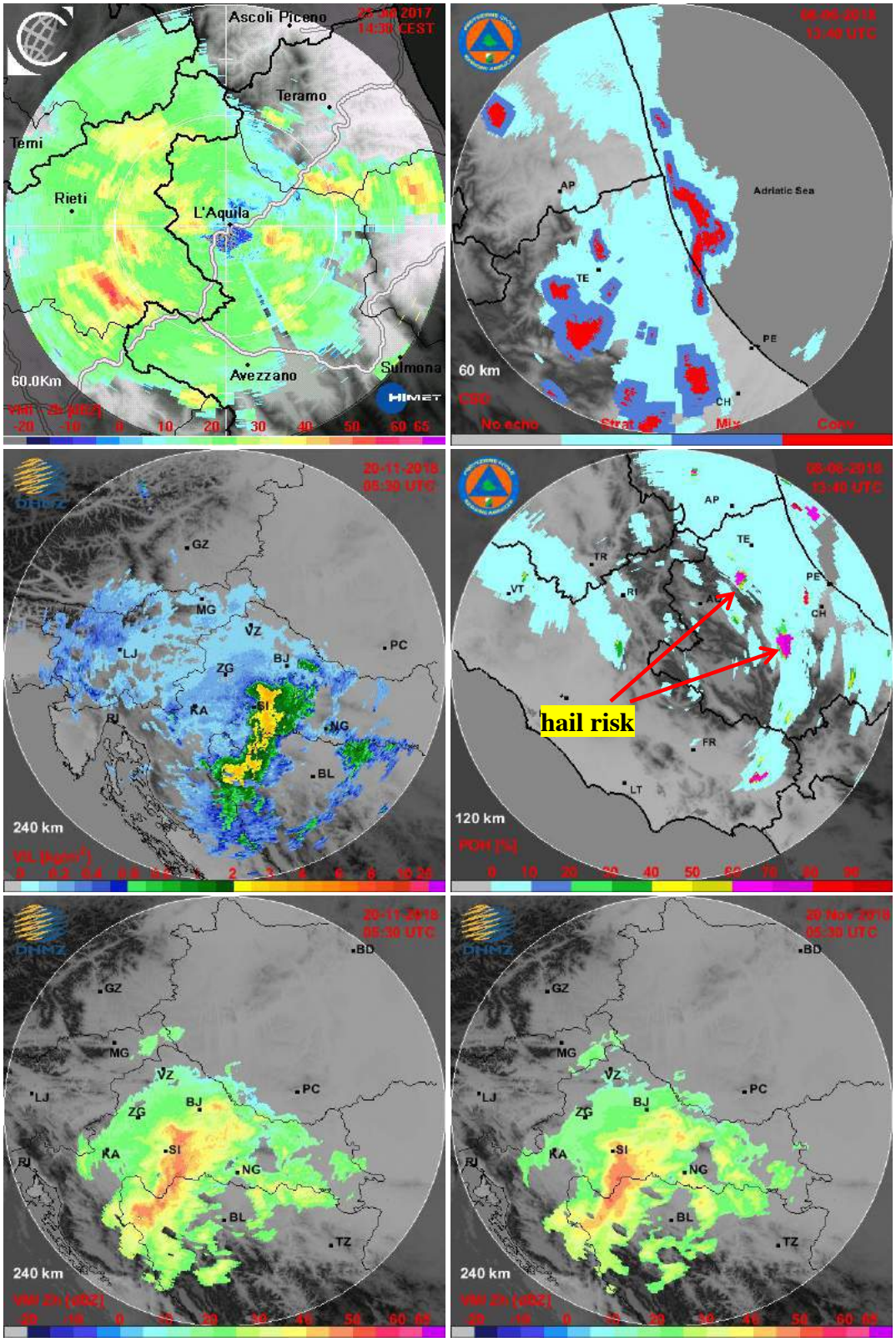


***Figure 5.15*** *Examples of the Maximum of reflectivity (VMI, top left) for L'Aquila radar, Convective storm detection (CSD, top right) for Tortoreto radar. Examples of the Vertically Integrated Liquid (VIL, central left) for Puntijarka radar and Probability of Hail (POH, central right) for Monte Midia radar. Example of observed (bottom left) and predicted (bottom right) reflectivity map for Bilogora radar*

### 5.4 Remapping onto a common 2D Cartesian grid

As described in the previous sections once a radar volume scan is fully received, the data are pre-processed through RAMP chain in the native radar (spherical) coordinates. After that, single radar reflectivity data are remapped from their native spherical coordinates to a specific cartesian coordinates system and then some valuable products (such as VMI, VIL, SRI) are generated at single radar level. At the same time 2D products from other available radar can be also used as input.

This module, highlighted in **figure 5.16**, is devoted to resample all products from their specific 2D Cartesian grid onto a common 2D Cartesian grid covering the whole area of mosaic domain.

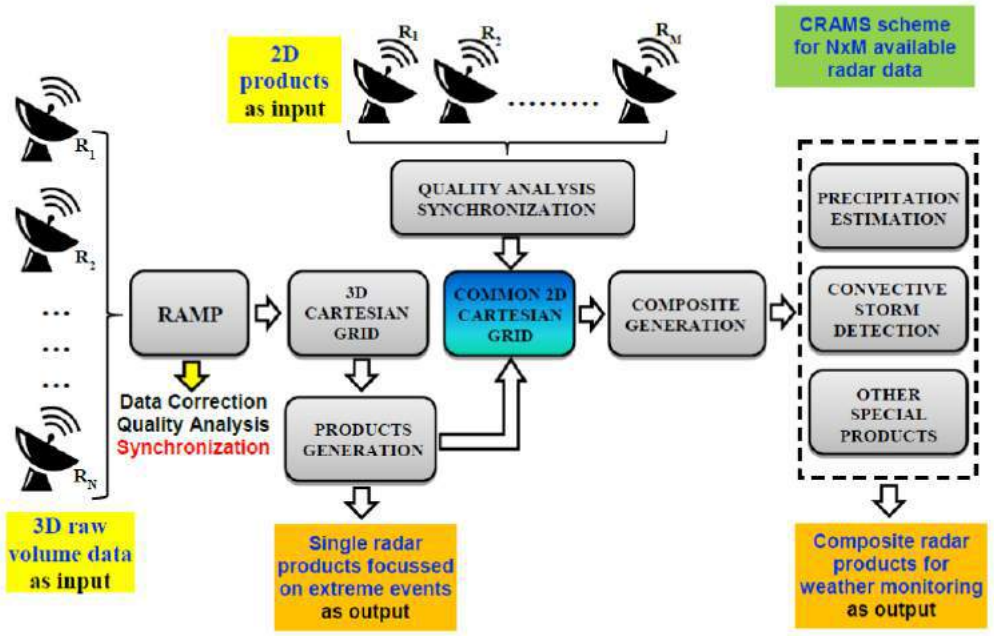


***Figure 5.16*** *Block diagram of the radar data processing and mosaicking algorithm (CRAMS), the module described in this section is highlighted*

Concerning Abruzzo network, the mosaicking domain was defined taking into account the technical characteristics of the radars, their geographical location and the peculiarities of the territory concerned. For each radar, the coverage area was set compatible with the size of the mosaicking domain, see **figure 5.17** where the coverage area utilized for each device (do not considering obstacles due to orography) is also depicted. The DPC composite products, if temporally available, are also used as input data by cutting out on a 60 km domain from Tufillo radar site.

We chose a common grid with a resolution of 0.4 x 0.4 $km^2$ and with a composite area of about 83.000 $km^2$ (310 x 268 Km), a compromise able to guarantee sufficient accuracy, ease of implementation and calculation speed in processing. The products of the individual radars, although in Cartesian coordinates X, Y and distributed in an almost regular way, cannot however be used as nodes in the new unified grid system due to the different resolution of each radar. It is therefore necessary to reconfigure the radar products on the nodes of the mosaic domain grid by means of a coordinate transformation applied to the nodes of the radar products. Then an interpolation will be performed, with the technique of the nearest neighbour.

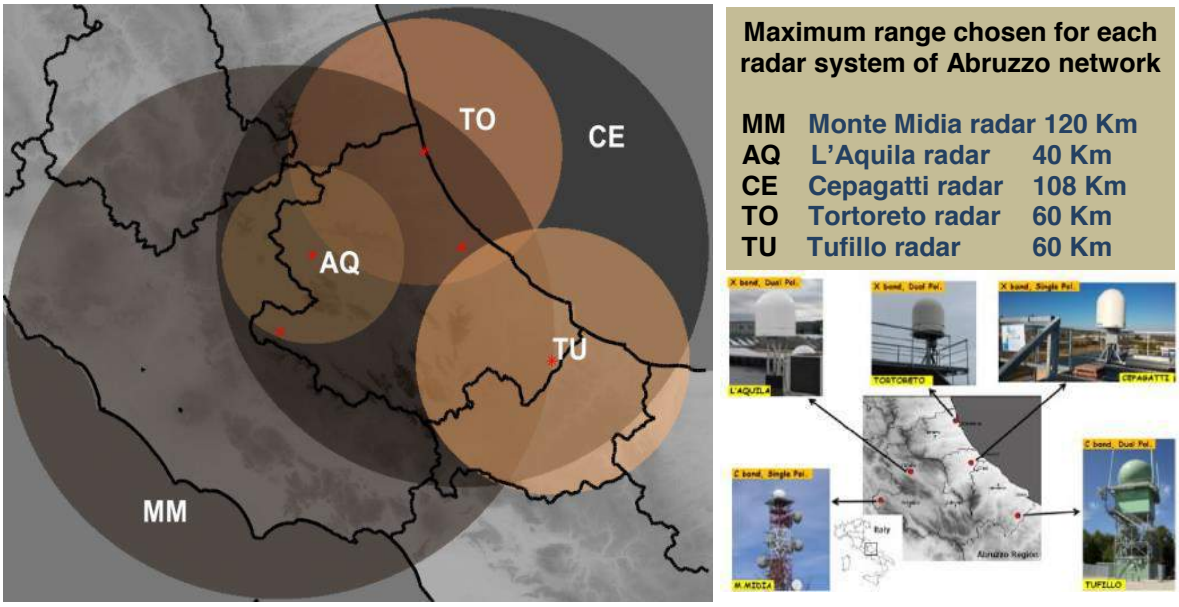


***Figure 5.17*** *The composite domain for Abruzzo network with the maximum coverage area chosen for each radar system whose location are indicated with a red spot*

**Figure 5.18** shows an example of remapping of the VMI product for the radars of the Abruzzo network within the mosaic domain shown in figure 5.17.

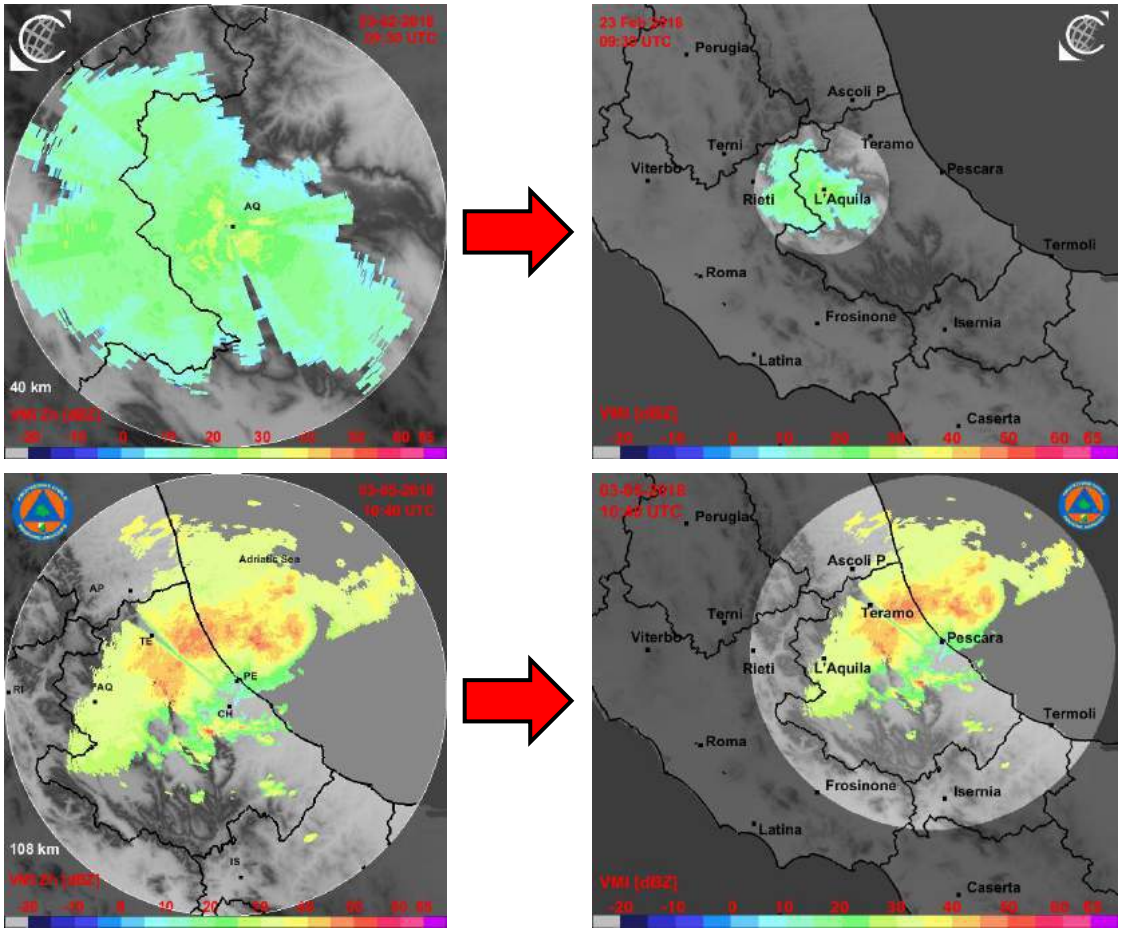

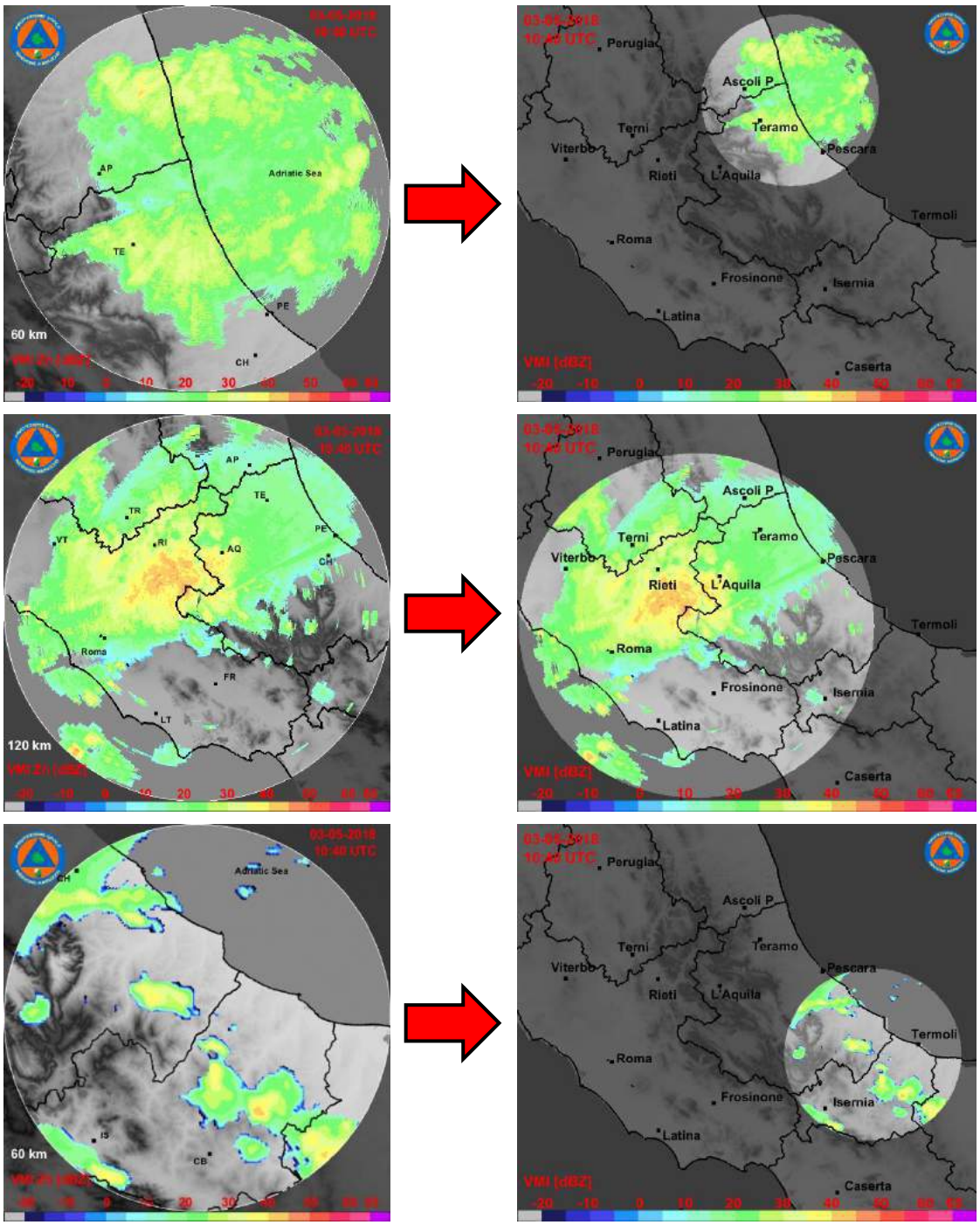


***Figure 5.18*** *Adaptation of VMI product to the common domain for the L'Aquila radar (first row), Cepagatti (second row), Tortoreto (third row), Monte Midia (fourth row) and Tufillo (fifth row)*

Concerning Croatian network for the mosaicking domain was chosen the same domain, shown in **figure 5.19**, utilized by the Meteorological and Hydrological Service of Croatia (DHMZ).

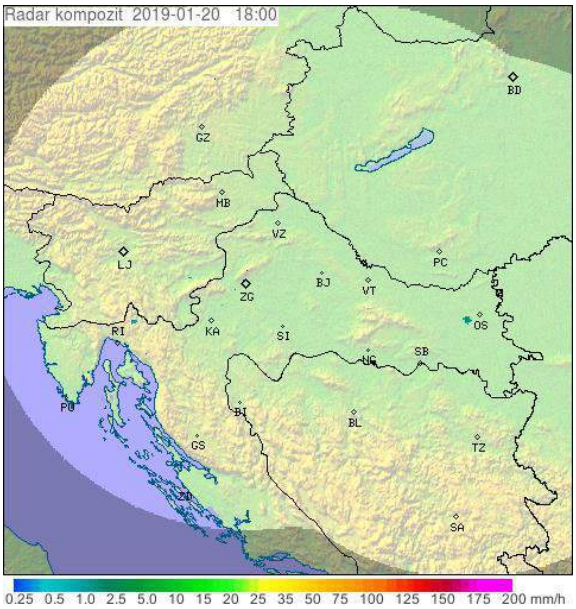


***Figure 5.19*** *The composite domain for Croatian network utilized by the DHMZ*

We chose a common grid with a resolution of 0.5 x 0.5 km$^2$ and with a composite area of about 266.000 km$^2$ (512 x 520 Km). The products of the single radars are at the same resolution and are reconfigured on the nodes of the domain grid by means of a coordinate transformation applied to the nodes of the radar products and then interpolated with the nearest neighbour's technique. See **figure 5.20** where the coverage area utilized for each device (do not considering obstacles due to orography) is also depicted.

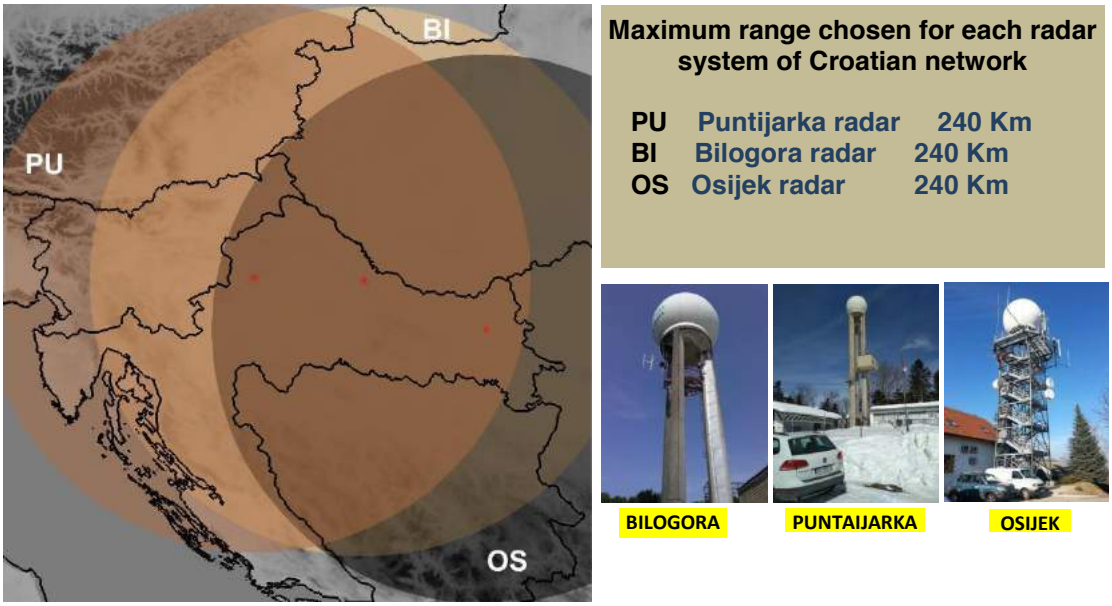


***Figure 5.20*** *The composite domain for Croatian network with the maximum coverage area chosen for each radar system whose location are indicated with a red spot*

**Figure 5.21** shows an example of remapping of the VMI product for the radars of the Croatian network within the mosaic domain shown in figure 5.20.

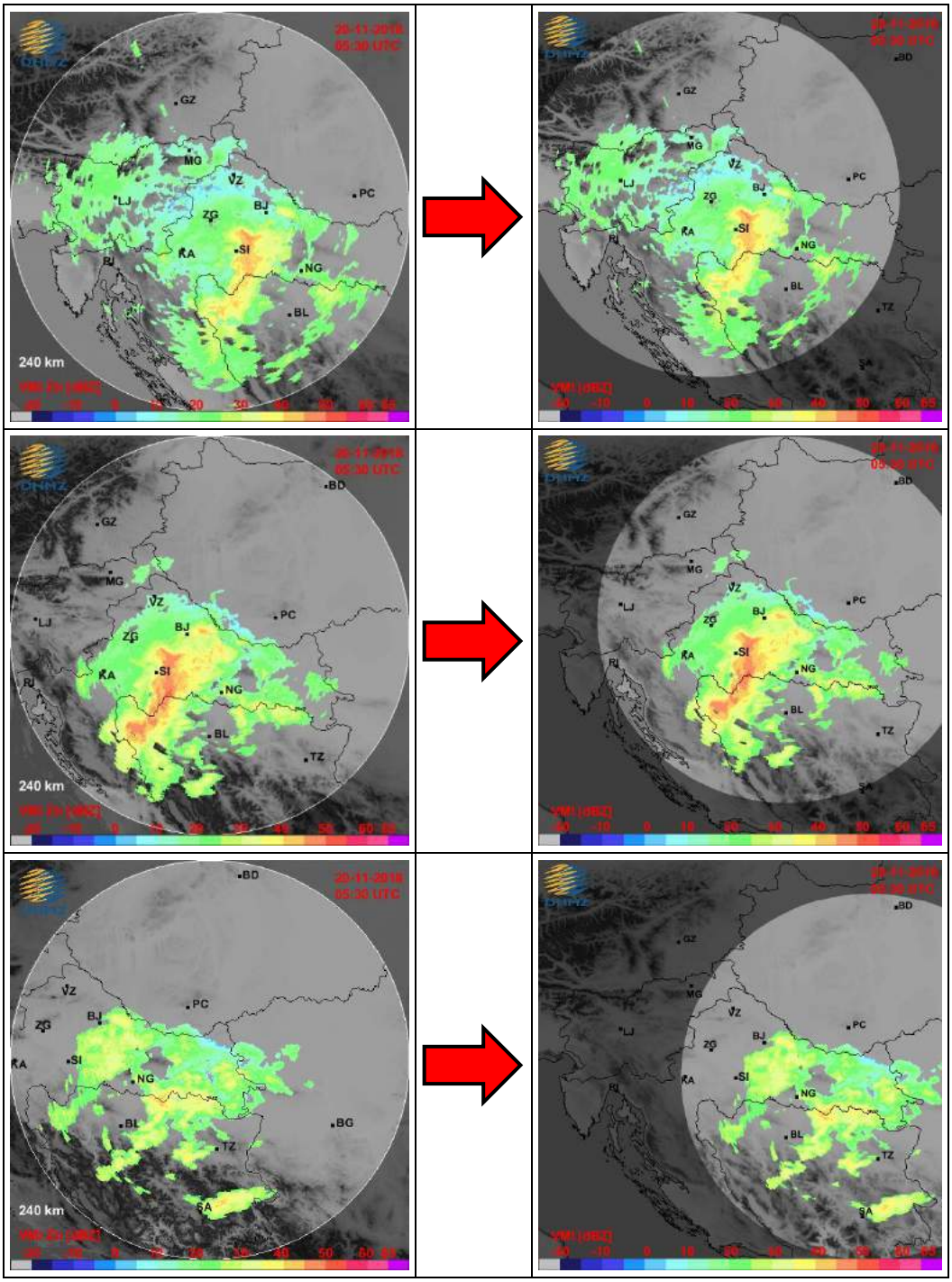


***Figure 5.21*** *Adaptation of VMI product to the common domain for the Puntijarka radar (first row), Bilogora (second row), and Osijek (third row)*

### 5.5 Mosaicking with different merging strategies

In this module of the CRAMS chain (highlighted in **figure 5.22**) the radar products, resampled within the mosaic domain, are suitably combined in order to obtain the final composite.

Selecting an optimal way to merge radar data is significant and must consider a number of factors such as the size and shape of the domain of interest, number and location of the network's nodes, and the resolution and type of the desired products. Our goal is to assess how different merging techniques can improve the quality of the products over the composite domain. There are several ways to generate a composite of radar data, after a thorough literature review in **table 5.3** are resumed the methods which have been taken into consideration, together with a brief description and relative bibliographic references.

These techniques can be applied to both 3D and 2D mosaic. The latter can be at first sight less accurate than 3D ones but have the advantage of being easier to implement in operational use, and have less computational complexity, especially if the scale of the domain is wide **[Lakshmanan, 2014]**.

In **figures 5.23a and 5.23b** are shown an example of VMI product composite of Abruzzo network for all the methods described in table 5.3 with reference at a precipitation event occurring on central Italy on March 11, 2018.

The mosaic methods of the table 5.3 have been tested, for a qualitative analysis, on the data of archived cases study considering diverse storm regimes. A quantitative analysis has been carried out in chapter 6 by using ground references data coming from a network of rain gauges.

Preliminary results show how the principle of Maximum Quality (method 6 of table 5.3) is a good compromise among the tested methods since it is comprehensive of the major problems affecting radar data.

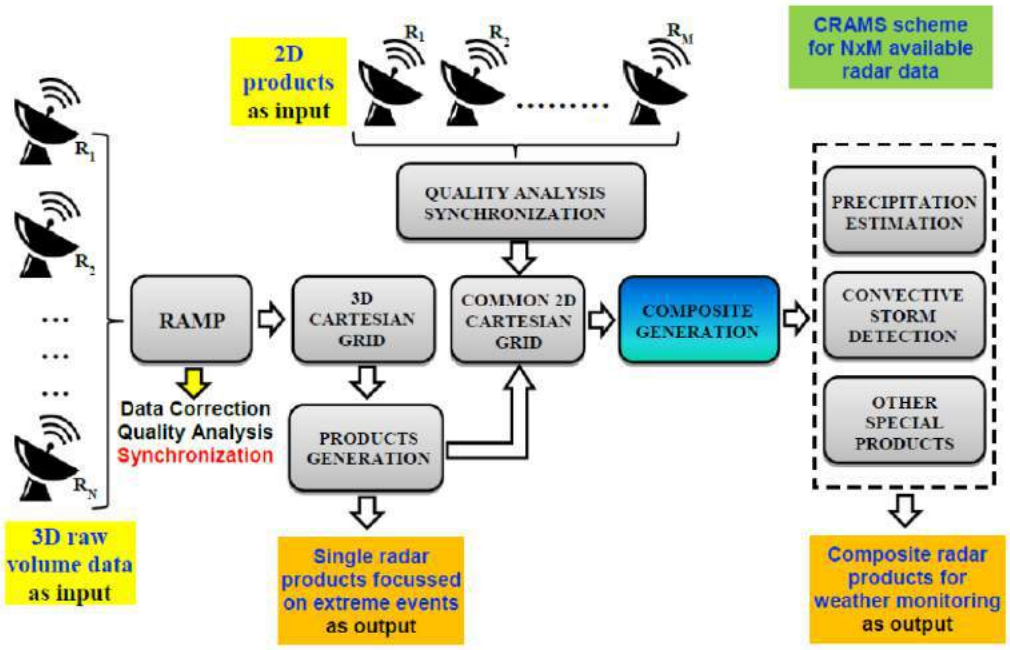


***Figure 5.22*** *Block diagram of the radar data processing and mosaicking algorithm (CRAMS), the module described in this section is highlighted*

| Num. | Mosaicking method | Bibliographic references |
|---|---|---|
| 1 | Assign to the common pixel the mean value of the available measurements | [Zhang, 2004] |
| 2 | Assign to the common pixel the maximum value of the available measurements | [Zhang, 2004] |
| 3 | Assign to the common pixel a value weighted with the distance from the radars, using linear weighting functions | [Einfalt, 2012] |
| 4 | Assign to the common pixel a value weighted with the distance from the radars, using exponential weighting functions | [Zhang, 2004] |
| 5 | Assign to the common pixel a value weighted by a defined inversely proportional power of the distance from the radar | [Shepard, 1968] |
| 6 | Assign to the common pixel the value corresponding to the maximum final quality (TQI) | [Fornasiero, 2006] [Peura, 2007] |
| 7 | Assign to the common pixel the value corresponding to the minimum PIA (Path Integrated Attenuation) | [Domaszczynski, 2012] |
| 8 | Assign to the common pixel a value weighed by the final quality (TQI) associated with the various radars | [Jurczyk, 2018] |
| 9 | Assign to the common pixel the value corresponding to the minimum distance | [Domaszczynski, 2012] |
| 10 | Assign to the common pixel a value weighed quadratically with the distance from the radar | [Zhang, 2004] |
| 11 | Assign to the common pixel a value weighted with the final quality (TQI) and a defined inversely proportional power of the distance from the radar | [Jurczyk, 2018] |

***Table 5.3*** *Different merging strategies tested and related bibliographic references*

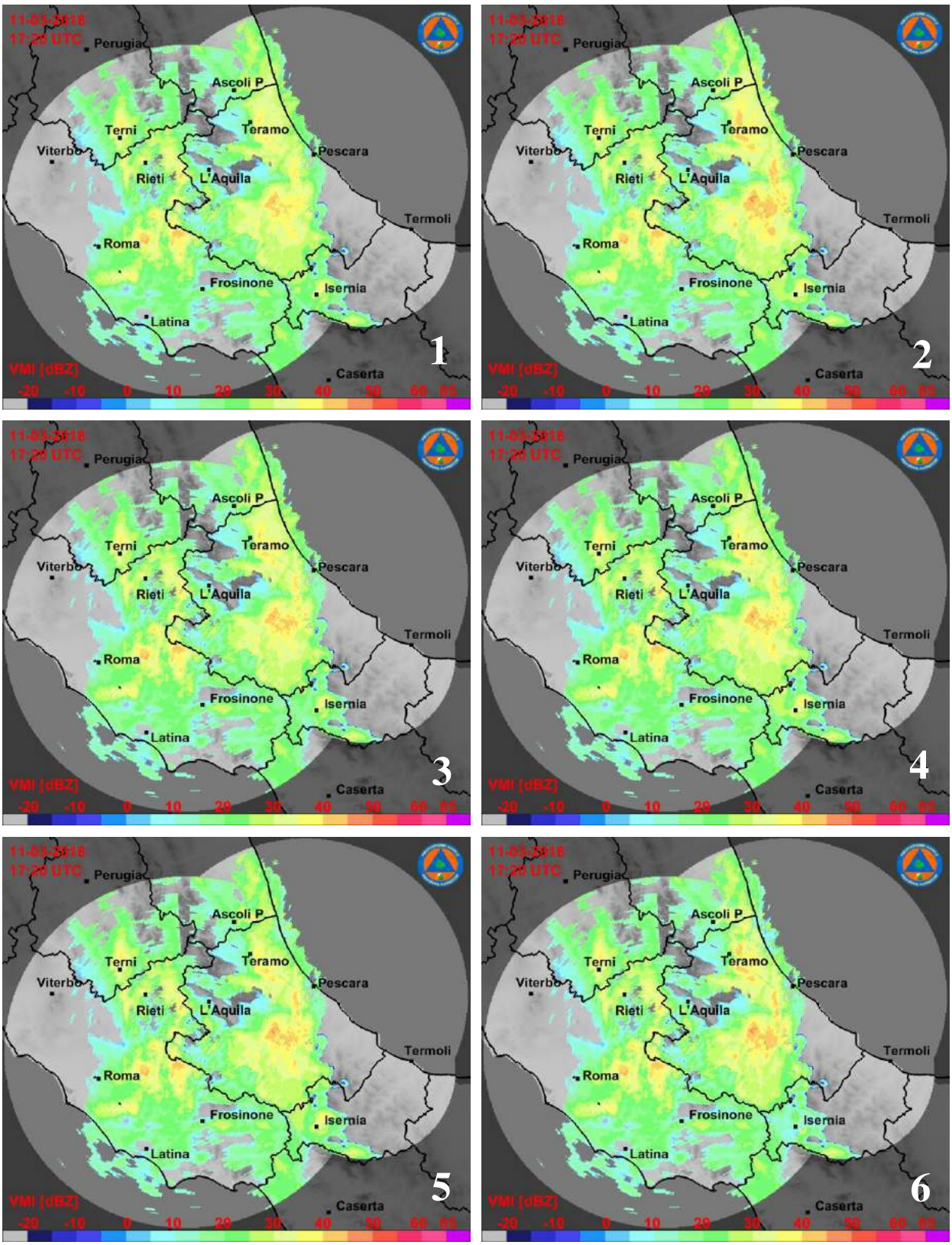


***Figure 5.23a*** *Example of mosaicking using methods from 1 to 6 of table 5.3 for the case of March 11, 2018*

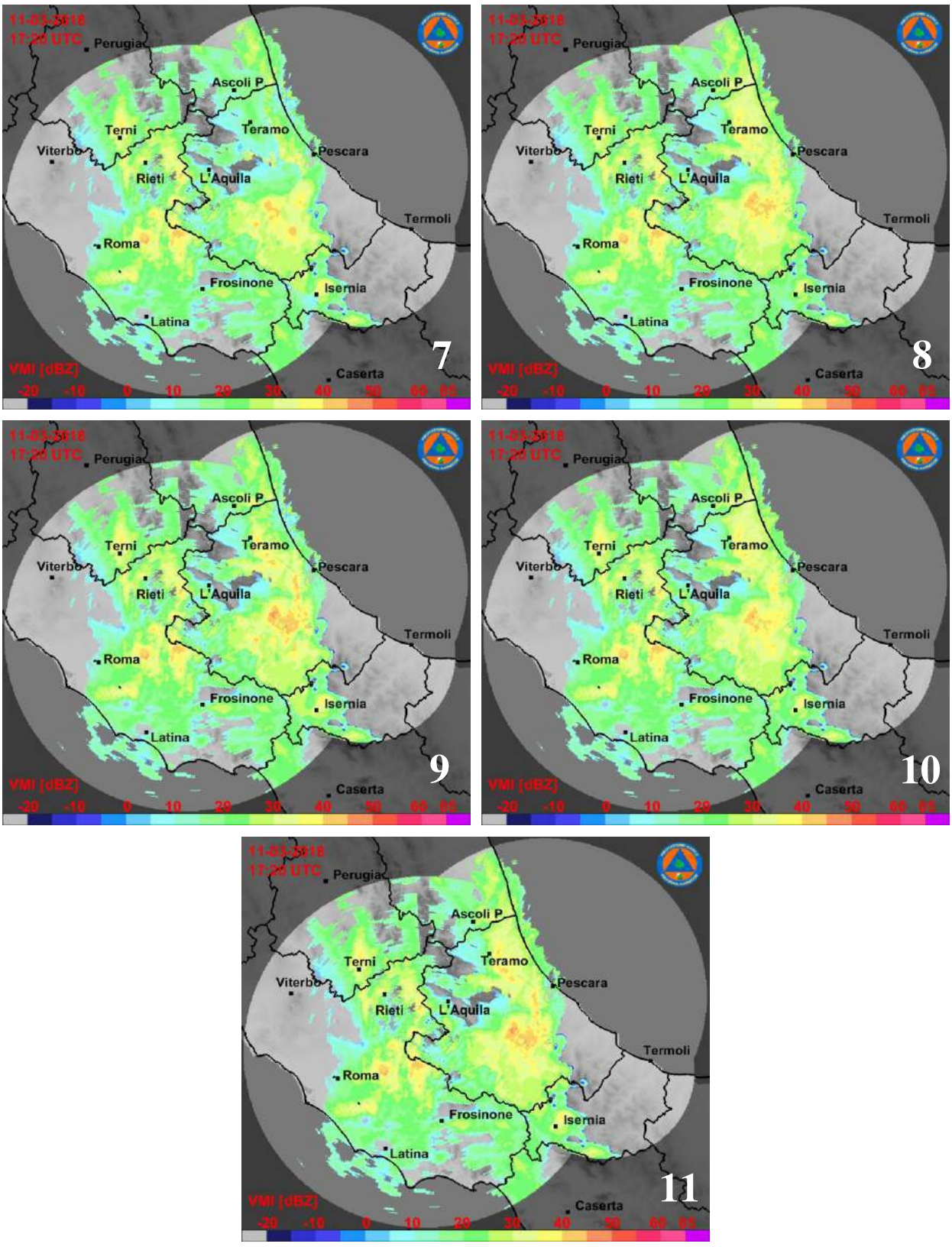


***Figure 5.23b*** *Example of mosaicking using methods from 7 to 11 of table 5.3 for the case of March 11, 2018*